Discovery of Peptide and Peptidomimetic Based Ligands Targeting the Melanocortin Receptors: A campaign in mixture-based positional scanning, chemical topology, and structure-activity relationships

A Dissertation

Submitted to the Faculty of the

University of Minnesota

By

Skye Ross Doering

In Partial Fulfillment of the Requirements

For the Degree of

Doctor of Philosophy

Carrie Haskell-Luevano, Advisor

July 2016

Acknowledgements

This work could not have been completed without the generous help and support of my advisor Carrie Haskell-Luevano. I would also like to acknowledge all of the current and past members of the Haskell-Luevano laboratory. All of these incredible people have significantly contributed to my scientific training (statistical analysis is not provided; however, I can assure you the reader this is certainly the case). I also had the wonderful opportunity to collaborate with the University of Minnesota Institute for Therapeutics Discovery & Development and the Torrey Pines Institute for Molecular Studies. I would also like to thank the University of Minnesota and the Department of Medicinal Chemistry for their investments, intellectually and financially, in my education. I also have to thank my fellow graduate students, particularly the ones who matriculated with me in 2011, who helped me along the way. A special thanks is due to my colleague and friend, Adam Zarth, who has help me, beyond measure, grow as a scientist and as a person. I also must acknowledge the unwavering support I have received from my boyfriend Derrick Berndt, family, and friends. Without everyone this simply would not have been possible. Thank you all.

Dedication

This dissertation is dedicated to all of those who have inspired me, supported me, and loved me throughout my life.

Table of Contents

List of Tables

List of Figures

Chapter 1

Introduction to Obesity and the Melanocortin Receptor System

Obesity

Despite aggressive public health initiatives over the last few decades, the proportion of the population who are obese and overweight continues to expand at an alarming rate. According to the World Health Organization, the prevalence of obesity has nearly doubled from 1980 to 2014 where now 11% of men and 15% of women are obese worldwide.[1] In the United States, more than one-third of adults in addition to 17% of the youth are obese (Figure 1-1).[2] This epidemic puts a substantial burden on the U.S. health care system by consuming an estimated 9.1%, or $147 billion dollars, of the total annual medical spending.[3] However, the impact of the disease is more than added pounds and dollars. As weight increases so does the risk for cardiovascular disease, diabetes, musculoskeletal disorders such as osteoarthritis, and cancers including endometrial, breast, and colon.[1] The risk for these comorbidities becomes moderate to severe with a body mass index (BMI) greater than 30 kilograms per meter squared.[1] Although BMI does not account for body composition (fat vs muscle tissue), a body mass index (BMI) greater or equal to 25 kg/m^2 and less than 30 kg/m^2 is defined as overweight while a BMI greater or equal to 30 kg/m^2 is defined as obese.[1] For reference, a person who is 5'10" tall, this would be 174 pounds and 209 pounds, respectively.

A multitude of external factors, such as easily accessible high-calorie foods and an overall lack of physical activity, are contributing to this epidemic; however, the basic regulatory pathways within the body are not completely understood. The sequencing of the human genome, identification of key signaling pathways, mutagenesis, synthesis of

chemical probes, in addition to a plethora of other scientific techniques have allowed scientists to begin to understand the molecular machinery involved in energy homeostasis.

Evidence suggests many of the signaling systems regulating energy homeostasis feed into the brain where the final step is mediated by the melanocortin receptors. There have been correlations found in the clinic that identified genotypes in obese patients that correlate with both molecular (i.e. *in vitro* intracellular cAMP accumulation assays) and clinical (i.e. feeding behavior) phenotypes.[4] Moreover, there is a peptide based drug candidate Setmelanotide from Rhythm Pharmaceuticals, with the sequence Ac-Arg-c[Cys-D-Ala-His-D-Phe-Arg-Trp-Cys]-NH_2, targeting the melanocortin-4 receptor.[5-7] This compound has passed early-stage clinical trials and is now being evaluated in patients with rare genetic mutations, Prader-Willi syndrome and proopiomelanocortin deficiencies, which result in obesity (clinicaltrials.gov identifiers NCT02507492 and NCT02311673).

The remainder of this chapter will discuss the biology of the melanocortin receptor subtypes, the endogenous ligands, a concise history of key discoveries in the field and structure-activity relationships (SAR), in addition to some of the challenges which have limited this field from developing a viable therapeutic treating metabolic disorders. In addition, the introduction will serve to put the following work reported herein in the context of the rest of the field and demonstrate how this work is fulfilling some of the unmet needs.

The Melanocortin System

Overview

The melanocortin receptors are a family of class A, rhodopsin-like, G protein-coupled receptors (GPCRs).[8-14] They signal primarily through the Gαs subunit which results in the accumulation of the secondary messenger cyclic adenosine monophosphate (cAMP).[15] There have been five melanocortin receptor (MCRs) subtypes cloned to date, labeled MC1R through MC5R, which mediate a myriad of functions (Figure 1-2).[8-14] The melanocortins control numerous and varied systems within the body and research in this field have found implications within the areas of Alzheimer's disease, skin pigmentation, sexual function, social behavior, cancer, and energy homeostasis, including both obesity and cachexia.[16-20]

There are numerous peptide agonists and antagonists with varying pharmacology at each of the receptor subtypes.[8-14] Even with the challenges associated with the therapeutic use of peptides compared to traditional "small molecules," including delivery and half-life, the potent, long-lasting melanocortin analog NDP-MSH has been approved under the tradename Scenesse (agency product number EMEA/H/C/002548) by the European Medicines Agency (http://www.ema.europa.eu/) for the treatment of erythropoietic protoporphyria, a severe skin sensitivity to sunlight.[21]

The Endogenous Receptors and Their Functions

The MC1R is found primarily in the skin and is involved in the regulation of pigmentation.[8-9] The MC2R is involved in steroidogenesis, is a key receptor in the hypothalamic-pituitary-adrenal axis, and is activated only by the adrenocorticotropic

hormone (ACTH).[22] Both the MC3R and MC4R are located in the brain and are integral in maintaining energy homoeostasis and body weight regulation.[10-11, 13] The MC5R has been identified to affect the exocrine gland function and grooming behavior in mice,[23] yet the function of this receptor in humans has yet to be fully elucidated.

The MC4R has been investigated as an obesity drug target due to the identification of numerous single nucleotide polymorphisms (SNPs) in the MC4R of obese individuals, making this receptor the largest monogenic determinant of severe childhood-onset obesity.[4] The Haskell-Luevano laboratory has pharmacologically characterized 70 hMC4R SNPs and results indicated these polymorphisms can alter the cell surface expression levels of the receptor, constitutive activity, in addition to altering the potencies of the endogenous agonists and agouti-related peptide (AgRP), an endogenous antagonist.[24-26] The Haskell-Luevano laboratory has also identified potent ligands for some of the specific polymorphisms and *in vitro* assays indicated these compounds were able to rescue the function of these mutant receptors.[27-28] Out of the two centrally expressed receptors, it has been hypothesized that the melanocortin-4 receptor affects immediate satiety whereas the melanocortin-3 receptor affects the long-term energy needs and food consumption in the body. In order to test this hypothesis there is a need for melanocortin-3 receptor selective compounds (greater than 100-fold) which currently do not exist.

The Endogenous Ligands

Stimulation of all five of the melanocortin receptors is mediated through proopiomelanocortin (POMC) gene-derived products[29] with additional reports indicating they can signal through other non-classical pathways including $G_{i/o}$, MAPK, and the

Kir7.1 channel.[30-32] These peptide ligands include α-, β-, and γ-melanocyte stimulating hormones (MSH) which stimulate the MC1, MC3, MC4, and MC5 receptors, and the ACTH ligand which stimulates all five of the receptor subtypes.[33-34] Extensive structure-activity relationship (SAR) studies have determined the conserved His-Phe-Arg-Trp motif found in all of the endogenous melanocortin agonists to be the minimum naturally occurring sequence necessary for receptor activation and it has been described as the core melanocortin signaling sequence.[35-36] Figure 1-3 illustrates the endogenous POMC ligands that stimulate the melanocortin receptors. For clarity, they are aligned and highlighted to better illustrate the core melanocortin signaling motif.

Receptor stimulation is inhibited at the melanocortin-1, -3, and -4 receptors by two endogenous antagonists: agouti-signaling protein (ASIP) and agouti-related protein (AGRP).[37-39] SAR studies on the 100+ amino acid sequences of human ASIP and AGRP have determined an Arg-Phe-Phe tripeptide sequence to be essential for antagonist activity.[39-42] *In vivo* mouse studies have demonstrated that melanocortin agonists decrease food intake while MC3R/MC4R melanocortin antagonists can promote food intake.[43-44] These results support the hypothesis the MC3R and MC4R may be viable drug targets for the treatment of metabolic diseases.

Synthetic Melanocortin Ligands

In the past decades, many synthetic melanocortin ligands have been identified. It would be beyond the scope of this work to discuss all of the reported SAR. Additionally, this work has been expertly reviewed elsewhere.[45-47] However, several of these synthetic compounds were used throughout this dissertation (Figure 1-4). It is beneficial to discuss

the SAR of these key melanocortin ligands and discuss how they were used as standard positive controls in the experiments reported herein.

Sawyer and co-workers reported one of the first potent and long lasting α-MSH compounds.[21] Substitutions at Met^4 and Phe^7 positions of α-MSH with norleucine (Nle) and D-Phe, respectively, resulted in the potent and long-lasting agonist pharmacology.[21] A Met^4 to Nle^4 replacement is a bioisosteric modification where the sulfur atom on methionine is replaced with a methylene group. This substitution produces a sidechain which is structurally similar to the native sidechain yet is more stable against degradation.[21] The Phe^7 to $DPhe^7$ replacement was discovered using an activity-guided fractionation method where both [Nle^4]-α-MSH and the native α-MSH peptides were subjected to heat-alkali-catalyzed racemization.[21] Typically, this peptide produces an EC_{50} value in the single-digit to sub-nanomolar range (0.1 to 10 nM) at the MC1, MC3, MC4, and MC5 receptor subtypes. In the literature this compound is commonly referred to as [Nle^4, $DPhe^7$]-α-MSH, NDP-MSH, or melanotan-1. Additionally, this compound is the one which is approved in the European Union for skin UV sensitivity and sold under the tradename Scenesse (agency product number EMEA/H/C/002548).

The Hruby laboratory continued investigations into potent α-MSH analogues. They first evaluated a series of truncated α-MSH and NDP-MSH analogues where they learned the minimal requirements needed for receptor activation.[35] Beginning from a truncated α-MSH analogue, sequence [Nle^4, $DPhe^7$]-α-MSH_{4-10}, they conducted molecular dynamic simulations and proposed the formation of a lactam bridge between Glu^5 and Lys^{10} may be beneficial.[48-49] They constructed a library of compounds varying the macrocycle from 20 to 24 atoms utilizing combinations of Glu^5 or Asp^5 and Lys^{10},

ornithine[10] (Orn[10]), 2,4-diaminobutyric acid[10] (Dab[10]), or 2,3-diaminopropionic acid[10] (Dpr[10]).[49] Results from the *Rana pipiens* frog skin and *Anolis carolinensis* lizard skin assays identified the Ac-Nle-c[Asp-His-DPhe-Arg-Trp-Lys]-NH_2 as the most potent compound.[49] Throughout the literature this compound has become known as melanotan-2 or MTII. Typically, MTII tends to be more potent than NDP-MSH at the four receptor subtypes. This non-selective compound has been used to elucidate the role the melanocortin system has on feeding behavior and obesity.[43] In addition, the effects on human sexual function have also been documented by "willing collaborators" with the Hruby laboratory, a practice not currently employed in the Haskell-Luevano laboratory, in addition to more traditional animal studies.[18, 50] This compound is not currently used clinically, although it has proven beneficial as a tool to probe the function of the melanocortin receptors with *in vitro* and *in vivo* models in the Haskell-Luevano laboratory.

A scientist may ask why use both NDP-MSH and MTII in the laboratory when a potent endogenous ligand like α-MSH exists? It takes relatively the same amount of effort to synthesize the synthetic analogues as it does α-MSH, yet MTII has a shorter sequence so it takes fewer resources in terms of chemical reagents. An important benefit from both NDP-MSH and MTII is their increased potency (> 10-fold) relative to α-MSH. Antagonist compounds are evaluated with a Schild analysis which measures antagonist activity by competitively shifting the dose-response curve of a known agonist at varying antagonist concentrations.[51] Since both NDP-MSH and MTII are a log more potent than alpha-MSH, there is a greater range for the dose-response curves to shift than for α-MSH.

In practice, this aspect is important when evaluating weaker antagonists, a common pharmacological result in new chemical libraries.

Further investigations into the MTII scaffold by conducting a single amino acid replacement study in the template led to the identification of SHU9119.[52] The sequence of this peptide is Ac-Nle-c[Asp-His-**DNal(2')**-Arg-Trp-Lys]-NH_2, and compared to MTII this analogue has a $DPhe^7$ to $DNal(2')^7$ single residue replacement.[52] The pharmacological profile of this cyclic peptide is well documented. It is a potent MC1R/MC5R agonist and an MC3R/MC4R antagonist.[52] An important aspect of this pharmacological profile is the partial agonist activity at the MC3R which is thoroughly discussed beginning in Chapter 3. This compound has been used as a control for *in vivo* studies to demonstrate the agonist-induced decreased food intake in mice can be competitively reversed.[43] It is used in the studies reported herein as a benchmark compound which all other antagonist compounds may be compared to.

The last compound to be introduced in this section is the Carrie Haskell-Luevano (CHL) tetrapeptide Ac-His-DPhe-Arg-Trp-NH_2. This tetrapeptide sequence was identified by a truncation study of NDP-MSH in the Haskell-Luevano laboratory to be a nanomolar agonist at the mouse MC1, MC3, MC4, and MC5 receptor subtypes.[53] This result was in agreement with a previous study,[54] and this sequence has since been the subject of more than a dozen published studies from the Haskell-Luevano laboratory.[28, 55-68] This peptide sequence has been referred to as the "HL-peptide" in the literature.[69] Studies about this tetrapeptide sequence have yielded compounds with a variety of pharmacological (agonists/antagonists) and selectivity profiles, and, as reported in subsequent chapters, this scaffold aided in the identification of first-in-class selective

(greater than 100-fold) MC3R ligands over the MC4R. One useful aspect of using a tetrapeptide scaffold, compared to longer α-MSH analogues, is the incorporation of a few unnatural amino acid residues can quickly produce more "drug-like" mimetics which are stable against endogenous processes like proteolytic degradation.

Therapeutic Use of Melanocortin Ligands

Treating Obesity via the Melanocortins

A brief historical perspective on the field of melanocortins highlighting some of the achievements, in addition to some of the unexpected challenges, illustrates one path to successfully develop an anti-obesity treatment. The field has a rich and long history of fruitful research, dating back 100 years.[70-71] Before the cloning of the receptors in the 1990's much of the early research focused on skin pigmentation and therefore the MC1R. It was not until 1986 when it was first demonstrated that intracerebroventricular (ICV) injection of both α-MSH and ACTH (1-24) decreased food intake and suggested the melanocortin receptors may play a role in the regulation of energy homeostasis.[72] Yet it was unknown which receptor, or receptors, were being activated. The development of routine DNA sequencing in the 1990s allowed for the identification of the five known receptor subtypes, it was during this decade that the identification of the lethal yellow allele and underlying molecular mechanism for the agouti obesity syndrome was discovered, first observed by mouse fanciers in the 1800s.[73] Identification of the lethal yellow (A^y) allele mutation in the agouti gene promoter region resulted in the ectopic expression of agouti and gave rise to the observed pleotropic effects of hyperphagia, hyperinsulinemia, and hyperglycemia.[37, 74] Intracerebroventricular injection of the potent melanocortin agonist MTII and antagonist SHU9119 demonstrated the role of

melanocortinergic neurons in feeding behavior and the agouti obesity syndrome.[43] With these encouraging results, many melanocortin compounds were brought into the clinic as potential anti-obesity therapeutics; however, the results were less than ideal.

Results from Past and Ongoing Clinical Trials

The development of an anti-obesity therapeutic drug targeting the melanocortin receptors has yet to reach the market. There has been a concerted effort by several large pharmaceutical companies, including Eli Lilly, Hoffman-La Roche, Merck, and Procter & Gamble, to develop a MC4R selective compound and, to date, all of them have failed in clinical trials. One compound which illustrates the promising yet ultimately negative results of this large research and development effort is LY2112688 (Eli Lilly and Company).

The cyclic octapeptide LY2112688, Ac-DArg-c[Cys-Glu-His-DPhe-Arg-Trp-Cys]-NH_2, is a truncated analog of α-MSH which is cyclized via a disulfide bridge, and the observed pharmacology indicated selectivity for the MC4R over both the MC1R and MC3R (30- and >100-fold increased affinity).[75] Results from a study with 26 obese or overweight individuals indicated that a once daily 1.0 mg subcutaneous infusion of LY212688 for 7-days resulted in significant increases in both systolic and diastolic blood pressures and these increases may complicate the therapeutic use of a MC4R compound.[75] Given these issues, it is curious to note that the closely related [Arg^1, $DAla^3$] Ly2112688 analog RM-493 is currently in clinical trials.

Setmelanotide (BIM-22493 or RM-493) Ac-Arg-c[Cys-DAla-His-DPhe-Arg-Trp-Cys]-NH_2 is being developed by Rhythm Metabolic. The *in vitro* pharmacology data indicates the compound has a sub-nanomolar EC_{50} at the hMC4R (0.27 nM), nanomolar

potencies at both the hMC1R and hMC3R (5.8 and 5.3 nM, respectively), and a micromolar potency at the hMC5R (1,600 nM).[7] *In vivo* animal studies indicated the peripheral administration induced weight loss in diet induced obese C57BL/6J (B6) mice and further studies with MC3R and MC4R KO mice indicated the weight-loss was primarily dependent on the MC4R; however, there were significant improvements on insulin sensitivity and it could not be concluded which of the melanocortin receptors were responsible for this activity.[7] Similar weight loss results and improvements on insulin sensitivity were observed for diet induced obese rhesus macaques.[6]

The phase 1 clinical trial has results which contradict the results for all other MC4R agonists. A clinical trial with 12 healthy obese adults indicated setmelanotide increased the resting energy expenditure and increased the amount of fat oxidation, and unexpectedly, there were no adverse effects on heart rate or blood pressure (clinicaltrials.gov identifier NCT01867437).[5] The short, 3-day, duration of the study and the small sample size could account for the lack of adverse heart effects. Moreover, the current phase 2 clinical trials are only recruiting obese patients with rare genetic mutations, either patients with POMC deficiencies or Prader-Willi syndrome (clinicaltrials.gov identifiers NCT02507492 and NCT02311673), so it is possible there will be set less stringent guidelines for possible heart effects. These patients may already have lower blood pressures and heart rates than normal patients since this anomaly has been observed for MC4R deficient patients.[75]

MC3R Selectivity and the Therapeutic Potentials

Animal knockout models indicate the MC3 and MC4 receptor subtypes have non-redundant roles in energy homeostasis. Mouse knockout models for each of the receptors

results in an increases in fat tissue, yet there are some phenotypic differences including the MC4R knockout mice are generally larger in size and the MC3R knockout mice are smaller in size.[76] However, both result in a fat to lean tissue ratio which is greater than their wild-type counterparts.[76] In addition, combined knockout results in an extreme obese phenotype.[76] The phenotypic differences in the single knockout mice and the extreme obese phenotype of the double knockout suggest the receptors have non-redundant roles and they may work together via a synergistic mechanism. Studies with patients in the clinic with selective MC4R and non-selective melanocortin agonists have indicated targeting the MC3R may prove to be better than the MC4R in terms of an anti-obesity therapy.[18, 50, 77-78]

Side effects observed when treating obesity with MC4R drugs in humans, as discussed above, include increasing blood pressure and increased erectile activity.[18, 50, 77-78] The hypertensive cardiovascular effects associated with central administration of the POMC derived peptides α- and γ_2-MSH were demonstrated in a rodent model may be an MC3R-independent (due to the absence of the effects when γ_2-MSH was administered) and an MC4R-dependent processes (due to the presence of the effects when α-MSH was administered).[77] Although these results may not correlate with humans since it was later reported γ_2-MSH has activity at both the mouse MC3R and mouse MC5R, furthermore this finding should be taken into consideration when interpreting *in vivo* results since the MC5R is found, among other places, in heart tissue.[79]

Although these studies are not conclusive, they are suggestive that targeting the MC3R to manage energy homeostasis may be more advantageous than targeting the MC4R. The simplest approach to evaluate the effectiveness and any potential side effects

of an anti-obesity therapeutic targeting the MC3R would be to administer a selective MC3R compound into an *in vivo* model. Although simple, the issue remains that there are, to the best of our knowledge, no selective (EC_{50} > 1,000-fold) MC3R compounds. Reports on MC3R selective compounds have been primarily limited to analogs of α-MSH and γ-MSH.[80-85] The identification of selective MC3R compounds with more drug-like properties, such as a lower molecular weight (MW < 1,000), may result in the development of a valuable therapeutic strategy for the current obesity epidemic, as compared to a therapeutic targeting of the activation the MC4R which has several undesirable side effects.

The Hypothesis and Approach

We hypothesize that of the five melanocortin receptors, selective modulation of the MC3R subtype may be able to alter energy homeostasis and be devoid of the undesirable side effects associated with the activation of the MC4R. In order to probe this hypothesis, there is a need for MC3R ligands that are selective over the MC4R. The work reported herein utilized classical peptide SAR strategies, such as single and double residue replacement on previously identified melanocortin ligands. In addition to these strategies, a high throughput campaign via mixture-based positional scanning was carried out in order to identify previously unidentified melanocortin peptide sequences. Research on this sequence was able to identify selective MC3R ligands with a first-in-class pharmacological profile. In addition to the completed studies reported, discussed in Chapter 6 are several ongoing projects using mixture-based positional scanning. This approach will be utilized to identify novel peptidomimetic melanocortin scaffolds and to answer fundamental questions about GPCR signaling.

Chapter 1 Figures:

Figure 1-1: Prevalence of Self-Reported Obesity Among U.S. Adults by State and Territory, As Reported by the Centers for Disease Control and Prevention, 2014

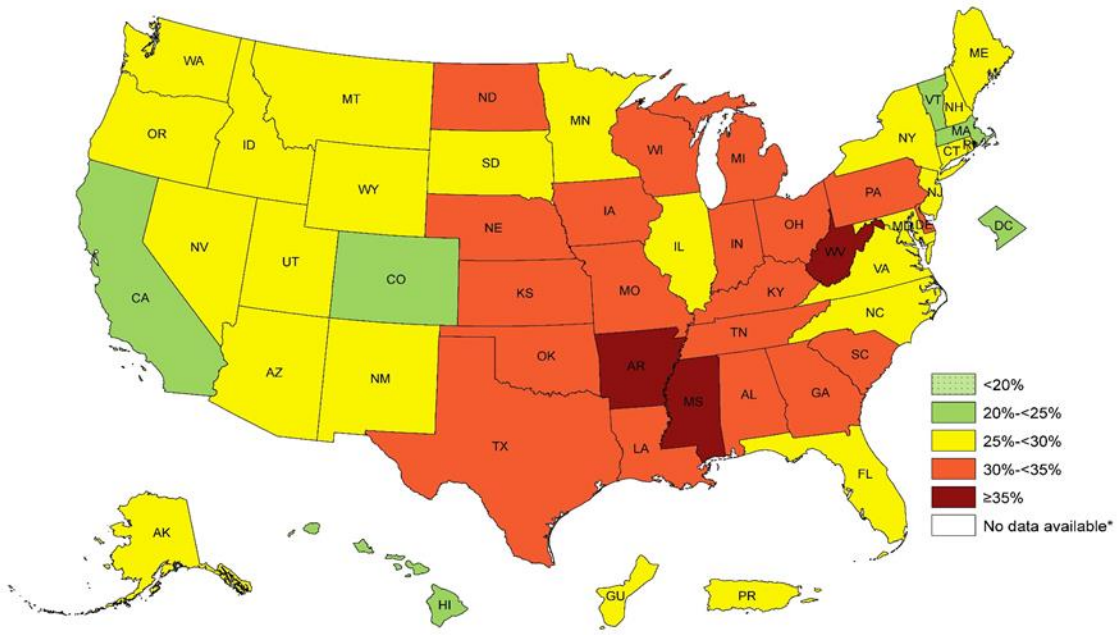

The obesity epidemic in the United States is astounding with 20% to more than 35% of the population by state considered obese (BMI > 30 kg/m^2). With an increase in weight, there is an increased risk for the comorbidities such as some cancers and type-2 diabetes. This image was originally produced by the Centers for Disease Control and Prevention and, "are royalty-free and available for personal, professional and educational use in electronic or print media, with appropriate citation."[86]

Figure 1-2: Brief Summary of the Melanocortin System

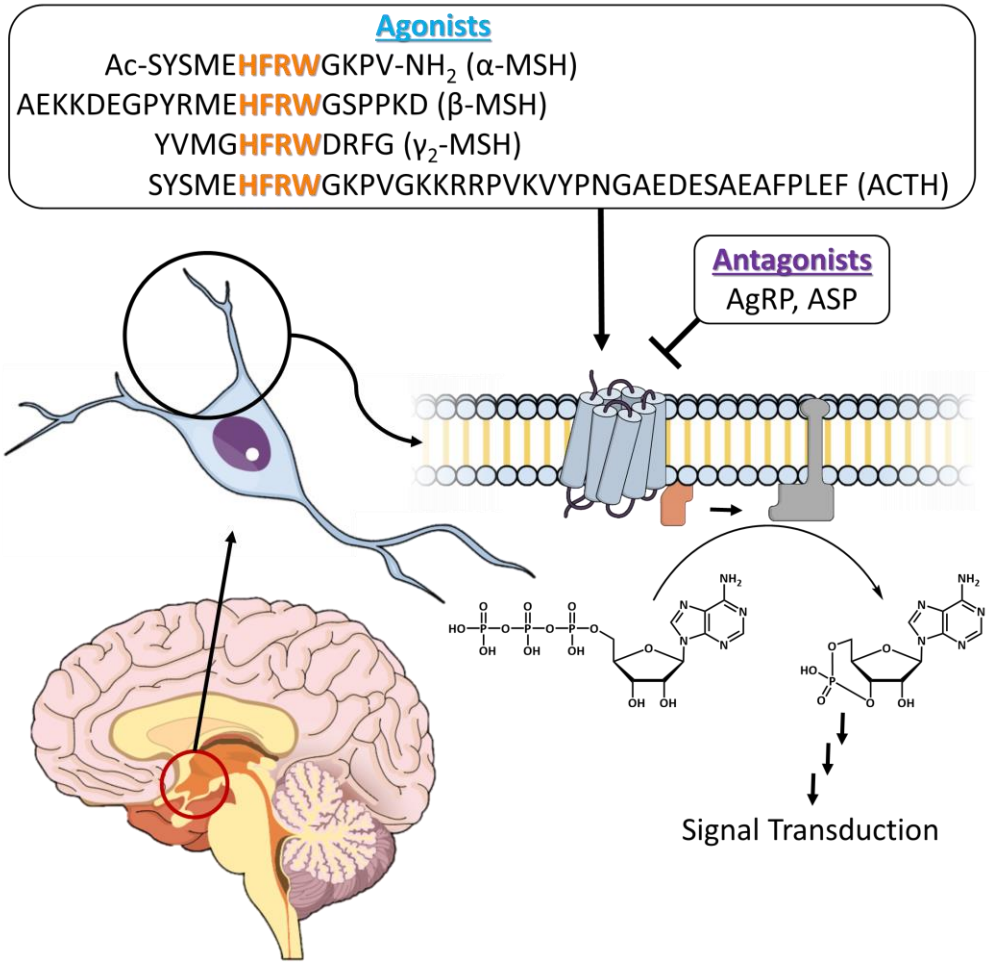

The melanocortin system is comprised of five stimulatory GPCRs. There are several endogenous peptide agonists and antagonists mediating the system. The MC3R and MC4R are expressed centrally, in the hypothalamus (circled in red), and it has been demonstrated that melanocortin agonists decrease food intake whereas antagonists increase food intake. These results indicate there is a therapeutic potential for targeting these receptors for the treatment of a variety of metabolic disorders from obesity to cachexia.

Figure 1-3: Sequence of POMC Derived Melanocortin Agonists

Peptide	Sequence
α-MSH	Ac-SYSMD**HFRW**GKPV-NH_2
β-MSH	HEKKDEGPYRMD**HFRW**GSPPKD-OH
γ_2-MSH	YVMG**HFRW**DRFG-OH
ACTH	SYSMD**HFRW**GKPVGKKRRPVKVYPNGAEDESAEAFPLEF-OH

All of the POMC derived melanocortin agonists share a common His-Phe-Arg-Trp motif which is the minimum signaling sequence. The numbering convention when describing the ligands and their analogs is generally based on the sequence of α-MSH (Ac-S^{1}-Y^{2}-S^{3}-M^{4}-D^{5}-**H^{6}-F^{7}-R^{8}-W^{9}**-G^{10}-K^{11}-P^{12}-V^{13}-NH_2).

Figure 1-4: The Pharmacology and Sequences of Common Melanocortin Ligands

α-MSH: melanocortin-1, -3, -4, -5 receptor agonist
Ac-Ser-Tyr-Ser-Met-Asp-His-Phe-Arg-Trp-Gly-Lys-Pro-Val-NH_2

NDP-MSH: super-potent and long lasting melanocortin-1, -3, -4, -5 receptor agonist
Ac-Ser-Tyr-Ser-**Nle**-Asp-His-**DPhe**-Arg-Trp-Gly-Lys-Pro-Val-NH_2

SHU9119: melanocortin-3, -4 receptor antagonist and melanocortin-1, -5 receptor agonist
Ac-**Nle**-**c**[Asp-His-**DNal(2')**-Arg-Trp-Gly-Lys]-NH_2

MTII: ultra-potent and stable melanocortin-1, -3, -4, -5 receptor agonist
Ac-**Nle**-**c**[Asp-His-**DPhe**-Arg-Trp-Gly-Lys]-NH_2

CHL peptide: melanocortin-1, -3, -4, -5 receptor agonist
Ac-His-**DPhe**-Arg-Trp-NH_2

Illustrated are the sequences and generally pharmacology for four synthetic melanocortin ligands which were utilized throughout this dissertation. The endogenous peptide α-MSH is included for reference. It is standard convention to indicate residue substitutions relative to α-MSH.

Chapter 2

General Methodologies

Chemistry

Peptides regulate numerous signaling pathways in the body. They may possess complex structures allowing for high selectivity, and the tiniest of changes can lead to pronounced biological effects. For example, as discussed in Chapter 1, MTII and SHU9119 differ by a DPhe to DNal(2') replacement, yet one is a potent agonist while the latter is a potent antagonist. Peptides are capable of numerous chemical interactions, and the elegant, yet sophisticated, biological machinery used to produce the peptides from the most basic amino acid building blocks is the result of more than a billion years of evolution. Advancements in computer science, molecular biology, and chemistry over the last century that have allowed scientists to better explore and understand the pathways regulated by peptides and discover new peptide sequences to regulate these pathways.

The importance of peptides has driven chemists to devise simple and robust methodologies to produce them. One key advancement was the use of a solid support in the synthesis of peptides. This permitted the facile stepwise addition of protected amino acids onto a growing peptide chain while eliminating the need for intermediate purifications. As Nobel Laureate R. Bruce Merrifield modestly stated in his seminal 1963 *J.A.C.S.* publication, "The advantages of the new method were speed and simplicity of operation."[87] Compared to traditional solution-phase chemistry, solid-phase peptide synthesis (SPPS) does not fully characterize each individual reaction in addition to any possible side products. Instead, SPPS relies on chemical methodology that drives each

reaction to nearly quantitative yields, and the use of a solid support allows for reagents to be simply filtered and washed off.

The synthesis of peptides using SPPS requires very robust chemical reactions. A tetrapeptide composed of four amino acids requires a minimum of eight steps to synthesize, and the overall theoretical yield for the entire reaction can be calculated by taking the average yield for each individual chemical reaction and raising it to number of steps. An average yield of 99.9% for each step would produce an overall theoretical yield of 99.2%, whereas an average yield of 90% for each step drops the overall theoretical yield to 43%. If the average yield of each reaction dropped to an average of 80% per step, then the overall yield drops to a dismal 17%. The steep drop off in overall yield grows exponentially with each additional residue. If the same theoretical yield calculations were done for a peptide possessing 13 amino acids, such as α-MSH, the minimum 26 steps needed for the synthesis would make the overall theoretical yields of 97% (99.9%^26 steps), 6% (90%^26 steps), and a trace 0.3% (80%^26 steps)!

Many chemists have devoted their careers to developing new robust methodologies, which has greatly benefited my syntheses and I gratefully acknowledge their contributions to the peptide community. The following discussion is not an all-encompassing description of SPPS and combinatorial library construction, but an overview of the concepts to introduce the reader on the subjects. This will be followed by a discussion of the specific chemistry reported in later chapters. This chapter will also discuss some of the nuances and pitfalls which are not prominently discussed in the literature but were learned by trial and error with the hope this knowledge may be useful for future students' projects.

Solid-Phase Synthesis – A General Overview

SPPS constructs peptides in a stepwise manner where the growing peptide chain is attached to, typically, a polystyrene support. There has been successful efforts to develop alternative resins, such as Cross-Linked Ethoxylate Acrylate Resin (CLEAR) that was developed by George Barany's laboratory, that are suitable in certain applications.[88] Figure 2-1 illustrates the basic concept of SPPS for the synthesis of a "typical" peptide which is simply a linear chain of amino acids that are not further modified. On the polystyrene support there is a linker to attach the first amino acid. The linker choice determines the functionality on the C terminus of the desired peptide. After "swelling" the resin in organic solvent (the resin beads increase in size in the presence of solvent), typically dichloromethane since it will cause the greatest amount of swelling, the first protected amino acid may be coupled on.[89] This is followed by the deprotection of the N-α-amine of the first amino acid. Since the growing peptide is attached to a solid support, the coupling and deprotection reagents can be washed off while the growing peptide chain is retained on the resin, which is kept by a course filter. This can be followed by the coupling and N-α-deprotection of the second protected amino acid. Additional amino acids may be added through successive couplings and deprotections until the desired peptide sequence is synthesized. The peptide is cleaved from the support and typically the cleavage conditions will also deprotect the protected sidechain functionalities. The crude peptide can then be isolated and purified by chromatographic means. Peptides are traditionally synthesized from the C terminus to the N termini in the laboratory, yet are reported from the N termini to the C termini, the direction peptides are synthesized in nature.

Resin Selection

The selection of the proper resin is key to synthesizing any peptide since this will determine the functionality on the C-termini of the final peptide, indicate the compatibility of one's reaction with solvents/reagents, and the substitution amount (milli-equivalents per gram) will govern the necessary equivalents for all of the subsequent chemistry. There are many resins commercially available for use in different applications. A 200-400 mesh, rink amide p-methylbenzhydrylamine (MBHA) resin with 1% divinylbenzene (DVB) copolymer was used for the synthesis of all peptides reported in this dissertation, typically with a 0.3-0.6 milliequivalents per gram (meq/g) substitution (Figure 2-2).[90] This polystyrene resin is compatible with organic solvents. The mesh size indicates the size of the screen which was used to sort the resin. The rink amide MBHA linker indicates the C termini of the peptides will be amidated. The resin substitution is analytically determined for each batch of resin and indicates how much resin will have to be used for a given synthesis scale in addition to the spacing of each peptide when it is bound to the resin. In practice, the 0.3-0.6 meq/g substitution rate is suitable for short to medium length (20 amino acids or less) peptides. When peptides exceed that length, bound peptides have the potential to interact with each other, and require a lower resin substitution.

Solid-Phase Synthesis and Fmoc Chemistry

The key to the synthetic approach is the selection of side chain and Nα protecting groups that are orthogonal to each other. The peptides reported in this dissertation were synthesized using standard Nα-fluorenylmethyloxycarbonyl (Fmoc) chemistry.[91-93] This approach utilizes amino acids which possess N-α-amines that are protected with the base-

labile Fmoc protecting group and the sidechains are orthogonally protected with acid-labile protecting groups, if there are sidechains which need protecting.[91-93] Out of the 20 naturally occurring amino acids, only 12 require sidechain protection. Amino acids such as alanine do not require sidechain protection since their sidechain functionalities are typically unreactive to amide bond coupling and deprotection conditions.

Fmoc protecting groups are removed using mild base conditions. A 20% piperidine solution in N,N-dimethylformamide (DMF) will effectively remove the Fmoc protecting group.[91-93] A reasonable mechanism for Fmoc removal would begin with base abstraction of the proton off of the carbon beta to the carbamate and on the fluorenyl ring system. The resonance stabilized electron pair induces collapse of the protecting group which is irreversibly driven to completion through the loss of carbon dioxide, and the amine is subsequently revealed (Figure 2-3). In practice, when utilizing microwave assisted SPPS, the Fmoc protecting group was removed in a two-step process. First, a 20% piperidine in DMF deprotecting solution was added to the reaction vessel and reacted for 2 minutes at room temperature. This was followed by removal of the solution, addition of fresh deprotecting solution, and placement of the reaction vessel in the microwave and allowed to react (75°C, 30W, 4 min). This reduces the probability of the products from the deprotection reaction to polymerize.[94]

Potential Problems with Piperidine

Issues can arise during the deprotection of Fmoc protecting groups with piperidine when Glu or the dipeptide sequence Asp-Gly is present. The protected carboxylic acids have the potential to react with piperidine and the resulting side products are either pyroglutamic acid (which is truncating) or an aspartimide (Figure 2-4). An

indication an aspartimide is present is the loss of 18 amu (one water molecule). In both cases, piperidine reacts with the tert-butyl ester on either the protected Glu or Asp sidechains. With the piperidine reacted Glu, the free amine alpha to the sidechain displaces the piperidine to form a lactam. This is in contrast to the aspartimide formation wherein the nitrogen originating from the Gly of the Asp-Gly dipeptide displaces the piperidine to form a heterocycle. A simple solution to minimize both side reactions is the addition of 5% formic acid to the 20% piperidine in DMF.[95]

Orthogonal Acid-Labile Sidechain Protecting Groups

All of the natural amino acids, in addition to many unnatural ones, are commercially available with Fmoc protection in addition to an orthogonal sidechain protection. Typically the sidechain protecting groups used in this dissertation were acid-labile protecting groups (illustrated in Figure 2-5); many additional sidechain protecting groups exist, which are orthogonal to acidic and basic conditions.[96] Sidechains protected with groups such as ω,ω′-bis-allyloxycarbonyl (alloc), removed with $Pd(PPh_3)_4$ and scavengers, can allow for the selective removal of those sidechain protecting groups while the peptide is still on solid support in order to perform additional chemistry, like lactam bridge formation.[97]

They can be categorized into five groups based upon the type of protecting group present and the resulting functionality after removal. Alcohols functionalities present in Ser, Thr, and Tyr are protected as tert-butyl ethers. Carboxylic acid functionalities present in Asp and Glu are also protected as tert-butyl esters. The nitrogen atoms found on the primary amine of lysine and the indole of tryptophan were protected with tert-butyloxycarbonyl (Boc) protecting groups. The amide nitrogen atoms on Asn and Gln,

one of the imidazole nitrogen atoms of histidine, and the sulfur on cysteine were protected with trityl protecting groups. Last, only one of the nitrogen atoms on the guanidinium sidechain functionality on Arg were protected with a 2,2,4,6,7-pentamethyldihydrobenzofuran-5-sulfonyl (Pbf) protecting group. Technically, the remaining unprotected nitrogen on the arginine is reactive; however, the Pbf protecting group is sufficiently deactiviating to render that nitrogen unreactive.[96] In practice, one drawback of coupling arginine was the need for increased amino acid equivalents. It is postulated arginine can form a six-membered δ-lactam ring, although this byproduct cannot be coupled to a growing peptide chain.[96]

All of the sidechain protecting groups listed were removed during cleavage of the peptide from the solid support with a cleavage cocktail consisting of trifluoroacetic acid, ethanedithiol, triisopropylsilane, and water (ratio of 91:3:3:3). The acid cleaves the peptide from the resin in addition to removing the sidechain protecting groups and the three scavengers prevent the re-addition of any protecting groups back onto the peptide. In part due to the unbelievably eye-watering strong and unrelenting odor of ethanedithiol in combination with the sometimes inadequate ventilation provided by the fume hoods in Weaver-Densford Hall, thioanisole was substituted at the same ratio.

Carboxylic Activation and Amino Acid Coupling

The coupling conditions selected for the reported peptides used N,N,N′,N′-tetramethyl-O-(1H-benzotriazol-1-yl)uronium hexafluorophosphate (HBTU) and diisopropylethylamine (DIEA) coupling reagents and typically microwave assistance was also utilized to increase the reaction speed. The selected coupling reagents go through a two-step process to activate the carboxylic acid on the amino acid before it is able to be

added onto the growing peptide chain (Figure 2-6). In the proposed reaction mechanism, the non-nucleophilic base DIEA removes the proton from the carboxylic acid. The oxygen on the carboxylic acid subsequently attacks the carbon on the uronium functionality and displaces the hydroxybenzotriazole (HOBt) from HBTU via a nucleophilic substitution style reaction. This is followed up by HOBt attacking back in, as the final step to activate the carboxylic acid, resulting in the loss of a urea. The free amine on the growing peptide backbone attacks the now activated carbonyl carbon of the activated carboxylic acid to result in the desired amide bond formation.

Table 2-1 summarizes the standard equivalents for coupling each amino acid in addition to the microwave irradiation settings. For a standard amino acid (i.e. not Arg, His, or Cys) 3.1 equivalents of the protected amino acid was used along with 3.0 equivalents of HBTU and 5.0 equivalents of DIEA. The slight excess of the protected amino acid relative to the HBTU equivalents decreases the formation of a peptide truncating guanidinium. The free amine on the growing peptide chain is sufficiently nucleophilic to displace HOBt at the uronium moiety of HBTU. The microwave conditions (75°C, 30W, 5 min) were optimized to sufficiently couple most amino acids in the least amount of time. As discussed above, the equivalents for Arg is greater than what was used for all other amino acids. The increased equivalents and a longer reaction time were necessary to drive the reaction to completion. Cys and His required a lower reaction temperature for the coupling to limit undesirable side reactions, particularly the epimerization of the residue.

Reaction Monitoring

In order to test for the presence of a free amine, during both the coupling and deprotecting stages of the synthesis, two colorimetric tests were employed. A small amount of resin was removed from the reaction vessel and either the ninhydrin (Kaiser) test was performed to determine for the presence of a primary amine or the chloranil reaction was performed to test for the presence of a secondary amine.[98-99]

The presence of a primary amine results in a vibrant blue ninhydrin test result.[98-99] First, a ninhydrin molecule condenses with the primary amine via a Schiff base. Subsequent hydrolysis results in the removal of the nitrogen from the growing peptide chain, and it is at this point the ninhydrin molecule containing the abstracted nitrogen atom then reacts with a second ninhydrin molecule to form a blue chromophore (Figure 2-7).

For secondary amines, equal parts of a saturated chloranil solution and acetone are added to the resin.[98] In this reaction, the acetone is conjugated to the secondary amine through an imine intermediate. A chloranil molecule is then nucleophilically attacked, via a Schiff base intermediate, at one of the four chlorine substituted carbons on the substituted quinone. The resulting adduct results in the dark black/brown color observed for the resin (normally the resin is translucent) indicating a positive test (Figure 2-8).

Peptide Purification and Characterization

After final cleavage and deprotection of the desired peptide, the next step is to purify the peptide from the crude mixture and analytically characterize the compound before it is submitted for biological evaluation. Peptides are purified via reverse-phase high-pressure liquid chromatography (RP-HPLC) coupled to a photodiode array (PDA)

detector. The column eluent is typically monitored at 214 and 280 nanometers since these are the wavelengths where amide bonds and aromatic rings absorb, respectively. Typically the HPLC system uses a C18 column with either methanol or acetonitrile along with 0.1% TFA in water as the solvent system. The exact purification settings are unique for each peptide and are discussed in detail in the experimental sections in the following chapters. The rationale for analytically characterizing the peptides in two different solvent systems is to reduce the possibility of having a small impurity hide under the absorbance of the main product peak. For the molecular mass determination of the peptides, any soft ionization like electrospray ionization (ESI) or matrix-assisted laser desorption/ionization (MALDI) is suitable for the MS analysis. Most MS facilities bill by the minute, so in order to maximize financial resources the selection of MALDI is more cost-effective. Compared to ESI, MALDI requires more preparation before going to the MS facility, in terms of spotting the plate and waiting for the matrix to dry; however, the MALDI is much quicker to run multiple samples since washing steps are not required between analyzing samples. So, unless ESI-MS in needed, one should preferentially use MALDI-MS because less instrument time is required per peptide.

Final Thoughts

Peptide chemistry is uniquely suited for SPPS. The robustness of the chemical methodology allows for the rapid synthesis of large libraries of peptides. As discussed above, SPPS is a simple solution to a complex problem.

Mixture-Based Combinatorial Screening Libraries

A large portion of the worked reported herein includes the utilization of mixture-based combinatorial screening libraries. This type of library allows for the rapid evaluation of millions and millions of compounds. An additional benefit of using this technology is that compound leads produced by this type of campaign use little to no previous knowledge of the particular system of interest. This results in unique compounds residing in areas of chemical space which has yet to be fully explored in one's field; in essence, the researcher is sowing seeds to produce new low hanging fruit.

This approach was pioneered and developed by Dr. Richard Houghten, the president and founder of The Torrey Pines Institute for Molecular Studies, and with whom the Haskell-Luevano laboratory has developed an extensive collaboration that is currently ongoing.[28] This technology has been applied to several disease states including diabetes,[100] immunology,[101] infectious disease,[101] cancer,[102] and pain management[103]. Important to the melanocortin field, this technology has been validated through a proof-of-concept study where tetrapeptides were identified which rescued the function of single nucleotide polymorphisms found within the human melanocortin-4 receptor that were identified in patients with severe childhood-onset obesity.[28] Mixture-based positional scanning was developed over several decades and required new innovations in both chemistry and biology.

A Historical Perspective

As described by Dr. Houghten himself in a perspective in the initial issue of the Journal of Combinatorial Chemistry, the first innovation came to him as a possible time

saving measure while he was synthesizing small libraries of compounds using solid-phase synthesis.

> "Some say that 'necessity is the mother of invention', but in my case I was drawn to the time saved by this synthetic method so that I had more time for intriguing scientific and extracurricular pastimes (this was, after all, San Francisco in the 1970s)."

While we can only postulate about the extracurricular pastimes of San Francisco in the 1970s, Houghten observed at the benchtop while synthesizing individual analog after analog, and repeating the same deporotection, neutralization, coupling, and washing steps over and over, that the common deprotection, neutralization, and washing steps could be done in parallel in a single reaction vessel.[104] This required a method to keep the compound resins separate. Trial and error lead to the development of the "tea bag" approach. Compounds are synthesized on resin contained within a polypropylene mesh bag which resembles a tea bag; hence the name.[105-106] Each tea bag is permanently sealed and contains a code so it can be tracked throughout the synthetic process. All of tea bags are then reacted in a single vessel for the common deprotection, neutralization, and washing protocols which are necessary for standard Merrifield solid-phase peptide synthesis, and the tea bags which shared common residues at a particular position could be coupled in parallel. This allowed for the increase in speed and efficiency at which individual compounds could be synthesized. It was first implemented in a study investigating the specificity of antigen antibody interactions in 1985 and later patented in 1986.[105-106]

The Theoretical Concept

The second key innovation for this technology was the development of the mixture-based screening approach. The key connection between the chemistry and biology was mixtures of compounds are part of the normal environment for any biological process and if mixtures could be synthesized in a particular way this would yield useful molecular information, then large libraries of compounds could be screened without having to synthesize and purify each individual compound.[104] A thought experiment can aide in understanding the fundamental theory why the mixture-based screening approach works and how one would implement a mixture-based screening library in practice.

In a typical *in vitro* assay, a single compound is dosed and the subsequent response is recorded. In this case, we are starting out with a compound which results in an EC_{50} of 1 nM. Now an additional completely inactive compound with no measureable functional or binding activity is added. The recorded response would be the exact same. We can now add a second completely inactive compound to our "typical" assay and repeat the measurement, and we would find the response is again the exact same. We could repeat this again and again until we reached a mixture that contained a thousand different compounds. Since only the first compound binds and activates the biological target of interest, the measurement for the overall assay of the mixture is effectively the same. However, the resulting potency of a mixture is altered upon the addition of a moderately active compound (EC_{50} = 1,000 nM).

What is the resulting potency when a moderately potent (EC_{50} = 1,000 nM) compound is added to a potent (EC_{50} = 1 nM) compound, and could the mixture still be

identified as containing a potent compound? The arithmetic mean of the two compounds, the sum of the means divided by the sample size, would predict a value of approximately moderate 500 nM mixture, and each additional moderate to weak compound added to the mixture would quickly shift the overall potency to even higher and higher values. Yet, in in practice, the resulting potency for mixtures of two compounds is closer to 2 nM. This is because the mixture potency follows a harmonic mean as opposed to the arithmetic mean.[107] This was experimentally determined through the use of model mixtures where the potency of each constituent was known.[107] The harmonic mean is calculated as the reciprocal of the arithmetic mean of the reciprocals:

$$Harmonic\ mean = \frac{n}{\left(\frac{1}{EC_{50}A} + \frac{1}{EC_{50}B} + \cdots + \frac{1}{EC_{50}X}\right)}$$

The overall potency is "weighted" towards the most potent compounds. What is concluded from this experiment is the overall potency observed for a large mixture of compounds containing potent, moderate, and inactive compounds can be attributed to mainly the most potent compounds.

Further Illustration of Mixture-Based Positional Scanning

This key conclusion allows for the development of mixture-based positional scanning libraries. In these libraries, compounds are synthesized around a common core with several points of diversity, and within each mixture one sidechain at a particular point of diversity is constant. Figure 2-9, adapted from Drug Discovery Today,[108] illustrates this principle. In this case, the scaffold is a tripeptide, there are four amino acid building blocks (A,R,T,W), and it is assumed the only active peptide has the sequence RAT. With mixture-based positional scan assays, all 64 possible tripeptides (4^3) in 12

mixtures (4+4+4), and the mixtures which produce a signal would be the mixtures with R in the first position, A in the second position, and T in the third position. The active mixtures have biological activity since the RAT tripeptide can be found within each mixture (Figure 2-9). In practice there are often active mixtures at each of the positions for a given scaffold; and therefore, linear combinations of the active mixture sequences are used to construct a list of sequences which will be synthesized as individual compounds for the deconvolution of the mixture-based positional scan.

An alternate approach to better understand mixture-based positional scanning is by looking at how each mixture is synthesized. Figure 2-10 illustrates how the mixtures are synthesized. For this example, we want to synthesize a mixture of tripeptides that contains an Arg at the first position and then a mixture of all of the selected building blocks at positions two and three (R-X-X). A polystyrene teabag of resin is activated and a mixture containing all of the building blocks is coupled. After the reaction is completed the peptide mixture is deprotected and again a mixture of building blocks is coupled. Following this reaction is another deprotection and coupling reaction, only this time the coupling solution only contains Arg. Following this final coupling, the mixture of peptides is cleaved and the result is a mixture of tripeptides where Arg is at the first position and the second and third positions represent mixtures of all of the building blocks (peptides are synthesized from C to N termini, yet standard convention dictates peptide sequences are reported from N to C termini).

One question a researcher may ask is do the mixtures represent equal molar quantities of each constituent? The short answer is yes, in theory. We would predict building blocks which are sterically less hindered, for example glycine, would react faster

than building blocks which are bulkier, something such as phenylalanine. Since this is the case, the coupling mixtures of building blocks are formulated to contain equal reactive mixtures of building blocks and not necessarily equal molar quantities of each building block. Chemical methodology studies have been performed so coupling mixtures containing the common amino acids may be quickly formulated.[109-112]

The benefit of this approach is (1) reduction of the number of wells required to assay a large number of compounds, especially for very large libraries, and (2) rapid development of an SAR about a particular target since all possible combinations are examined. Since the primary contribution to the potency of an active mixture can be attributed to a single compound and not the additive effect of many moderately potent compounds, linear combinations of active mixtures can be used to create a list of sequences for individual compounds which will be synthesized and assayed.

Translation to Therapy

As already stated, this combinatorial technology has been applied to study numerous disease states, and it has now been employed in the field long enough to begin to see results being translated into promising novel therapies. There has been particular successful in the area pain management. Historically, the gold standard for analgesia are the opiates. These compounds have varying pharmacology at the μ, κ, and δ receptors, and although they are effective analgesics, they have numerous undesirable side effects including CNS depression and tolerance.[113] Furthermore they have a high propensity for abuse.[113] A different approach to solving this problem is the development of peripherally-selective compounds (avoiding CNS side effects) which are selective for specific opiate receptor subtypes (avoiding side effects such as constipation which is resultant of μ

activation).[114] A κ agonist compound is therefore of interest since it could be used therapeutically for analgesia, yet it would be devoid of the deleterious side effects dysphoria and sedation.[114-115] A successful collaboration using mixture-based positional scanning as a starting point in the identification of new ligands has resulted in a κ selective ligand which has completed phase 2 clinical trials (clinical trials.gov identifier NCT00877799).

A mixture-based positional screening library of tetrapeptides, constructed from 50 distinct amino acid building blocks resulting in a total diversity of 6,250,000 compounds, was assayed at the μ, κ, and δ opioid receptors.[116] Upon library deconvolution and subsequent synthesis of individual peptides, selectivity was achieved for each of the receptor subtypes,[116] and subsequent binding studies on the peptide DPhe-DPhe-DNle-DArg-NH_2 (FE200041) in an *in vitro* radiolabeled binding experiment with the cloned human opiate receptors indicated a selectivity greater than 30,000-fold for κ/μ or κ/δ.[117] Further development by Ferring Research Institute Inc. (San Diego, CA) in partnership with TPIMS yielded two C terminal functionalized analogs, pyridin-4-yl methanamine (FE200665) and morpholine (FE200666), resulting in an even greater selectivity profile with κ/μ/δ selectivity profiles of 1/16,900/84,600 and 1/88,600/>1,250,000, respectively.[103] It was also observed and interpreted as greater peripheral selectivity (i.e. not CNS penetrant), the dosage to induce centrally-mediated effects of sedation/impairment was 182-fold greater than the dosage needed for antinociception.[103] The FE200665 (CR665) is now being further developed by Cara Therapeutics (Shelton, CT), and they are now researching closely related peptide H-DPhe-DPhe-DLeu-DLys-[ω(4-aminopiperidine-4-carboxylic acid)]-OH (CR845).[118] Intravenous formulations have

proven safe and efficacious in phase 2 clinical trials for acute postoperative pain (clinical trials.gov identifier NCT00877799) and there is an ongoing phase 2 study looking at the safety and efficacy of oral formulations for osteoarthritis of the hip or knee (clinical trials.gov identifier NCT02524197).

These positive results in the clinic demonstrate the therapeutic potential for the mixture-based positional scan paradigm in the development of new peptide leads which can translate into viable therapies. Both the opiate and melanocortin receptors are peptide-mediated rhodopsin-like, class A, GPCRs that share the common POMC endogenous signaling precursor. Given the similarities between the two families of receptors, it was hopeful a mixture-based positional scanning could lead to the identification of a selective MC3R, over the MC4R, peptide sequence for the treatment of energy homeostasis disorders.

Synthesis of Mixture-Based Positional Scanning Libraries in Practice

Libraries of compounds can be rapidly synthesized using standard solid-phase chemistry using Houghten's tea bag approach.[105] This approach has been applied to peptides and other scaffolds which can be readily synthesized with very high-yielding reactions that are amenable to solid-phase synthesis. Examples of different scaffolds include: tetrapeptides[28], cyclic guanidines[119], conotoxins[120], piperazines[121], and triamines.[121]

In a mixture-based positional scanning library, each building block (e.g. amino acid) is sampled at each position while the rest of the positions along the scaffold are varied so they contain all possible combinations of all the selected building blocks. The total number of compounds represented in the library is the product of the number of

building blocks at each position along a scaffold (# of building blocks at position 1 x # of building blocks at position 2 x … x # of building blocks at position n) whereas the number of mixtures is simply the sum of the building blocks at each position (# of building blocks at position 1 + # of building blocks at position 2 + … + # of building blocks at position n). The use of solid phase methodology allows for the rapid synthesis of these chemical libraries.

As described in the beginning of this chapter, synthesizing a compound using solid-phase synthesis uses an iterative deprotecting, washing, coupling, and washing process for the synthesis of individual compounds. The synthesis of large mixture-based libraries is not fundamentally different from the synthesis of individual compounds. Important to library construction is the optimization of the chemistry. This may be more critical than with the synthesis of individual compounds since the incorporation of reagent mixtures into a growing scaffold could exponentially insert unwanted side reactions into millions of analogs. Mixtures of building blocks are reacted in quantities such that the resulting mixture of compounds have equimolar incorporation of each building block. The ratio of reagents is determined by measuring their relative activity and then mixing them in ratios which are inversely proportional to their reactivity; that is to say, a faster reacting building block will be a relatively smaller constituent in the reagent mixture than a slower reacting building block.[109-112] The tea bag method allows for nearly all of the chemistry to be performed in parallel. The cleavage of the compounds is also done in parallel and the mixtures are generally assayed as crude mixtures; a consideration which becomes important in assay selection.

Screening

Any chemical library that is not compatible for biological analysis cannot be utilized from a drug discovery standpoint. Luckily, as reviewed in the literature, mixture-based positional scanning has been used in a variety of biological targets with a variety of biological assays.[122] This is an indication of the robustness of this technology. The Haskell-Luevano laboratory has used these combinatorial libraries in conjugation with the live whole cell colorimetric β-galactosidase CRE reporter gene assay in a 96-well format.[28, 123] The assay is typically performed as a two-point dose response for each mixture to reduce the rate of false positives. An advantage to this assay is in addition to assessing intracellular cAMP accumulation, the health of the cells can also be assessed for each individual well. This is important because some types of the compounds kill the cells at the concentrations at which they are assayed. This is a gain-of-function experiment as well, therefore, cell death equates to no signal.

Data Handling and Library Deconvolution

It will become apparent in later chapters that the amount of data produced by this technology is large and organizational skills are a necessity. However, relative to the number of compounds assayed, the amount of data is relatively minimal. The lead tetrapeptide introduced in Chapter 4 used a mixture-based positional scanning library (TPI924) to identify it. Briefly, the library consisted of a tetrapeptide scan consisting of 60 amino acid building blocks at each position representing more than 12 million compounds, yet the all of the compounds fit into less than three 96-well plates. The same library was used in the previously mentioned proof-of-concept study demonstrating the compatibility of this technology with the melanocortin receptors, and the table of

contents graphic illustrates (Figure 2-11) the type of data which the assay produces.[28] Along the x-axis is each of the amino acid building blocks that were scanned while the y-axis is the relative activity for each mixture. After setting an appropriate cut-off point, the "hit" mixtures can then be identified. The construction of data matrixes and plots, using data visualization software such as Spotfire, can prove useful to see trends in the data. There are also useful features within Excel, such as pivot tables and plots, which are convenient for data visualization and analysis.

The data produced by a mixture-based positional scan indicates what residues and functionalities are important at specific positions along a scaffold. It could be thought of an SAR analysis, although the data for the mixtures of compounds and the library must be deconvoluted through the synthesis of individual compounds to confirm the SAR. There are several approaches which may be employed. Two distinct approaches our lab has used to deconvoluted a mixture-based positional scan include performing a single-residue replacement about a known tetrapeptide sequence, resulting in a biased library, in addition to synthesizing new unbiased libraries of tetrapeptides which use combinations of the "hit" mixtures.[28]

Use of This Combinatorial Technology within this Dissertation

This combinatorial technology was used throughout the studies reported within this dissertation, and a general workflow can be compartmentalized into three areas of study each with their own unique features and challenges (summarized in Figure 2-12). The discovery of mMC3R selective tetrapeptide sequences, starting in Chapter 4, begins with the identification of a new sequence, followed by a mixture-based positional scan about the peptide. The final variation on this combinatorial technology is discussed in

Chapter 6. This chapter consists of two separate vignettes both using mixture-based positional scanning. The first section discusses an effort to identify selective melanocortin peptidomimetics while the second is a decapeptide screen on the human MC4R. Results from the decapaptide screen are being used to identify previously unknown endogenous modulators.

Conclusions

This chapter discussed the general methodologies that were used in this dissertation. Solid-phase synthesis is a well-suited method for synthesizing libraries of individual compounds, and I am indebted to the chemists and the wide breadth of their methodology studies which have matured the field of peptide chemistry such that it is relatively routine to synthesize compounds. Mixture-based positional scanning was also discussed. This technology is a novel way of evaluating exceedingly large libraries of compounds (millions of compounds) in a relatively short amount of time (within a PhD project timeline).

Chapter 2 Tables and Figures:

Table 2-1: Standard Coupling Conditions

Amino Acid	AA Eq.	HBTU Eq.	DIEA Eq.	Microwave Conditions
Arg	5.1	5.0	7.0	75°C, 30W, 10 min
Cys or His	3.1	3.0	5.0	50°C, 30W, 5 min
All others	3.1	3.0	5.0	75°C, 30W, 5 min

The standard coupling conditions used in the solid-phase synthesis of peptides using microwave assistance can be categorized into three categories for all 20 of the natural amino acids. Arg is typically the hardest amino acid to couple, therefore it uses the highest equivalents in addition to longest reaction times. Cys and His are more sensitive to side reactions so the reaction temperature is kept minimal. The last group containing all of the other amino acid residues uses reaction conditions that were optimized by the Haskell-Luevano laboratory to efficiently couple the residues in a reasonable amount of time.

Figure 2-1: Synthetic Approach for Solid Phase Synthesis

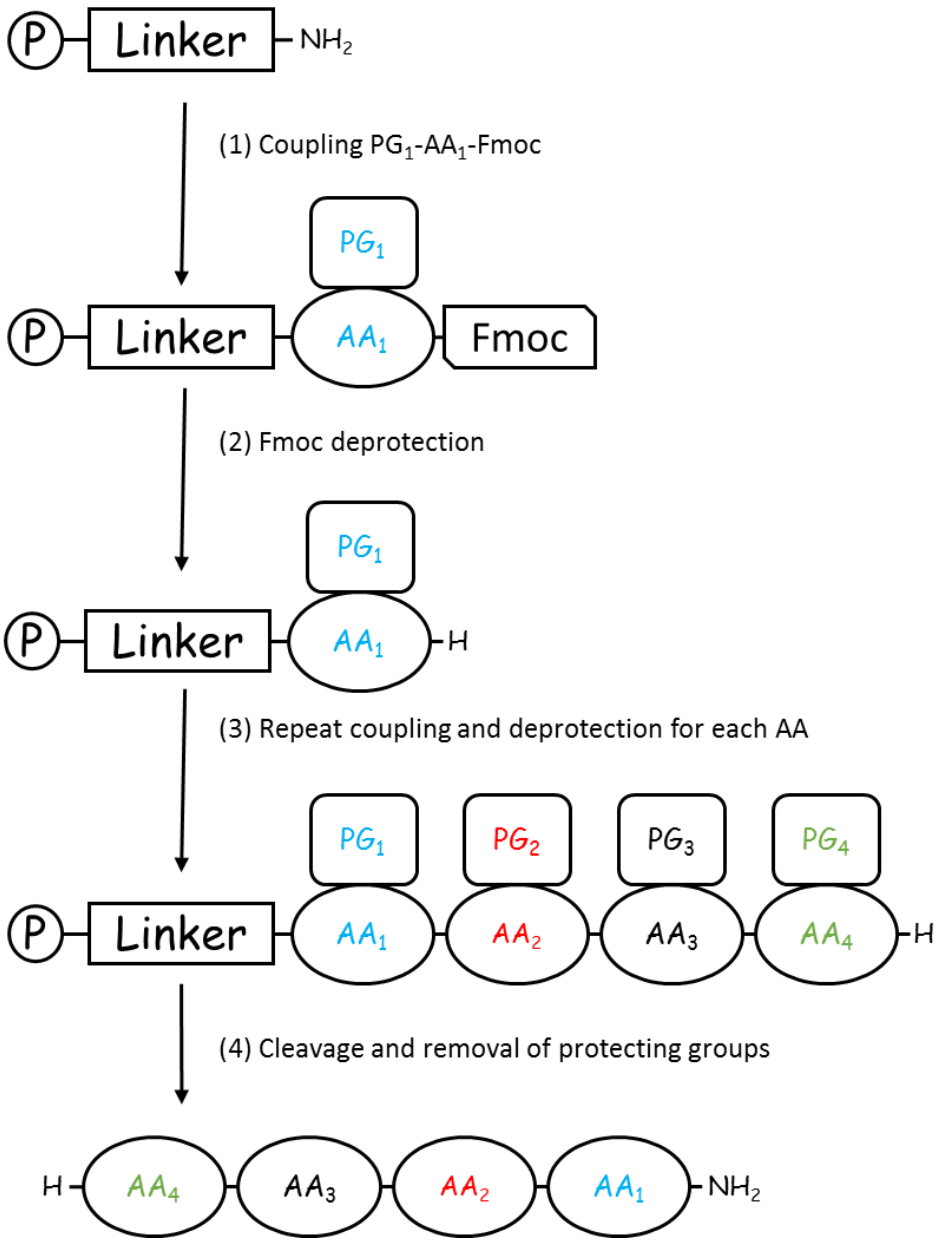

Conceptually, peptides are synthesized attached to a solid support. The peptides are synthesized in a stepwise manner, using protected amino acids, where successive coupling and deprotecting reactions allow for the sequence to grow starting from the C termini (in this case it is a carboxamide) to the N termini. The final cleavage removes the peptide from the solid support and removes the sidechain protecting groups.

Figure 2-2: Rink Amide p-Methylbenzhydrylamine (MBHA) Resin

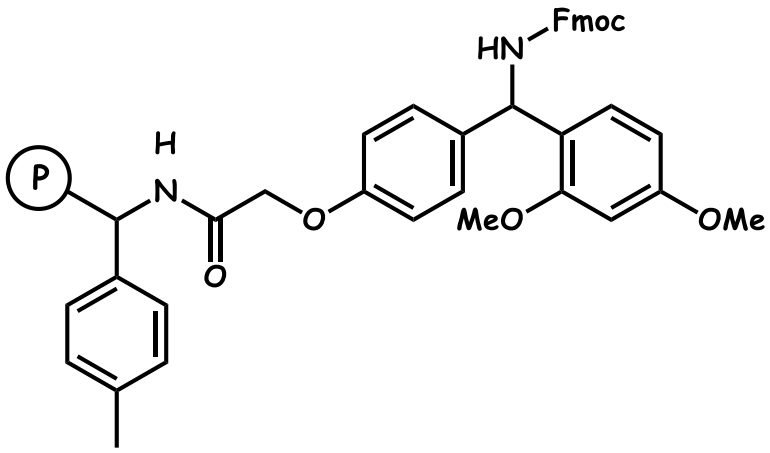

All of the individual peptides synthesized contain an amidated C terminal. This modification was achieved through the use of Rink amide MBHA resin (is commercially available and sold as Fmoc protected), which contains an acid labile linker.

Figure 2-3: Proposed Mechanism for the E1$_{CB}$ Nα-Fluorenylmethyloxycarbonyl Deprotection

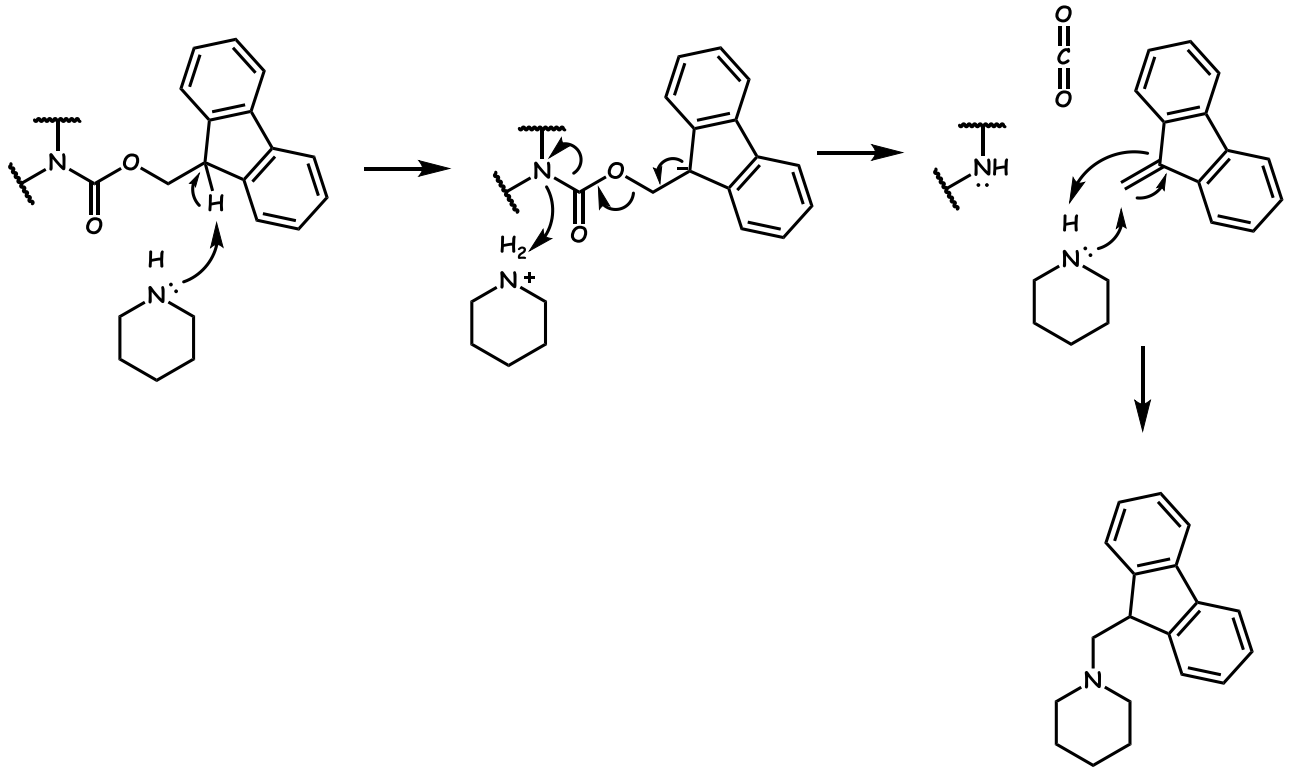

Illustrated is the proposed mechanism for the removal of the Nα-Fmoc protecting group via piperidine to yield a amine which can be subsequently coupled to an additional residue.

Figure 2-4: Aspartamide and Pyroglutamic Acid Formation and Side Reaction Products

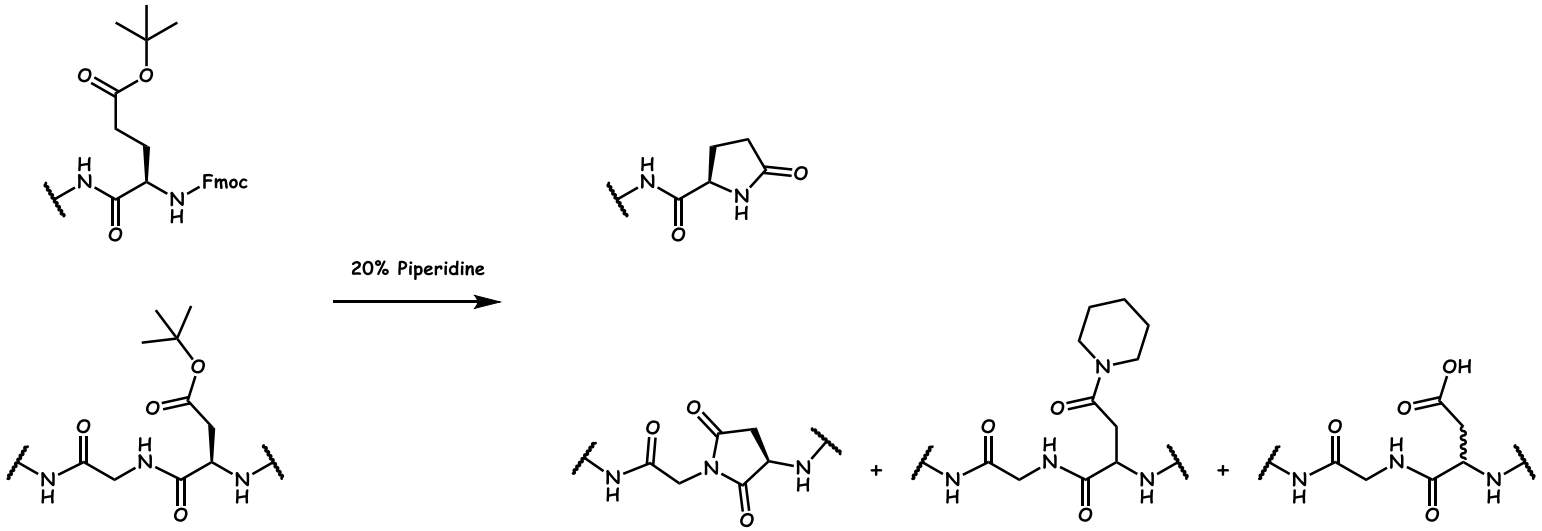

Glutamic acid and the dipeptide sequence glycine-aspartic acid are susceptible to an undesirable side reactions with piperidine when the peptide is being deprotected.

Figure 2-5: Common Sidechain Protecting Groups

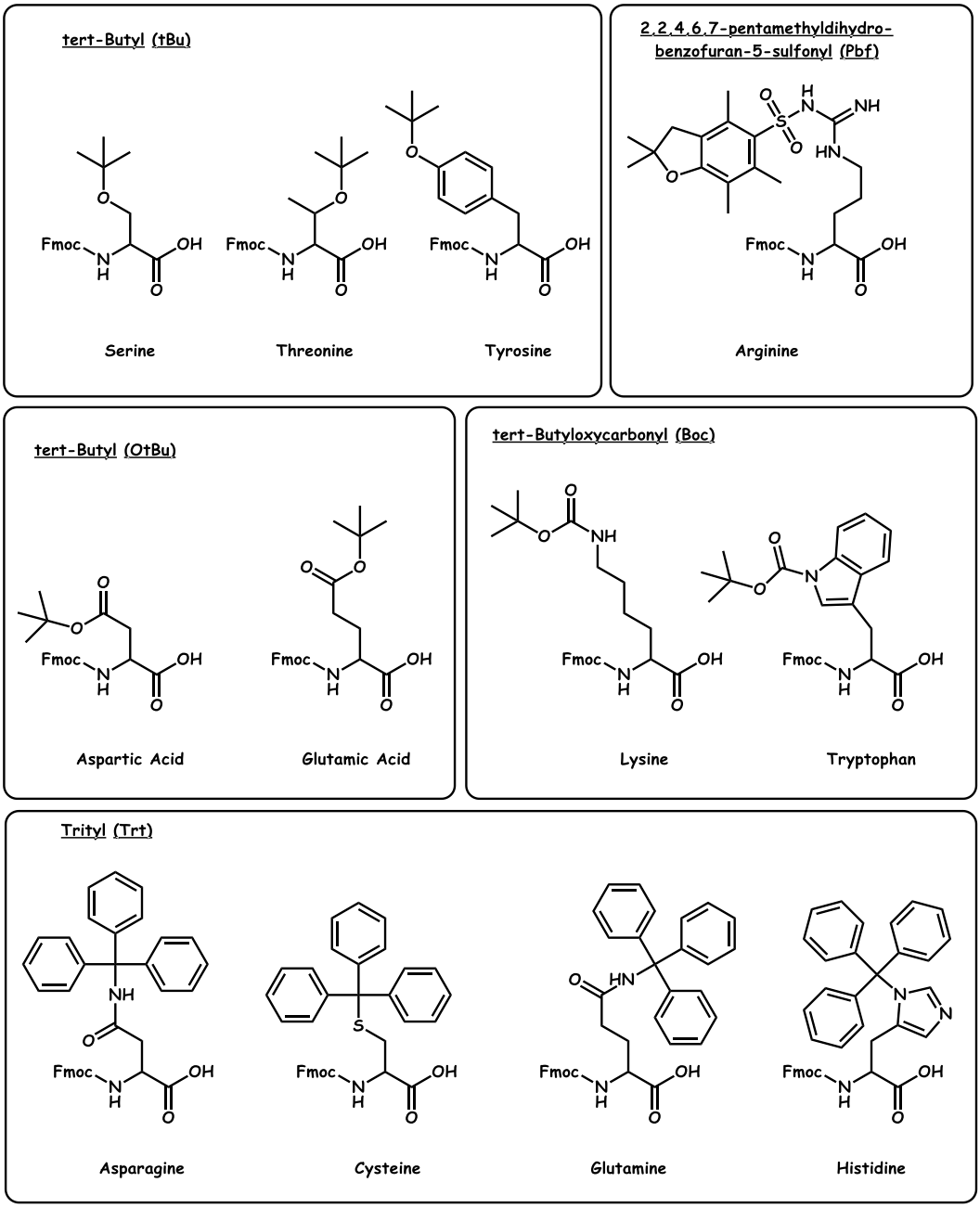

The natural amino acids that require sidechain protection illustrated with the acid-labile protecting groups that are compatible with standard Fmoc chemistry which was utilized in the synthesis of the individual peptides reported.

Figure 2-6: Carboxylic Acid Activation and Amide Bond Condensation Mechanism

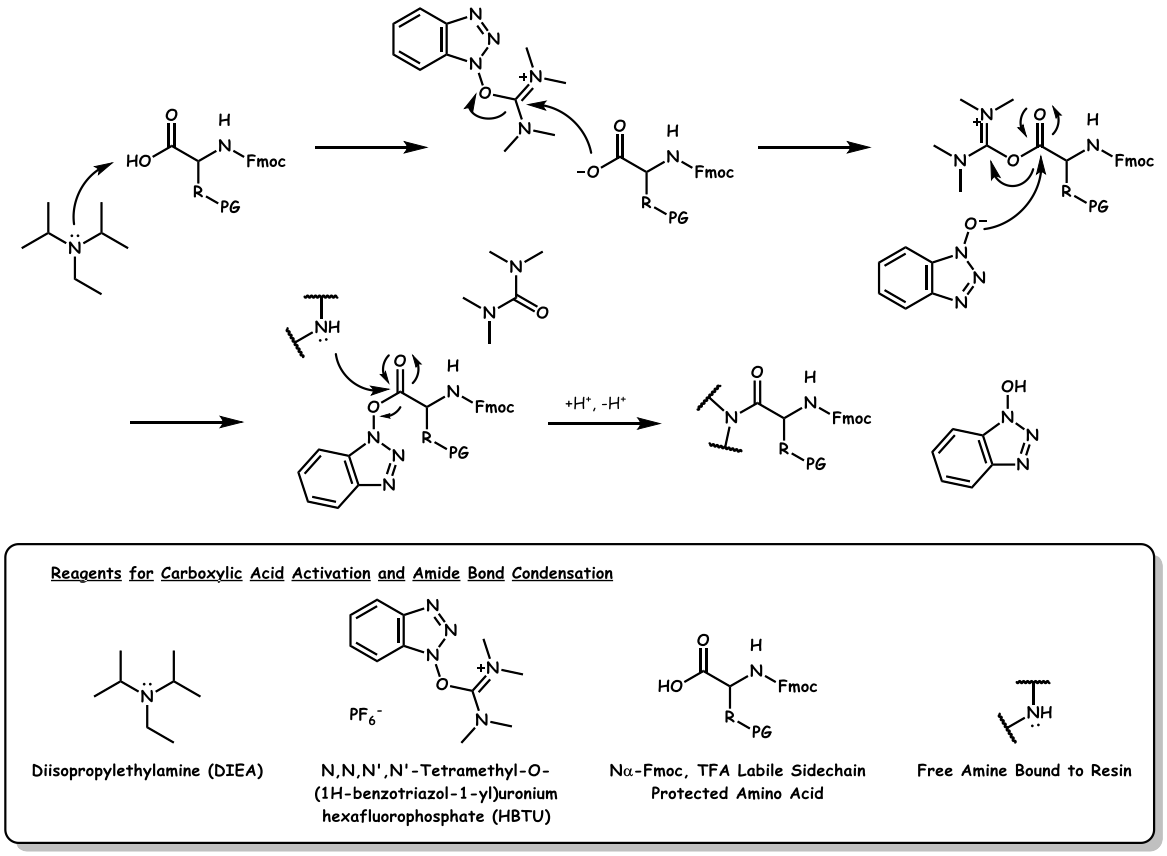

Illustrated is the proposed two-step mechanism for carboxylic acid activation using HBTYU/DIEA coupling conditions

Figure 2-7: Proposed Mechanism for Ninhydrin Test for Primary Amines

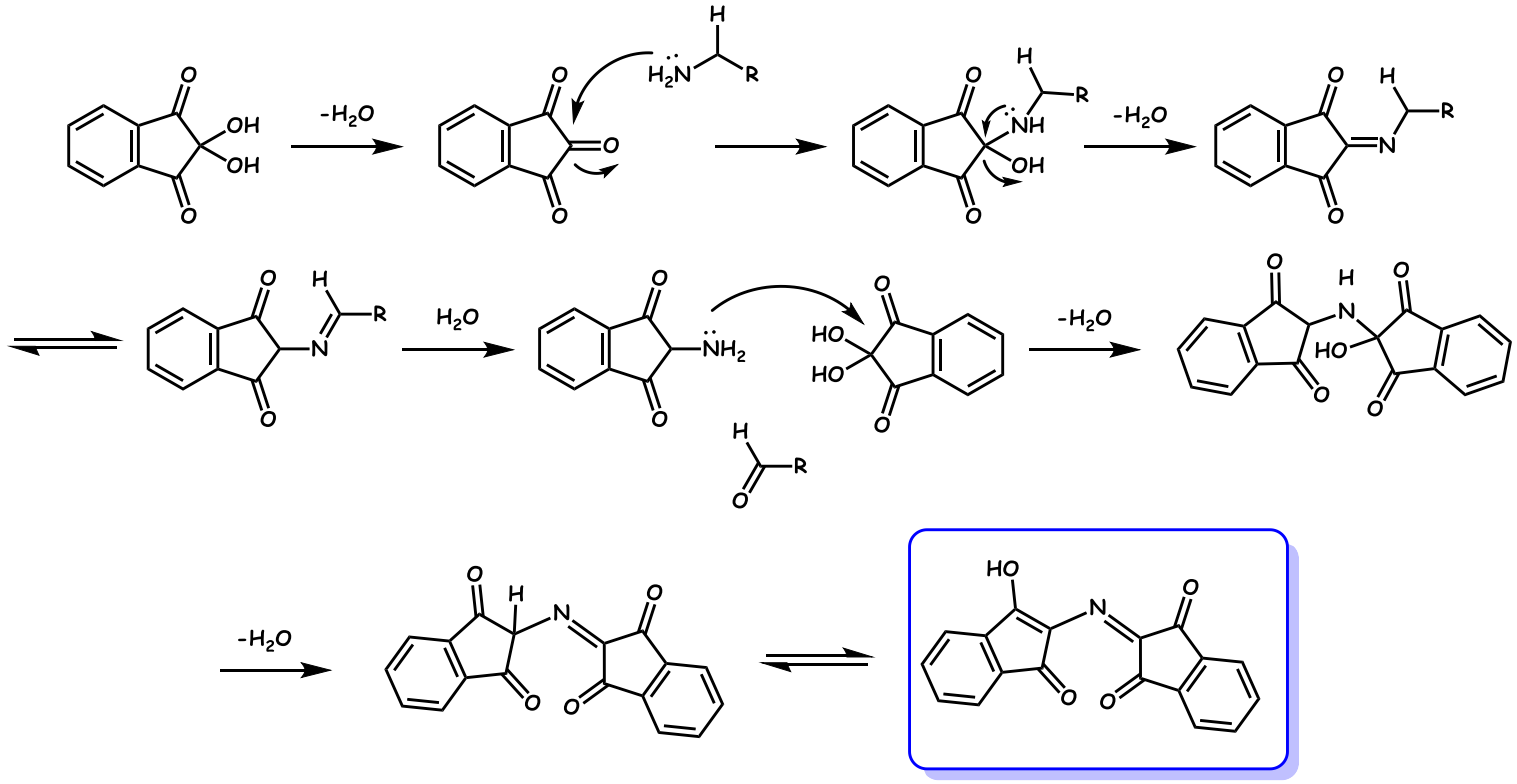

Illustrated is the proposed mechanism for the ninhydrin (Kaiser) test for a free primary amine.

Figure 2-8: Proposed Mechanism for Chloranil Test

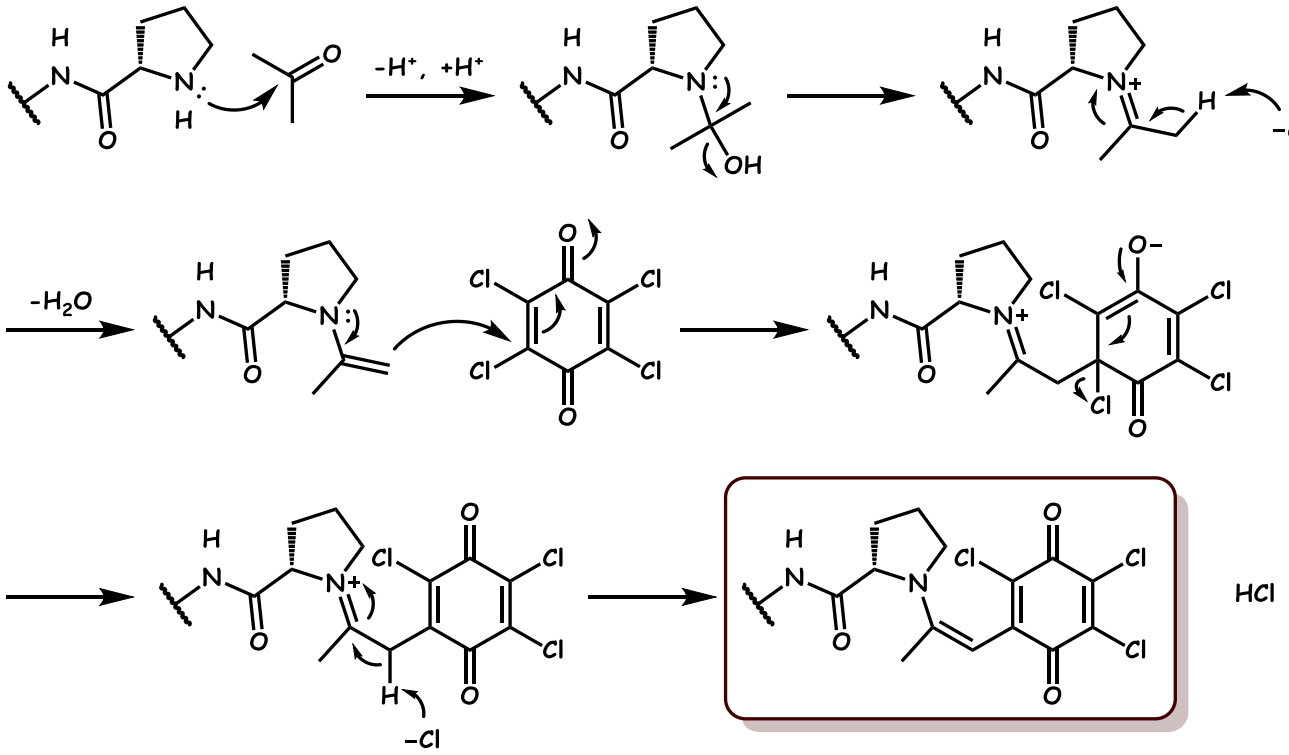

Illustrated is the proposed mechanism for the chloranil test that was employed for the detection of a free secondary amine. The reaction mechanism rationalizes why only the resin, as opposed to the solution, turns color.

Figure 2-9: The Fundamentals of Mixture-Based Positional Scanning

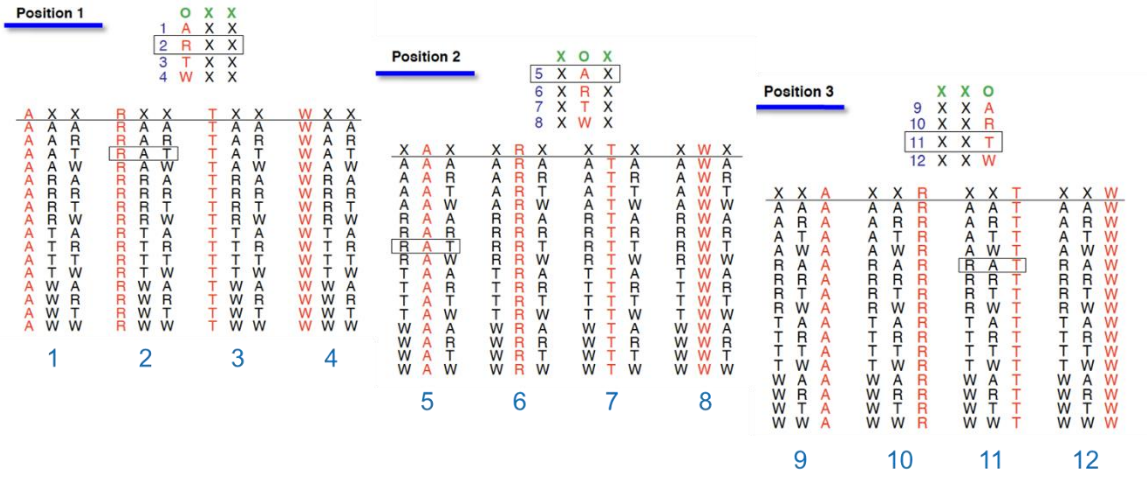

Mixture-based positional scanning is a high throughput method which is well suited for peptides. In each mixture one amino acid is held constant and the remaining residues are varied to contain each of the desired building blocks. Above illustrates an example for a tripeptide with four amino acid building blocks (R, T, A, and W) at each position.[108] If the "hit" compound had the sequence R-A-T, then wells 2, 5, and 11 would indicate a positive result in the assay since that peptide is represented in each mixture. Following the primary screen, the mixture-based positional scanning library would have to be deconvoluted and the individual compound would have to be synthesized and subsequently assayed. The image was adopted from Drug Discovery Today[108] and written permission for reuse in this dissertation was obtained May 2, 2016 from Elsevier via RightsLink® license number 3860841295998.

Figure 2-10: Overview of Mixture Based Positional Scanning Synthesis

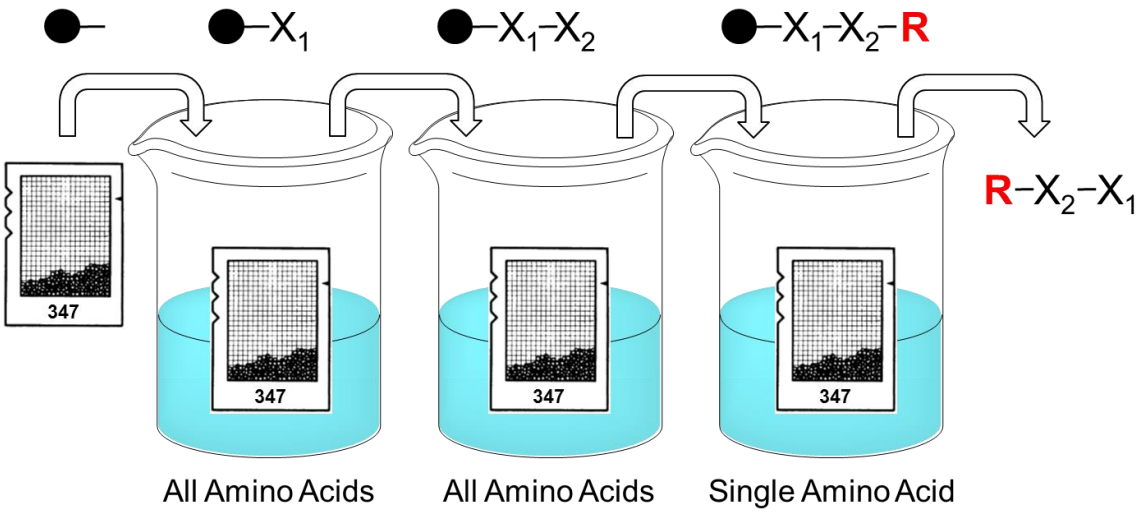

A conceptual illustration of using SPPS to construct mixtures which are used in mixture-based positional scanning combinatorial libraries.

Figure 2-11: Example of data collected with a mixture-based positional scanning library

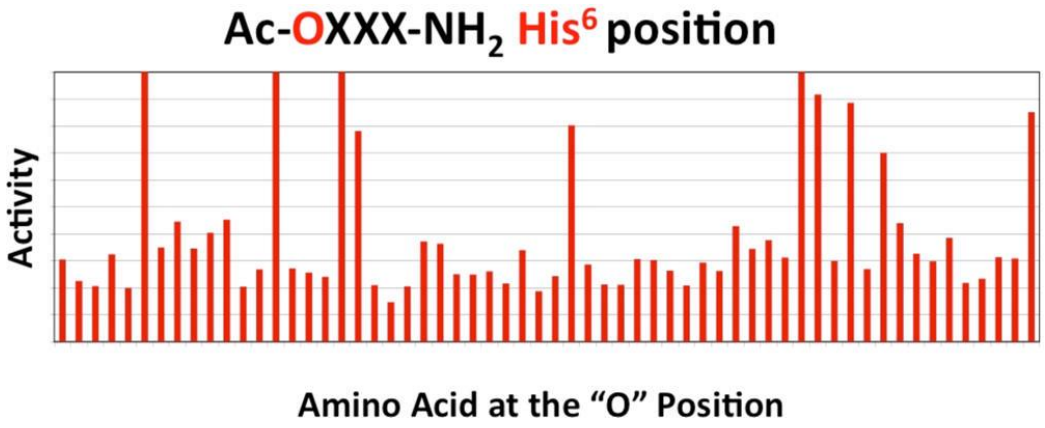

This illustrates the type of data which is expected from a mixture-based positional scan. Along the x-axis is each of the amino acid building blocks that were scanned while the y-axis is the relative activity for each mixture. This graphic is adapted from a published ACS journal article http://pubs.acs.org/doi/abs/10.1021/jm500064t with a standard ACS AuthorChoice/Editors' Choice usage agreement and, "This is an unofficial translation of an article that appeared in an ACS publication. ACS has not endorsed the content of this translation or the context of its use."

Figure 2-12: Workflow for the Discovery of Ligands Using a Mixture-Based Positional Scanning Approach

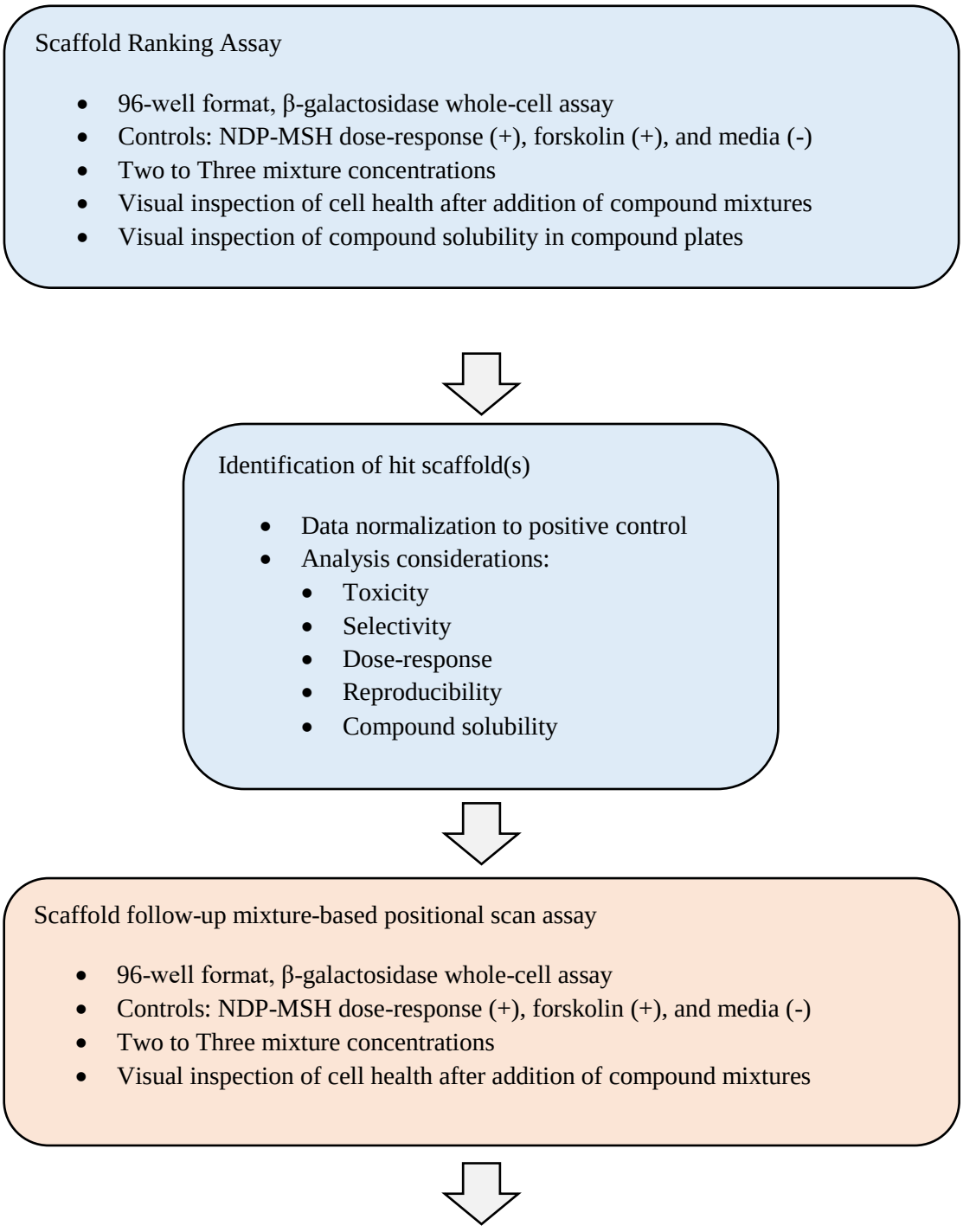

Identification of hit side-chains and positions

- Data normalization to positive control
- Rank according to potency
- Analysis considerations:
  - Toxicity
  - Selectivity
  - Dose-response
  - Reproducibility
  - Compound solubility

Selection and synthesis of individual compounds

- Based on selected side-chain and position hits
- Two possible approaches for library construction
  1. Make a combinatorial library from selected side-chain and position hits yielding a totally unbiased library (e.g. If scaffold has three points of diversity and R_1 = 3 hits, R_2 = 3 hits, R_3 = 4 hits; then the total library consist of 3x3x4 = 36 compounds)
  2. Make a library of analogs based on a known ligand which uses the selected scaffold (e.g. A library of single-point substitution analogs based on the melanocortin tetrapeptide Ac-His-DPhe-Arg-Trp-NH_2)

Function and binding testing and analysis of individual compounds

1. Screen for functional activity and selectivity via 384-well ALPHA (Perkin-Elmer) screen
2. Select desired hits (considering selectivity and potency) and assay for functional activity and selectivity via the orthogonal 96-well β-galactosidase assay
3. Assess desired hits for binding activity via an I^{125} labeled NDP-MSH competitive binding experiment

The use of mixture-based positional scanning is useful in the identification of new ligand scaffolds and unique compounds with desired pharmacological profiles. This type of high-throughput campaign begins with the identification of a scaffold(s), followed by the mixture-based positional scanning, and last, followed by the synthesis and evaluation of discrete compounds. Special consideration is given to matching the assay to the type of library which is being tested. This type of high throughput campaign has a high attrition rate, and therefore allows for the rapid evaluation of millions of compounds.

Chapter 3

Identification of Clean Melanocortin-3 Receptor Antagonists Based on the Classic "HFRW" Signaling Motif

All peptides were synthesized, purified, and characterized by Skye Doering under the supervision of Carrie Haskell-Luevano. Lead peptide was identified by Dr. Aleksandar Todorovic, a previous graduate student in the Haskell-Luevano laboratory. Functional assays were performed by Skye Doering, and function assay data analysis was done by Carrie Haskell-Luevano and Skye Doering. This study was published in ACS Medicinal Chemistry Letters (DOI: 10.1021/ml500340z). The published article is provided by the ACS http://pubs.acs.org/doi/abs/10.1021/ml500340z under the terms of the standard ACS AuthorChoice/Editors' Choice usage agreement and, "This is an unofficial translation of an article that appeared in an ACS publication. ACS has not endorsed the content of this translation or the context of its use." The last section of this chapter "Future Directions and Preliminary Feeding Studies" briefly discusses an animal study conducted which was performed by Cody Lensing, Danielle Adank, and Stacey Wilber under the supervision of Carrie Haskell-Luevano.

Introduction

Briefly, as already discussed, the melanocortin receptors are seven transmembrane spanning α-helical GPCRs that signal through Gs to increase the amount of intracellular cAMP.[8-13, 124] Five melanocortin receptors have been cloned to date. The

MC1R is found primarily in the skin and regulates skin pigmentation. The MC2R is a key component in steroidogenesis and only responds to ACTH. Both the MC3R and MC4R are expressed within the central nervous system and are involved in energy and weight homeostasis.[10-11, 13] The MC4R has been more extensively studied than the MC3R in the field of obesity, and SNPs of the hMC4R account for one of the largest monogenic determinants of obesity.[4] It has been demonstrated that mMC3R and mMC4R agonist ligands reduce food intake, while antagonist ligands at these receptors result in increased food intake upon central administration.[44] The use of selective MC4R agonists induce hypertension through a MC4R mediated process, which is currently not completely understood.[75] Therefore, targeting the MC3R selectively may be a more suitable for energy homeostasis therapies, yet very few selective and "clean" MC3R ligands exist in the field, which can be used to fully elucidate the receptor function. The melanocortin-5 receptor (MC5R) is implicated in exocrine gland function in mice with other physiological functions unknown.[23]

Previous Studies Based on the Classic "HFRW" Signaling Motif

All of the melanocortin receptor subtypes are stimulated by a series of endogenous peptide agonists that are derived from the POMC protein.[125] The POMC derived α-, β-, and γ- MSH bind to and only stimulate the MC1R, MC3R, MC4R, and MC5R subtypes, while ACTH has activity at all five of the melanocortin receptor subtypes. Since the MC2R is only stimulated by the ACTH peptide and not any

melanocortin-based tetrapeptides, it has been excluded from this study. The MSH hormones contain a highly conserved His-Phe-Arg-Trp motif.

Extensive truncation and SAR studies have identified this as the core melanocortin messaging sequence.[35] Multiple studies on the SAR of the tetrapeptide Ac-His-DPhe-Arg-Trp-NH_2 using single substitution strategies have been reported by our group.[55-58, 61-62, 64, 66] Similar work has been reported by others studying a linear pentapeptide template for receptor selectivity and potency.[126-127] There have been numerous additional studies with cyclic templates targeting the melanocortin receptors. On the basis of these previous studies, a simultaneous double substitution study was conducted around this tetrapeptide scaffold by Todorovic et al.[128] The substituted residues had been previously identified as important in dramatically altering potency and the mMC3R and mMC4R selectivity profiles.[55, 57] Some of these substitutions, such as a DPhe to (pI)DPhe, switched the pharmacology of the ligands from agonist to antagonist at the mMC3R.[57, 66]

Antagonist Library Design and Rationale

Results from single position scanning studies can be used in double substitution strategies to discover potent, selective, and pharmacologically unique ligands. The concept for this strategy is based upon the hypothesis that additive combinations of substitutions identified in single position scanning studies may produce ligands resulting in distinct pharmacological profiles. Conversely, the possibility of distinct pharmacological profiles may result and be different than simply the additive effect of the

single substitutions. The double substitution strategy herein, of the tetrapeptide template, led to the identification of lead compound SKY2-23-7, Ac-Trp-(pI)DPhe-Arg-Trp-NH_2.[128] This compound had micromolar full agonist activity at the mMC1R and mMC5R with competitive antagonist activity at both the mMC3R and mMC4R (pA_2 = 5.4 and 7.8, respectively). What is unique about this compound, however, is that it possessed only minimal agonist activity at 100 μM concentrations at the mMC3R (Figure 3-1).

A survey of human and mouse MC3R and MC4R antagonists, particularly the SHU9119 ligand[52] used extensively for in vivo physiological studies, reveals the in vitro pharmacological profile of an MC4R competitive antagonist with no partial agonist activity; however, at the MC3R, partial agonist activity is observed in addition to the competitive antagonism. Figure 3-1 illustrates the antagonist/partial agonist pharmacological profile of SHU9119 at the mMC3R and mMC4R. The SHU9119 ligand displays competitive antagonist activity at both receptor subtypes, in addition to partial agonist activity, approximately 50% of maximum response, at the mMC3R subtype. The SHU9119 ligand has also been used for in vivo feeding studies and demonstrated an ability to significantly induce feeding in mice.[44] Because of the mixed partial agonist/antagonist MC3R pharmacology of ligands like SHU9119, unless melanocortin receptor knockout mice are used in conjunction with such mixed antagonist ligands, deconvolution of the physiological behavior becomes confounding. Thus, the discovery of molecular probes that are "clean" mMC3R and mMC4R antagonists, lacking any partial agonist activities, are still needed in the field.

On the basis of this unmet need and the discovery of this novel tetrapeptide template possessing these mMC3R and mMC4R antagonistic pharmacological profiles, additional SAR studies of this Ac-Trp-(pI)DPhe-Arg-Trp-NH_2 template are described herein. With this template, the Trp^1 position is held constant, and the Trp^4 position is substituted with the following six tryptophan side chain modifications: Phe, β-(3-benzothienyl)-alanine (3Bal), tetrahydroisoquinoline (Tic), (2-naphthyl)-alanine [Nal(2′)], DNal(2′), and 4-4′-biphenylalanine (Bip) (Figure 3-2). It was hypothesized that, by performing this SAR, potency and selectivity profiles at the mMC3R and mMC4R could be explored with the goal of retaining the unique antagonist pharmacology at the mMC3R observed for the compound Ac-Trp-(pI)DPhe-Arg-Trp-NH_2.

We selected to screen the library at the mouse melanocortin receptors since these *in vitro* results can be readily translated to the *in vivo* knockout mouse models our laboratory routinely uses to further develop our understanding of the role the melanocortin receptors play in energy homeostasis.[44] We speculate the results from this study identifying ligands for the mouse melanocortin receptors would have similar pharmacological profiles when assayed at the human melanocortin receptors; however, this would need to be verified experimentally. Generally, the potency and selectivity profiles observed for peptidic ligands assayed at the mouse melanocortin receptors have been reported in the literature to possess similar SAR profiles at the human receptors. This is supported by data reported by numerous studies including both MC4R peptide ligand SAR as well as receptor mutagenesis studies. The melanocortin agonist MTII has single digit nM potencies when assayed at the hMC3R, hMC4R, and hMC5R is

comparable to the subnanomolar potencies reported herein.[83] The MC3R/MC4R antagonist SHU9119 has comparable pA_2 values at the hMC3R and hMC4R (pA_2 = 8.3 and 9.3, respectively); in addition, partial agonist activity is also observed at the hMC3R when SHU9119 is assayed alone.[52] The tetrapeptide Ac-His-DPhe-Arg-Trp-NH_2 has been used in previous studies probing the function of the human MC4R, and the EC_{50} determined for the mouse MC4R in this study is comparable to the human receptor subtype.[27, 53-54]

Results and Discussion

Table 3-1 summarizes the agonist receptor pharmacology at the mMC1R and mMC5R subtypes, and Table 3-2 summarizes the agonist and antagonist pharmacology at the mMC3R and mMC4R subtypes. Compound SKY2-23-7 possessed micromolar full agonist potency at the mMC1R and mMC5R. At the mMC3R, SKY2-23-7 is a micromolar antagonist with minimal agonist activity at 100 μM concentrations and a nanomolar mMC4R antagonist (Figure 3-1). This feature is unique to the field since mMC3R mixed partial agonist/antagonist pharmacology is commonly observed for peptides that function as dual mMC3R/mMC4R antagonists. A representative example of this type of mixed pharmacology can be seen with the tetrapeptide Ac-His-(pI)DPhe-Arg-Trp-NH_2 and illustrated with the SHU9119 mMC3R/mMC4R antagonist in Figure 3-1.[52, 55, 66] Previous SAR studies of the tetrapeptide template substituted at the Trp^4 position resulted in the identification of amino acids at this position that modified MC3R potencies and receptor selectivity profiles; thus, these amino acid modifications (Figure

3-2) were incorporated into the lead template herein in attempts to increase receptor potency and selectivity while probing the Trp^4 side chain moiety.

Substitution at the Trp^4 position on the tetrapeptide template SKY2-23-7 herein yielded flat SAR at the mMC1R and mMC5R subtypes with full agonist ligand potencies in the micromolar range. At the mMC3R and mMC4R subtypes, more varied SAR resulted. Tetrapeptide SKY2-23-1, containing the Bip^4 (4-4′-biphenylalanine) residue, resulted in 10-fold decreased agonist potency at the mMC1R while maintaining equipotent agonist activity at mMC5R, as compared to SKY2-23-7 and within the 3-fold inherent experimental error associated with this assay in our hands. Compound SKY2-23-1 did not possess agonist or antagonist activity at the mMC3R at up to 100 μM concentrations but was a 480 nM mMC4R antagonist, albeit 30-fold less potent than SKY2-23-7. Peptide SKY2-23-2, containing the 3Bal [β-(3-benzothienyl)-alanine] sulfur analogue of Trp, resulted in 4-fold to 8-fold decreased agonist potency at the mMC1R and mMC5R respectively, compared to SKY2-23-7. Compound SKY2-23-2 did not stimulate or antagonize the mMC3R at up to 100 μM concentrations but possessed nanomolar antagonist potency at the mMC4R that was 6-fold less potent than SKY2-23-7. Tetrapeptide SKY2-23-3, containing the sterically constrained Tic (tetrahydroisoquinoline) substitution (Figure 3-2), resulted in agonist activity equipotent at the mMC1R and the mMC5R as compared to SKY2-23-7. At up to 10 μM, SKY2-23-3 did not possess antagonist activity at the mMC3R although it possessed some agonist activity (48% of the maximal MTII-induced response) at 100 μM. At the mMC4R, SKY2-23-3 resulted in a 1 μM antagonist that possessed some stimulatory activity (44%

of the maximal MTII-induced response at 100 μM) and was a 76-fold less potent antagonist compared to SKY2-23-7. The Phe^4 containing substitution SKY2-23-4 resulted in an equipotent agonist, compared to SKY2-23-7, at both the mMC1R and the mMC5R when taking into account the inherent experimental error. Compound SKY2-23-4 lacked any antagonist activity at the mMC3R and possessed nanomolar MC4R antagonist potency, and partial receptor activation was observed at both the mMC3R and the mMC4R at 100 μM concentrations (66% and 44% activation, respectively). Tetrapeptide SKY2-23-5, containing the $Nal(2')^4$ [(2-naphthyl)-l-alanine] substitution, resulted in an equipotent agonist at the mMC1R and possessed a modest 7-fold decreased agonist activity at mMC5R, as compared to SKY2-23-7. The tetrapeptide did not possess any agonist activity at mMC3R and mMC4R, and similar to the lead compound SKY2-23-7, it did possess equipotent antagonist activity at the mMC3R and mMC4R. The DNal(2′) [(2-naphthyl)-d-alanine] containing tetrapeptide SKY2-23-6 resulted in similar pharmacology compared to its diastereomer compound SKY2-23-5. Tetrapeptide SKY2-23-6 was equipotent for agonist activity at the mMC1R, compared to SKY2-23-7 and SKY2-23-5, but resulted in 7-fold decreased agonist potency at mMC5R as compared to SKY2-23-7 but equipotent with SKY2-23-5. At concentrations up to 100 μM, SKY2-23-6 was unable to stimulate the mMC3R or mMC4R subtypes. However, SKY2-23-6 resulted in an equipotent mMC3R and mMC4R antagonist as compared to SKY2-23-7.

Conclusions

In conclusion, a focused seven-membered library of tetrapeptides was designed and synthesized based on the scaffold Ac-Trp-(pI)DPhe-Arg-Xaa-NH_2. Three of the tetrapeptides, SKY2-23-7, SKY2-23-5, and SKY2-23-6 possessed distinct antagonist pharmacology at the mMC3R. These peptides possessed antagonist activity with minimal agonist activity at 100 μM concentrations and, to the best of our knowledge, are the first low molecular weight (M.W. < 900) antagonist mMC3R ligands that display this *in vitro* pharmacological profile. The tetrapeptides possessed potent antagonist activity at the mMC4R, and two of them, compounds SKY2-23-5 and SKY2-23-6, had pA_2 values greater than 8.3 (K_i < 6 nM). Tetrapeptides SKY2-23-1 and SKY2-23-2 are selective antagonists for the mMC4R versus the mMC3R. The distinct pharmacology ascertained from this small library may aid in the future development of more potent and selective antagonists for the melanocortin receptors to more clearly identify *in vivo* roles of the various receptors.

We achieved in the identification of “clean” melanocortin-3 receptor antagonists which were based on the classic “HFRW” signaling motif, yet all of the compounds tended to be more potent at the mMC4R over the mMC3R. In order to evaluate the activity of these compounds at the mMC3R in an *in vivo* model, an mMC4R knockout model is required. Our laboratory has an in house mMC4R knockout model available for testing; however, this genetic modification approach cannot be used in human patients if future studies conclude the selective activation/blocking of the MC3R is an ideal target for the therapeutic modulation of energy homeostasis. The following chapters discuss the

use of an alternative unbiased screening method, mixture-based positional scanning, that is not based on the classic "HFRW" motif, and we were able to titrate back the functional activity at the mMC4R to yield selective mMC3R antagonists.

Future Directions and Preliminary Feeding Studies

The lead compound SKY2-23-7 has been advanced to *in vivo* mouse testing in both male and female wild-type mice. We observed SKY2-23-7, in our hands, affects female and male wild type littermate mice differently. The following is a brief summary of the experimental paradigm and results performed by Cody Lensing, Stacey Wilber, and Danielle Adank. The summary is adapted from a manuscript written by Cody Lensing. This study is in preparation for dissemination in ACS Chemical Neuroscience, and at the time of this dissertation had been submitted for review.

The initial pilot study consisted of the administration of SKY2-23-7 via intracerebroventricular (ICV) injection to both male and female mice in a conventional nocturnal feeding paradigm and housed in conventional cages.[129] The cannula was implanted into the lateral ventricle and validated as previously described.[44] Consistent with other melanocortin antagonists, such as SHU9119, an increase in food intake was observed for male mice;[43] however, these results were not consistent for female mice. This observation was further investigated with the use of TSE Phenotypic metabolic cages which measures food intake, water intake, changes in CO_2 and O_2, and activity.

SKY2-23-7 was administered ICV to mice, male and female, housed in metabolic cages. A total of five doses, 7.5 nmol, 5 nmol, 2.5 nmol, 1 nmol, and 0.5 nmol, were

tested. During crossover experiments, female and male mice were split between the compound group and the vehicle groups. The crossover paradigm was used for the 7.5 nmol dose, 5 nmol dose, and 2.5 nmol dose. A second 5 nmol administration and the 1.0 nmol and 0.5 nmol dosing were performed on both groups simultaneously. Illustrations of the binned data for cumulative food intake (Figure 3-3), hourly respiratory exchange ratio (Figure 3-4), average hourly energy expenditure (Figure 3-5), and average hourly activity (Figure 3-6) are presented herein.

Central ICV administration of SKY2-23-7 to mice housed in metabolic cages resulted in a dose dependent increase in food intake in male mice ($p<0.0001$, Figure 3-3), whereas, ICV administration of SKY2-23-7 to female mice did not result in the same dose response pattern. At the 7.5 nmol and 5 nmol dose, no significant effect was observed in females (Figure 3-3). A normal dose response pattern emerges at the doses 2.5 nmol, 1 nmol, and 0.5 nmol doses in females. A significant increase in food intake was observed at every two hour time point bin from 6-24 hours. It was unanticipated that the 7.5 nmol dose that caused the greatest increase in food intake in male mice resulted in no significant differences in female littermates. Also, the 2.5 nmol dose that caused the greatest increase in food intake in female mice resulted in no significant effect in the male littermates.

In the current study, a 7.5 nmol dose of antagonist SKY2-23-7 increased the average respiratory exchange ratio (RER) in male mice during the first dark cycle (0-14 hrs) (Figure 3-4). The RER was increased at the individual time points 2-7, 10-14 hours after compound administration. In the following light cycle (14-26 hrs), the average RER

drops most likely due to inactivity and decreased food intake. No significant effect was observed on the average RER during the light cycle in male mice (Figure 3-4). However, RER was significantly increased at early light cycle time points (15-18 hr in reverse light cycle). In female mice, no effect was seen at the 7.5 nmol dose. Unlike in the male mice, in female mice the 2.5 nmol dose of SKY2-23-7 significantly increased the average RER throughout both dark and light cycles (Figure 3-4). Significant effects on RER were observed at 3-7, 9, 13-19, and 21-22 hour time points. A significant effect on the average RER was seen at the 1.0 nmol dose as well in the dark cycle.

Decreases in energy expenditure were seen in male mice at 4, 20, 21, 23 and 24 hours post 7.5 nmol administration of SKY2-23-7 compared to control administration (Figure 3-5). No significant effect was seen at lower doses. There was no effect observed in the total calories spent in 24 hours after administration in male mice. In female mice, a significant increase in energy expenditure was observed after a 2.5 nmol administration of SKY2-23-7. This was observed at 5, 6, 15, 21, and 22 hours post administration (Figure 3-5).

Locomotor activity was quantified by the consecutive infrared beam breaks along the sides of the cage. There was no significant effect on the total activity observed between compound administration and saline administration in male mice in either the dark cycle (0-14 hours) or light cycle (14-26 hours). There was significant increases in activity observed at time points 8, 15, 18, and 24 hours in male mice at the 7.5 nmol dose (Figure 3-6). In female mice, there was a significant decrease in activity at the 5 nmol dose in the light cycle, but no other dose resulted in a significant change in total activity

in either the light cycle (0-14 hours) or dark cycle (14-26 hours). Significant increases in activity was observed at the 5 hour time point, and a significant decrease in activity was observed at the 24 hour time point in female mice after 2.5 nmol compound administration.

Experimental

Peptide Synthesis

The peptides were synthesized using a manual microwave peptide synthesizer (Discover SPS System, CEM Corporation, Matthews, NC) applying standard solid-phase Fmoc methodology.1-2 Fmoc-Nω-(2,2,4,6,7-pentamethyldihydrobenzofuran-5-sulfonyl)-arginine [Fmoc-Arg(Pbf)-OH], Fmoc-N(in)-tButyloxycarbonyl-tryptophan [Fmoc-Trp(Boc)-OH], Fmoc-Phenylalanine (Fmoc-Phe-OH), Fmoc-3-(2-naphthyl)-Lalanine [Fmoc-Nal(2')-OH], Fmoc-3-(2-naphthyl)-D-alanine [Fmoc-DNal(2')-OH], and N,N,N′,N′-Tetramethyl-O-(1H-benzotriazol-1-yl)uronium hexafluorophosphate (HBTU) were purchased from Peptides International (Louisville, KY). Fmoc-D-4-iodophenylalanine [Fmoc-(pI)DPhe-OH], Fmoc-L-4-4'-Biphenylalanine (Fmoc-Bip-OH), and Fmoc-L-tetrahydroisoquinoline-3-COOH (Fmoc-Tic-OH) were purchased from Synthetech (Albany, OR). Fmoc-β-(3-benzothienyl)-alanine (Fmoc-3Bal-OH) was purchased from Bachem (Torrance, CA). Anhydrous ethyl ether, methanol (MeOH), Acetonitrile (ACN), dichloromethane (DCM), and acetic anhydride were purchased from Fisher (Fair Lawn, NJ). 1,2-Ethanedithiol (EDT) and triisopropylsilane (TIS) were purchased from Aldrich (Milwaukee, WI). The reagents N,N-dimethylformamide (DMF), piperidine, pyridine, trifluoroacetic acid (TFA), and N,N-diisopropylethylamine (DIEA) were purchased from Sigma-Aldrich (St. Louis, MO). All reagents were ACS grade or better and used without further purification. The peptides were synthesized on rink-amide-MBHA resin (0.37 mmol/g substitution) purchased from Peptides International.

Each peptide was synthesized individually using a 25 mL reaction vessel fitted with a coarse frit (CEM Corporation).

Approximately 270 mg (0.1 mmol) of resin was added to the reaction vessel and allowed to swell in DCM for two hours. After swelling the resin it was then continually stirred by bubbling nitrogen gas through the mixture. The resin was washed in DMF (5 times, 15 mL, mixed 1 min) and subsequently deprotected with the addition of 15 mL 20 v/v % piperidine in DMF deprotection solution to the reaction vessel that was stirred for 2 minutes at room temperature. The reaction vessel was then drained by vacuum and an additional 15 mL of deprotection solution was added. The vessel was placed in the microwave and heated (75 °C, 30 W, 4 min). Following a positive Kaiser test,[99] the first amino acid residue was coupled. The general protocol for the growing peptide chain began with the addition of a 3.1-fold excess of the Nα-Fmoc-protected amino acid (5.1-fold for Arg) and a 3-fold excess of HBTU (5-fold for Arg) both dissolved in DMF. A 5-fold excess of DIEA (7-fold for Arg) was added, and the reaction was placed in the microwave synthesizer and heated (75 °C, 30 W) for 5 minutes (10 min for Arg). Following a negative Kaiser test,[99] the cycle was repeated beginning with the room temperature piperidine deprotection until the final amino acid was added according to the desired peptide sequence. Following a final deprotection cycle and positive Kaiser test, the peptide was acetylated with the addition of 15 mL acetic anhydride and 5 mL pyridine, and mixed for 30 minutes at room temperature. Following a negative Kaiser test, the peptide was washed in DCM (5 times, 15 mL, mixed 1 min) and dried overnight in a desiccator.

Side chain deprotection and peptide cleavage from the resin was performed by mixing the dried peptide-resin with 8 mL of cleavage cocktail (91% TFA, 3% EDT, 3% TIS, and 3% water) for a minimum of 2 hours. The peptides and cleavage solution were drained from the reaction vessel into a pre-weighed 50 mL conical tube. The cleaved resin was rinsed with an additional 2 mL of cleavage cocktail and mixed for 1 minute, the solution was drained into the conical tube, and the peptides were precipitated using cold (4 °C) anhydrous diethyl ether (up to 45 mL). The turbid mixture was placed in an ice bath for 30 minutes, followed by centrifugation at 4 °C and 4000 RPMs for 4 minutes (Sorval Super T21 high-speed centrifuge, swinging bucket rotor). The supernatant was decanted off, the crude peptide was then washed with cold (4 °C) diethylether, and again pelleted. The washing process was repeated for a total of three times. The pellet was dried *in vacuo* overnight.

A 10-20 mg sample of the crude peptide was purified using a Shimadzu RP-HPLC gradient system with a photodiode array detector and a semipreparative RP-HPLC C18 bonded column (Vydac 218TP1010, 1 cm x 25 cm). A typical purification RP-HPLC gradient ranges from 30% to 75% acetonitrile in water with 0.1% TFA over 15 minutes. Collection times and gradients varied dependent upon impurities found in a particular crude sample. After purification the peptide was then lyophilized. Analysis of the purified peptides by analytical RP-HPLC (Vydac 218TP104, 4.6 mm x 25 cm) indicated their purity was 95% or greater and ESIMS (University of Minnesota Department of Chemistry Mass Spectrometry Laboratory) indicated they had the correct molecular mass.

Functional Assay

HEK-293 cells were stably transfected with the mouse melanocortin receptors using a $pCDNA_3$ expression vector using a calcium phosphate method and G418 selection as previously reported by our laboratory.[28, 130] Stably transfected HEK-293 cells expressing the mouse melanocortin receptors were transiently transfected with 4 μg of CRE-PBKS per 10 cm plate using the calcium phosphate crystal method.[123] Briefly, $1x10^6$ to $3x10^6$ cells were plated into 10 cm dishes 24 hours prior to the transfection such that the confluency was approximately 40% at the time of transfection. The cells were transfected with a N,N-bis(2-hydroxyethyl)-2-aminoethanesulfonic acid (BES) buffered saline solution containing 0.125 M $CaCl_2$ and 4 μg of CRE/β-galatosidase reporter gene construct and the plates were then incubated at 35 °C and 3% CO_2 overnight. Twenty-four hours post transfection the cells were plated onto collagen treated Nunclon Delta Surface 96 well plates (Thermo Fischer Scientific) and incubated at 37 °C and 5% CO_2 overnight. Forty-eight hours post-transfection the cells were stimulated with 50 μL of peptide (10^{-4} to 10^{-10} M) or forskolin (10 μM) in assay media (1.0 mL 1% bovine serum albumin [BSA] in phosphate buffered saline [PBS] and 1.0 mL 100x isobutylmethylxanthine in 98.0 mL Dulbecco's Modified Eagle Medium [DMEM]) for 6 hours at 37 °C and 5% CO_2. The assay media was aspirated and 50 μL of lysis buffer (250 mM Tris-HCl pH=8.0, Triton X-100 in water) was added and the plates stored at -80°C for up to 2 weeks.

The plates were thawed and 10 μL sample of cell lysate was removed from each well and put into another 96 well plate for relative protein level determination. To each

well 40 μL 0.5% BSA in PBS was added, followed by, the addition of 150 μL of β-galatosidase substrate solution (60 mM Na_2HPO_4, 1 mM $MgCl_2$, 10 mM KCl, 50 mM 2-mercaptoethanol, and 660 μM 2-nitrophenyl β-galactopyranoside [ONPG]). The absorbance was read on a 96 well plate reader (Molecular Devices) at $\lambda = 405$ nm. The relative protein levels were determined through the addition of 200 μL of BioRad protein dye solution (1 dye: 4 water per manufacturer's instructions) to the 10 μL sample of cell lysate; the absorbance was recorded at $\lambda = 595$ nm on a 96 well plate reader. The β-galatosidase activity data was normalized to both protein levels and the forskolin positive controls, plotted in PRISM (v4.0, GraphPad Inc.), fitted with a sigmoidal dose-response curve, and EC_{50} values were determined. Each experiment consisted of duplicate replicates and was performed in at least three independent experiments. The values reported represent the mean with the associated standard error of the mean.

Chapter 3 Tables and Figures:

Table 3-1: Summary of the Tetrapeptide Agonist (EC_{50}) Receptor Pharmacologically at the mMC1R and mMC5R (Mean ± SEM)

Analogue	**Structure**	**mMC1R (nM)**	**mMC5R (nM)**
MTII	Ac-Nle-c[Asp-His-DPhe-Arg-Trp-Lys]-NH_2	0.22 ± 0.14	0.57 ± 0.07
SHU9119	Ac-Nle-c[Asp-His-DNal(2′)-Arg-Trp-Lys]-NH_2	0.67 ± 0.11	2.4 ± 0.4
NDP-MSH (6−9)	Ac-His-DPhe-Arg-Trp-NH_2	71 ± 20	4.6 ± 1.2
SKY2-23-7	Ac-Trp-(pI)DPhe-Arg-Trp-NH_2	2000 ± 600	2800 ± 1100
SKY2-23-1	Ac-Trp-(pI)DPhe-Arg-Bip-NH_2	20700 ± 7400	7800 ± 2600
SKY2-23-2	Ac-Trp-(pI)DPhe-Arg-3Bal-NH_2	8300 ± 1900	23700 ± 4300
SKY2-23-3	Ac-Trp-(pI)DPhe-Arg-Tic-NH_2	2700 ± 600	5300 ± 1500
SKY2-23-4	Ac-Trp-(pI)DPhe-Arg-Phe-NH_2	6500 ± 1200	1800 ± 600
SKY2-23-5	Ac-Trp-(pI)DPhe-Arg-Nal(2′)-NH_2	5500 ± 300	20300 ± 3200
SKY2-23-6	Ac-Trp-(pI)DPhe-Arg-DNal(2′)-NH_2	5800 ± 1700	19700 ± 4400

The reported errors are the standard error of the mean of at least three independent experiments. MTII, SHU9119, and NDP-MSH (6-9) are included as control compounds.

Table 3-2: Agonist (EC_{50}) and Antagonist (pA_2) Receptor Pharmacologically at the mMC3R and mMC4R (Mean ± SEM)

		mMC3R		mMC4R	
Analogue	**Structure**	**EC_{50} (nM)**	**pA_2**	**EC_{50} (nM)**	**pA_2**
MTII	Ac-Nle-c[Asp-His-DPhe-Arg-Trp-Lys]-NH_2	0.35 ± 0.02	none	0.05 ± 0.01	none
SHU9119	Ac-Nle-c[Asp-His-DNal(2′)-Arg-Trp-Lys]-NH_2	54% at 1 μM 3.0 ± 0.7	8.7 ± 0.3	>100,000	9.7 ± 0.2
NDP-MSH (6−9)	Ac-His-DPhe-Arg-Trp-NH_2	64 ± 19	none	5.4 ± 2.0	none
SKY2-23-7	Ac-Trp-(pI)DPhe-Arg-Trp-NH_2	>100,000	5.4 ± 0.2	>100,000	7.8 ± 0.1
SKY2-23-1	Ac-Trp-(pI)DPhe-Arg-Bip-NH_2	>100,000	none	>100,000	6.3 ± 0.1
SKY2-23-2	Ac-Trp-(pI)DPhe-Arg-3Bal-NH_2	>100,000	none	>100,000	7.1 ± 0.1
SKY2-23-3	Ac-Trp-(pI)DPhe-Arg-Tic-NH_2	48% at 100 μM	none	44% at 100 μM	6.0 ± 0.2
SKY2-23-4	Ac-Trp-(pI)DPhe-Arg-Phe-NH_2	66% at 100 μM	>100,000	44% at 100 μM	6.8 ± 0.2
SKY2-23-5	Ac-Trp-(pI)DPhe-Arg-Nal(2′)-NH_2	>100,000	5.9 ± 0.2	>100,000	8.3 ± 0.1
SKY2-23-6	Ac-Trp-(pI)DPhe-Arg-DNal(2′)-NH_2	>100,000	5.7 ± 0.1	>100,000	8.3 ± 0.1

The reported errors are the standard error of the mean of at least three independent experiments. The pA_2 values were calculated by a Schild analysis and used MTII as the agonist compound. A value of >100,000 nM indicates that no agonist activity was observed at the concentrations tested. A % at 100 μM indicates some agonist activity was observed with the corresponding percentage indicating the amount of activity relative to the MTII-induced maximal response.

Table 3-3: Table analytical data for the peptides synthesized in this study

Analog	Structure	HPLC k' 1	HPLC k' 2	M^{+1} Calc'd	MS Analysis (M^{+1}), Purity
SKY2-23-7	Ac-Trp-(pI)DPhe-Arg-Trp-NH_2	7.3	11.1	861.3	861.3, >97%
SKY2-23-1	Ac-Trp-(pI)DPhe-Arg-Bip-NH_2	8.5	12.7	898.3	898.3, >95%
SKY2-23-2	Ac-Trp-(pI)DPhe-Arg-3Bal-NH_2	7.7	12.0	878.2	878.3, >97%
SKY2-23-3	Ac-Trp-(pI)DPhe-Arg-Tic-NH_2	7.4	11.3	834.3	834.3, >96%
SKY2-23-4	Ac-Trp-(pI)DPhe-Arg-Phe-NH_2	7.2	11.0	822.3	822.4, >95%
SKY2-23-5	Ac-Trp-(pI)DPhe-Arg-Nal(2')-NH_2	8.0	12.2	872.3	872.3, >96%
SKY2-23-6	Ac-Trp-(pI)DPhe-Arg-DNal(2')-NH_2	7.8	11.7	872.3	872.3, >96%

HPLC k' = (peptide retention time - solvent retention time) / solvent retention time. System 1 is a 10% to 90% gradient of acetonitrile in water containing 0.1% triflouroacetic acid over 35 minutes, and system 2 is the same gradient with methanol replacing acetonitrile. The HPLC method is run on a 250 mm x 4.6 mm C18 column (Vydac 218TP C18 10 μ) with a flow rate of 1.5 mL/min. Product purity is determined using system 2 and integrating the area under the curves of the spectra collected at 214 nm.

Figure 3-1: Illustration of Dose-Response Antagonist Curves Observed for the Tetrapeptides Based on the Scaffold Ac-Trp-(pI)DPhe-Arg-Xaa-NH_2

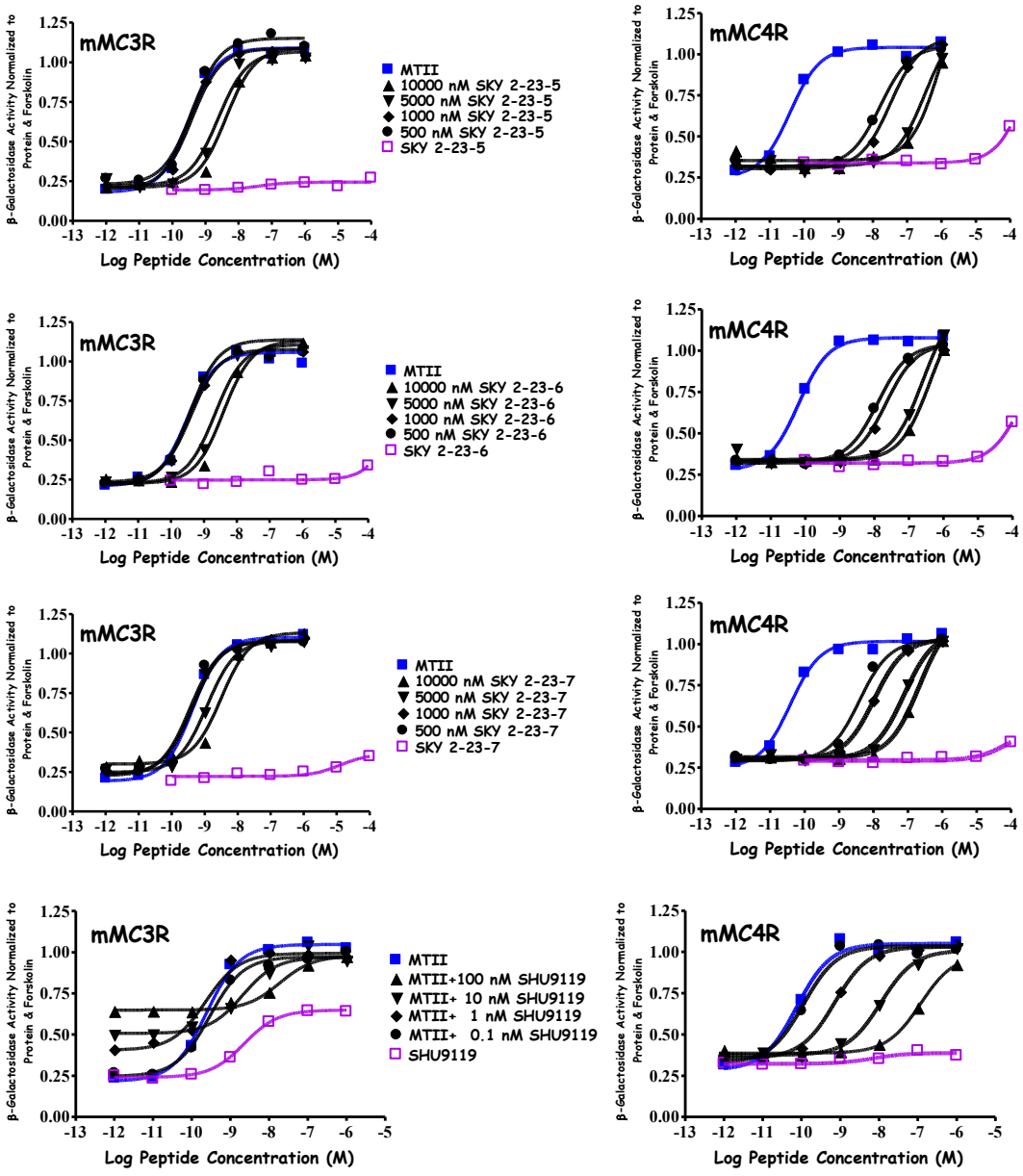

Illustration of the *in vitro* receptor pharmacology at the mMC3R and mMC4R for tetrapeptides SKY2-23-7 (Trp), SKY2-23-5 [Nal(2′)], and SKY2-23-6 [DNal(2′)], Ac-

Trp-(pI)DPhe-Arg-Xaa-NH_2 and SHU9119 Ac-Nle-c[Asp-His-DNal(2′)-Arg-Trp-Lys]-NH_2. The SHU9119 is a representative mMC3R/mMC4R antagonist that possesses mMC3R partial agonist activity, whereas SKY2-23-7, SKY2-23-5, and SKY2-23-6 possess minimal agonist activity at concentrations of 100 μM. Compounds SKY2-23-5, SKY2-23-6, and SKY2-23-7 were assayed for agonist activity at concentrations from 10^{-4} to 10^{-10} M. SHU9119 was assayed for agonist activity from 10^{-6} to 10^{-12} M. The compounds SKY2-23-5, SKY2-23-6, and SKY2-23-7 were assayed using the standard Schild experiment and analysis where MTII was assayed with the indicated concentrations of the indicated SKY compound.

Figure 3-2: Building Blocks for Tetrapeptide Antagonist Study Based on the Tetrapeptide Template Ac-Trp-(pI)DPhe-Arg-Xaa-NH_2

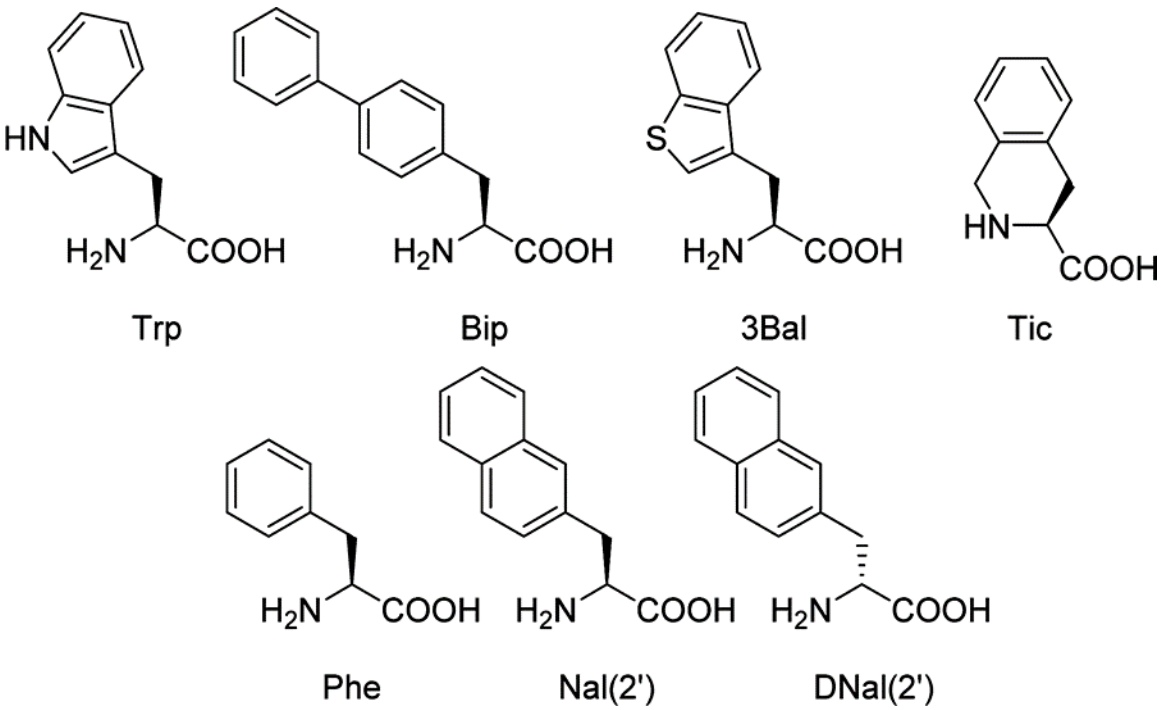

Illustration of the amino acid building blocks incorporated at the Trp^4 position in the tetrapeptide template Ac-Trp-(pI)DPhe-Arg-Trp^4-NH_2. Abbreviations for the nonstandard 20 amino acids are (3Bal) β-(3-benzothienyl)-alanine, (Tic) tetrahydroisoquinoline, [L/D-Nal(2′)], (2-naphthyl)-alanine, and (Bip) 4-4′-biphenylalanine.

Figure 3-3: Cumulative Food Intake for the ICV Administration of SKY2-23-7

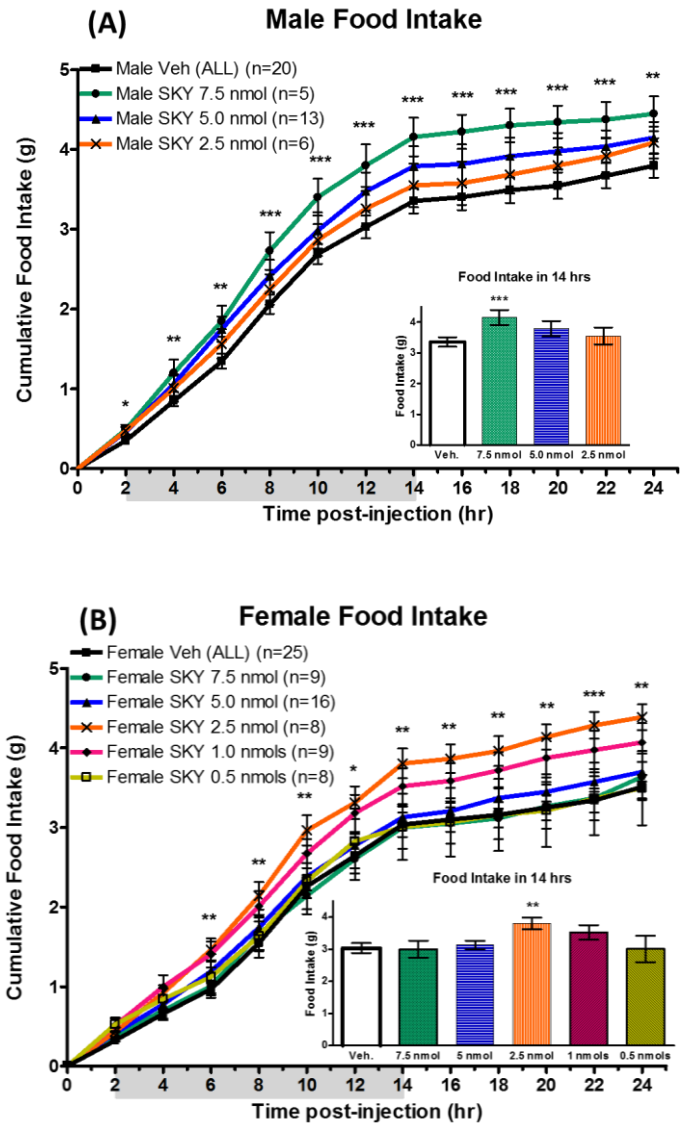

Cumulative food intake of (A) males and (B) females after ICV administration of SKY2-23-7. *p<0.05, **p<0.01, ***p<0.001. The dark band (x-axis) indicates the night cycle. Experiments performed by Cody Lensing and Danielle Adank.

Figure 3-4: The Hourly Respiratory Exchange Ratio (RER) for the ICV Administration of SKY2-23-7

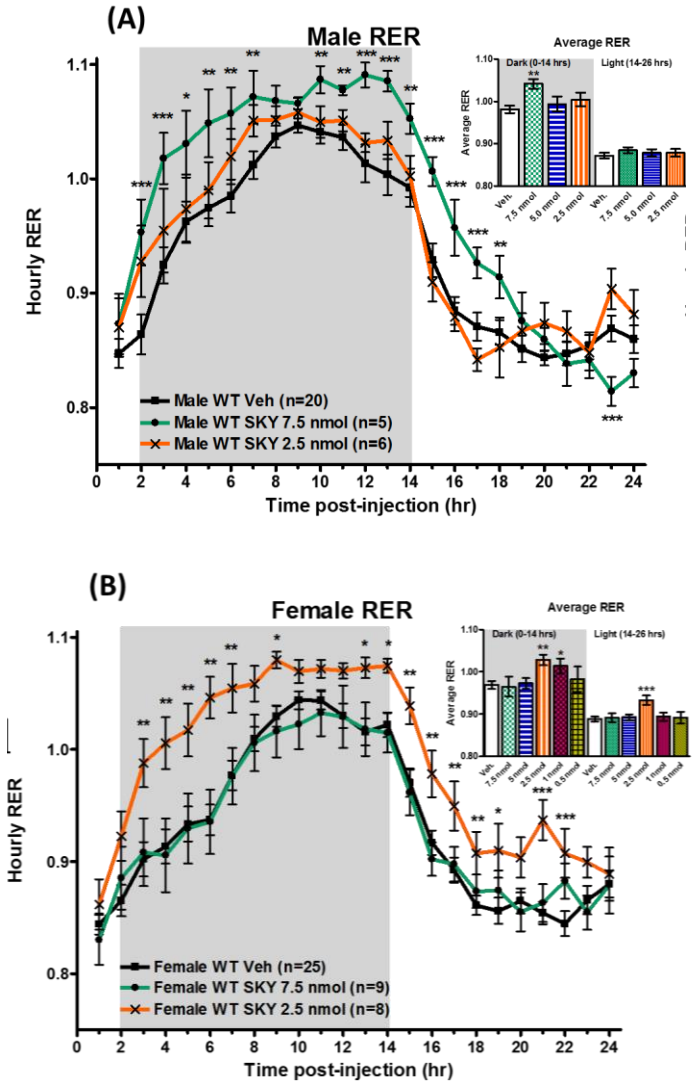

Average hourly RER values of (A) males and (B) females after ICV admiration of SKY2-23-7. *p<0.05, **p<0.01, ***p<0.001. The dark band (x-axis) indicates the night cycle. Experiments performed by Cody Lensing and Danielle Adank.

Figure 3-5: The Energy Expenditure (EE) for the ICV Administration of SKY2-23-7

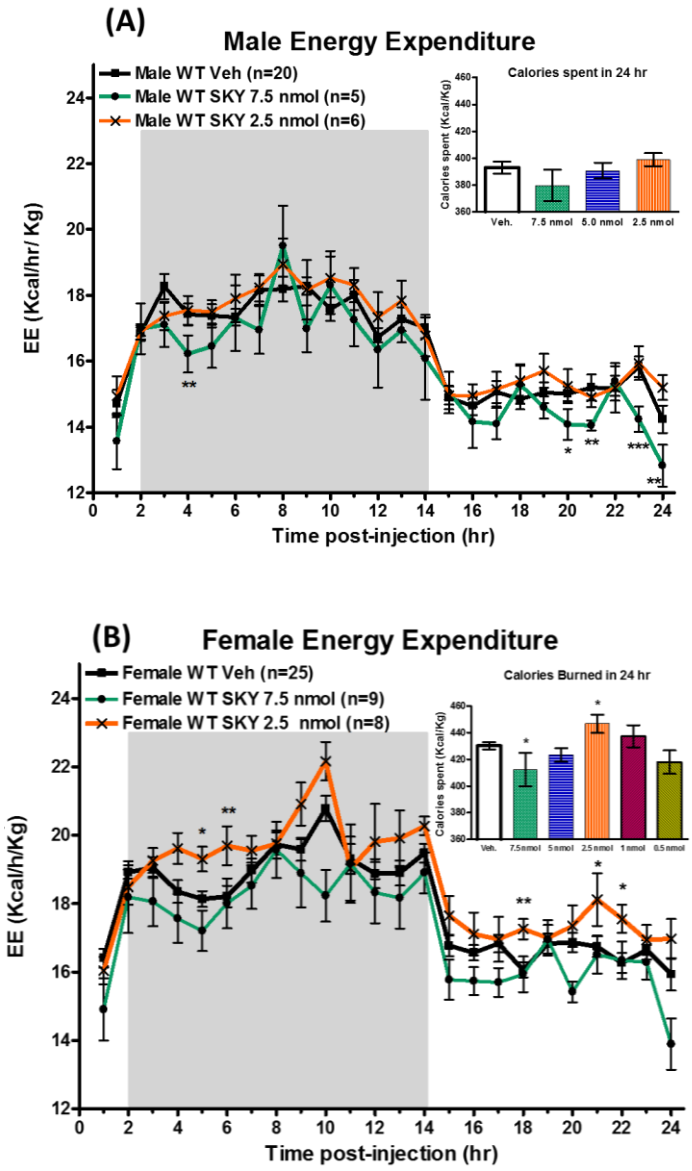

Average hourly energy expenditure (EE) normalized to body weight (Kcal/hr/Kg) of (A) males and (B) female after ICV admiration of SKY2-23-7. *p<0.05, **p<0.01, ***p<0.001. The dark band (x-axis) indicates the night cycle. Experiments performed by Cody Lensing and Danielle Adank.

Figure 3-6: The Ambulatory Activity for the ICV Administration of SKY2-23-7

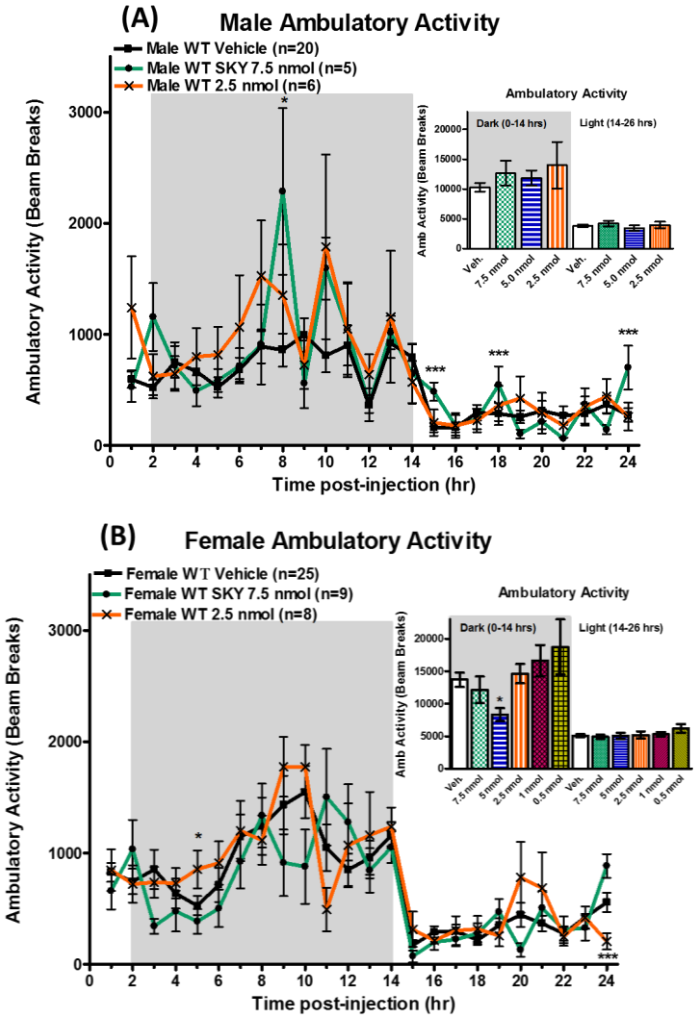

Average hourly activity of (A) males and (B) females after ICV admiration of SKY2-23-7. *p<0.05, **p<0.01, ***p<0.001. The dark band (x-axis) indicates the night cycle. Experiments performed by Cody Lensing and Danielle Adank.

Chapter 4

Identification of Dual Melanocortin-3 Agonists/Melanocortin-4 Antagonists Derived From Mixture-Based Positional Scanning

All peptides were synthesized, purified, and characterized by Skye Doering under the supervision of Carrie Haskell-Luevano. Lead peptide sequence was identified as part of a mixture-based screening campaign (TPI924) conducted by Erica Haslach, Marvin Dirain, Ginamarie Debevec, Phaedra Geer, Radleigh Santos, Marc Giulianotti, Clemencia Pinilla, Jon Appel, Richard Houghten, and Carrie Haskell-Luevano. Function and binding assays were designed and performed by Katie Freeman, Sathya Schnell, and Skye Doering. The data were analyzed by Skye Doering and Carrie Haskell-Luevano. The ^{125}I-NDP-MSH radiolabel was radio iodinated by Robert Speth. This work is currently in preparation for dissemination.

Introduction

As outlined in Chapter 1, one of the primary goals reported in this dissertation was the identification of potent and selective MC3R compounds. The following chapter presents a study which utilized a combination of mixture-based positional scanning in parallel with the more classical SAR strategy of double amino acid replacement. This study can be compared to Chapter 3, which used simply a single amino acid replacement around a lead peptide sequence based on the traditional melanocortin signaling motif "His-Phe-Arg-Trp." In this study, a novel tetrapeptide scaffold [Ac-Xaa^{1}-Arg-(pI)DPhe-

Xaa^4-NH_2] is reported. It was identified using a screening and mixture-based positional scanning approach. A 48 compound library of doubly-substituted tetrapeptides were designed based on this scaffold and characterized at the mouse melanocortin-1, -3, -4, and -5 receptors. This resulted in the serendipitous discovery of a first-in-class pharmacological profile for a tetrapeptide ligand at the central MC3 and MC4 receptor subtypes. Nine ligands with mixed pharmacology, MC3R agonist and MC4R antagonist, were discovered. Results indicated these compounds to be MC3R agonists (EC_{50} < 1,000 nM) and MC4R antagonists (5.7 > pA_2 > 7.8). The three most potent MC3R agonists, SKY4-48-18 [Ac-Arg-Arg-(pI)DPhe-Tic-NH_2] (EC_{50} = 16 nM), SKY6-24-2 [Ac-His-Arg-(pI)DPhe-Tic-NH_2] (EC_{50} = 40 nM), and SKY4-48-42 [Ac-Arg-Arg-(pI)DPhe-DNal(2')-NH_2] (EC_{50} = 57 nM) were more potent than melanocortin tetrapeptide Ac-His-DPhe-Arg-Trp-NH_2 (EC_{50} = 73 nM). This novel template contains an "Arg-Phe" sequence that is in reverse order with respect to the classical "His-Phe-Arg-Trp" melanocortin signaling motif, and this modification results in a pharmacological profile that is unique for the centrally located melanocortin receptors.

We report on the discovery of a series of dual MC3R agonist/MC4R antagonist compounds that, to the best of our knowledge, are first-in-class for melanocortin ligands. Therefore, resulting *in vivo* phenotype from the central administration of this class of compounds is unknown; however, it is not an unreasonable conjecture that the observed effect on energy homeostasis and body weight regulation could be greater than the sum of stimulating/blocking each receptor alone. That is to say, the MC3R and MC4R could be working in synergy and the expected decrease in food intake with the central administration of an agonist at the MC3R could be allosterically modulated via the

central administration of an antagonist at the MC4R.[44] Perhaps, the administration of these dual agonist/antagonist compounds would yield an amplified weight-loss benefit from stimulating the MC3R in addition to inducing a decrease in blood pressure from antagonizing the MC4R, which is a noted difference in patients with MC4R-deficent mutations.[75] The use of co-therapies is not novel and recent developments in this area illustrate the power of receptor synergy in relationship to weight-loss. This is illustrated by recent reports of a unimolecular co-agonist targeting both the glucagon-like peptide-1 (GLP-1) and glucose-dependent insulinotropic polypeptide (GIP) receptors, in addition to, a tri-agonist targeting the GLP-1, GIP, and glucagon receptors as a potential therapeutics for the treatment of so called diabesity.[131-133] The discovery of the reported dual agonist/antagonist compounds utilized a combination of different peptide methodologies.

Classical peptide structure-activity relationship (SAR) approaches, such as truncation studies and single residue replacement scans (example in Chapter 3), have yielded a variety of ligands with differing potencies and selectivity profiles at the receptor subtypes.[21, 35, 81, 134] These studies build upon preexisting knowledge and have been valuable in the development of potent, selective ligands. While useful, this approach has not generated a low molecule weight (M.W. < 1,000) MC3R selective ligand. To date, an unbiased approach that does not rely on prior scientific biases, such as mixture-based positional scanning, may be used in order to generate radically new previously unknown scaffolds.[28] Herein, we applied mixture-based positional scanning in conjunction with a classic double residue replacement scan to yield a first-in-class central MC3R antagonist MC4R antagonist dual pharmacological profile.

Mixture-based positional scanning has been extensively reviewed in the literature[108, 122, 135] in addition to Chapter 2, and this methodology has been previously validated for studying the melanocortin receptors wherein tetrapeptides were identified that rescued the function of selected human MC4R single nucleotide polymorphisms (SNPs).[28] Compounds sharing a common scaffold are assayed in mixtures where each compound within the mixture shares a common side chain at a particular position. There is a propensity for large mixtures containing only a few potent compounds to demonstrate an overall moderate activity, since the activity of a particular mixture is the harmonic mean of the constituents.[107] These active mixtures are then identified as "hits," and combinations of "hits" can be synthesized and assayed as individual compounds. This technology allows for the rapid screening of millions of compounds/peptides, the development of an extensive SAR, and the prioritization of individual compounds that could be studied as part of the deconvolution process. The ability to efficiently screen millions of compounds/peptides enables a larger area of chemical space to be explored in an unbiased and efficient manner. Thus, novel scaffolds can be identified that are not based upon any previously performed SAR studies, and may generate ligands with novel potency and selectivity profiles.

Herein, we describe the identification of a new synthetic tetrapeptide sequence, compound SKY6-24-2, Ac-His-Arg-(pI)DPhe-Tic-NH_2, derived from a mixture-based positional scanning library at the MC3R. A key feature of this compound is an apparent structure reversal in the melanocortin signaling sequence residues of arginine and phenylalanine compared to the conserved His-Phe-Arg-Trp motif. Analysis from the screening campaign identified Ac-Xaa^1-Arg-(pI)DPhe-Xaa^4-NH_2 as a scaffold warranting

further exploration due to the pharmacophore rearrangement. Based on this template, it was hypothesized that substituting the first and fourth positions with several aromatic sidechains, previously indicated to alter the selectivity and potency profiles of other melanocortin peptides, could result in the discovery of new mMC3R scaffolds with novel pharmacology that could be used as molecular tools to probe the mechanism between the MC3 and MC4 receptors *in vitro* and *in vivo*.[55-56]

Results and Discussion

Identification of the Lead Compound SKY 6-24-2, Ac-His-Arg-(pI)DPhe-Tic-NH_2

The mixture-based positional scan library TPI 924 consisted of 60 individual building blocks of D-amino acids, L-amino acids, and unnatural amino acids resulting in 240 mixtures each containing 216,000 compounds with an overall library representing 12,960,000 compounds. Each member of the combinatorial library shared a common Ac-tetrapeptide-NH_2 scaffold, and within each mixture a particular residue was held constant at a particular position. For example, all of the peptides in the first mixture shared the structure Ac-Ala-X-X-X-NH_2, where X indicates a mixture of all 60 building blocks and therefore resulting in 216,000 (1x60x60x60) compounds within the mixture. The scanning library was constructed using the standard solid-phase synthesis N-α-tert-butyloxycarbonyl (Boc) protecting scheme, and the mixtures of compounds were synthesized using the previously reported teabag method.[105]

The library was screened using a 96-well cAMP based colorimetric β-galactosidase assay using HEK293 cells stably expressing the cloned mMC3R.[123] The primary screen assessed for mixture activity at a stimulatory concentration of 100 µg/mL.

The data were normalized to both protein content and the responses of the potent synthetic agonist NDP-MSH and forskolin; the melanocortin receptor independent activator of adenylate cyclase. A positive mixture "hit" was considered for a mixture which produced a response greater than or equal to 70% of maximal response of the positive controls. A secondary screen was conducted at two concentrations, 100 μg/mL and 50 μg/mL, to confirm the "hits" observed in the primary screen were not false positives. Mixtures Ac-His-X-X-X-NH_2, Ac-X-Arg-X-X-NH_2, Ac-X-X-(pI)DPhe-X-NH_2, and Ac-X-X-X-Tic-NH_2 were confirmed as positive "hit" mixtures and the resulting tetrapeptide Ac-His-Arg-(pI)DPhe-Tic-NH_2 was selected for further evaluation based on the unusual Arg-Phe reversed template.

The lead compound Ac-His-Arg-(pI)DPhe-Tic-NH_2, SKY6-24-2, was synthesized using standard microwave assisted solid-phase N-α-fluorenylmethyloxycarbonyl (Fmoc) chemistry.[97-98] The compound was assessed for functional activity by the measurement of intracellular cAMP accumulation using the whole cell Amplified Luminescent Proximity Homogeneous Assay Screen (AlphaScreen®, Perkin-Elmer) in the same stably transfected HEK293 cells as the initial screen in a 384-well format.[68, 97, 136] Preliminary results indicated the compound was equipotent, within the 3-fold inherent error associated with this assay in our hands, to the previously reported melanocortin tetrapeptide, SKY4-48-1, Ac-His-DPhe-Arg-Trp-NH_2 (40 vs 73 nM) at the mMC3R.[53, 55-58] In addition, minimal agonist activity was observed at a concentration of 100 μM for the mMC4R and subsequent antagonist experiments indicated the compound demonstrated antagonist activity at the mMC4R (pA_2 = 7.0, K_i = 100 nM). To the best of our knowledge, this compound with agonist activity at the mMC3R and antagonist activity at

the mMC4R is a pharmacological profile that is first-in-class and can serve the unmet need which currently exists in the field. It was at this point we affectionately named this scaffold the Tetrapeptide Agonist Compound (TACO) scaffold, due to the propensity for this tetrapeptide to stimulate the MC3R (Figure 4-7).

Double Substitution Library Design, Synthesis, and Evaluation

Based upon the initial experiments, the first and fourth positions were selected for further investigations as part of a double-substitution library. It was hypothesized that the second and third positions would be held constant [(Ac-Xaa^1-Arg-(pI)DPhe-Xaa^4-NH_2], since previous studies on the linear truncated tetra- and penta-peptide analogs of α-MSH, Ac-His-DPhe-Arg-Trp-NH_2 and Bu-His-DPhe-Arg-Trp-Gly-NH_2, indicated alterations at these positions within the His-Phe-Arg-Trp signaling motif were generally detrimental to the activity at all of the receptors.[57-58, 63, 126, 137] The substitutions selected for the library contain both natural and unnatural amino acids which have been previously shown to alter either the selectivity and/or the potency at the selected melanocortin receptor subtypes in the aforementioned linear, Ac-His-DPhe-Arg-Trp-NH_2 based, peptides (Figure 4-1).[55-56, 137] For the first position of the tetrapeptide, arginine (Arg), histidine (His), biphenylalanine (Bip), β-(3-benzothienyl)-alanine (3Bal), 1,2,3,4-tetrahydroisoquinoline-3-carboxylic acid (Tic), phenylalanine (Phe), D/L 2-napthylalanine [DNal(2') and LNal(2')] were selected (Figure 4-1).[55] At the fourth position, Bip, 3Bal, Tic, Phe, DNal(2'), and LNal(2') were selected.[56] The library resulted in a total of 48 (8x1x1x6) analogs which included the resynthesis of the lead peptide SKY6-24-2 for a control; in addition, Ac-His-DPhe-Arg-Trp-NH_2 and NDP-

MSH were also included for reference and comparison purposes. All peptides were synthesized manually in a microwave in parallel using standard Fmoc solid phase peptide synthesis.[97-98]

They were purified by reverse phase high pressure liquid chromatography (RP-HPLC) on a semipreparative scale, and the purification was done, whenever possible, as a mixture of two crude peptides to reduce instrument time and solvent usage by nearly half. Typically, in order to isolate 5 to 10 mg of a pure (>95% by UV absorption at λ=214 nm) tetrapeptide for a single compound, 40 mg of crude peptide would be dissolved and injected onto a semipreparative Vydac C18 column (10 micron, 10 x 250 mm, Vydac Cat#218TP1010) over the course of 25 injections with a flow rate 5 mL/min in a mixture of 0.1% trifluoroacetic acid in water and acetonitrile. A typical RP-HPLC method would consist of a 10 minute run, followed by a 10 minute column flush, and then a 10 minute column equilibration for a total of 30 minutes per injection. Over the course of the purification of a single peptide, the RP-HPLC would be in use for 12.5 hours and 1.9 liters of acetonitrile (approximately, 50% of the total RP-HPLC solvent). The selection process in pairing crude peptides for purification consisted of first running an analytical of each crude peptide on a standard 10% to 90% acetonitrile gradient in 0.1% TFA in water over 35 minutes at a rate of 1.5 mL/min using an analytical Vydac C18 column (10 micron, 4.6 x 250 mm, Vydac Cat#218TP104). Pairs of RP-HPLC traces wherein the desired peptide peaks came off within 5 minutes of each other without the introduction of impurities were paired up and then the peptides were combined for purification (Figure 4-2a). With a modest 5 minute increase in the semipreparative RP-HPLC method, parallel purification of two crude peptides could be achieved (Figure 4-2b). It was estimated this

effort reduced the amount of RP-HPLC time by approximately 210 hours, or 8.75 days, in addition it reduced the amount of total solvent by 62.5 liters, of which approximately 50% was acetonitrile. Compounds were confirmed by matrix-assisted laser desorption ionization time of flight (MALDI-TOF) mass spectrometry at the University of Minnesota Mass Spectrometry Laboratory. They were assessed for purity by analytical RP-HPLC analysis using two different solvent systems (Table 4-4). Analytical characterization of the compounds indicated their purity >95% as indicated by UV absorbance at $\lambda = 214$ nm (Table 4-4).

The double-substitution library was screened for *in vitro* agonist activity using the 384-well cAMP based AlphaScreen technology at concentrations ranging from 10^{-4} M to 10^{-10} M in duplicate replicates with three independent experiments at the mMC1R, mMC3R, mMC4R, and the mMC5R. Since the MC2R is only stimulated by ACTH, it was excluded from this study.[22] The data were normalized to NDP-MSH, and the response observed for NDP-MSH at 10^{-6} M was defined as 100% response. Additional positive (forskolin) and negative (assay buffer) controls were included in the screening. Compounds which failed to produce full dose-response curves at the mMC3R or the mMC4R were further assessed for antagonist activity via a Schild analysis and pA_2 values were determined.[51] In a typical antagonist experiment, cells were co-treated with NDP-MSH (full dose-response, 10^{-6} to 10^{-12} M) and the compound of interest (10,000 nM, 5,000 nM, 1,000 nM, and 500 nM) and the apparent shift in NDP-MSH response was quantified. NDP-MSH was selected over α-MSH since it is a more potent analog,[21] and in our hands, NDP-MSH proved to give a more consistent result in the AlphaScreen over the other commonly used potent cyclic MSH analog, MTII. The apparent shifts in

NDP-MSH's agonist activity (EC_{50} values) were recorded and a Schild analysis was performed to yield a pA_2 value [$pA_2 = -Log(K_i)$].[51] These experiments were also performed with duplicate well replicates and three independent experiments.

Overview of the SAR results at the mouse melanocortin-1, -3, -4, and -5 receptors

The double-substitution library produced a varied SAR between the receptors at the four selected subtypes which ranged from potent agonists to potent antagonists. Given the large volume of data, they are separated by receptor subtypes with the mMC1R/mMC5R together and mMC3R/mMC4R together. The combined agonist and antagonist results for the mMC3R and mMC4R are tabulated in Table 4-1 and the agonist results for the mMC1R and mMC5R are tabulated in Table 4-2. Additional figures illustrate a summary of the agonist and antagonist activity as a function of both substitutions at the first and fourth positions of the TACO scaffold (Figure 4-3 for the mMC1R/mMC5R agonist, Figure 4-4 for the mMC3R/mMC4R agonist, and Figure 4-5 for the mMC3R/mMC4R antagonist data). The most potent agonist activity was observed at the mMC1R, followed by similar agonist activities at the mMC3R and mMC5R, while little to no agonist activity was observed at the mMC4R. As already discussed, compounds demonstrating little to no agonist activity at the mMC3R or the mMC4R were selected for antagonist activity via a Schild analysis.[51] Compounds with antagonist activity at the mMC3R are generally observed to be weak, $pA_2 < 6$, ($K_i > 1{,}000$ nM) whereas seventeen compounds evaluated at the mMC4R possessed $pA_2 > 6$ ($K_i < 1{,}000$ nM). Notably lead compound SKY6-24-2, Ac-His-Arg-(pI)DPhe-Tic-NH_2, and the closely related compound SKY4-48-18, Ac-Arg-Arg-(pI)DPhe-Tic-NH_2, were observed

to be an antagonists at the mMC4R with a pA_2 greater than 7.0 (K_i < 100 nM) and potent nanomolar agonists at the mMC3R (EC_{50} = 40 and 16 nM, respectively). Lastly, compound SKY4-48-42 was observed to be a potent nanomolar agonist at the mMC3R (EC_{50} = 57 nM) which was 5-fold selective over the mMC1R and 9-fold selective over the mMC5R. In addition, this compound was a 400 nM antagonist at the mMC4R (pA_2 = 6.4).

Comparison of the library to Ac-His-DPhe-Arg-Trp-NH_2

Seven compounds were equipotent to more potent than the tetrapeptide Ac-His-DPhe-Arg-Trp-NH_2 at the mMC1R, compared to four at the mMC3R, one at the mMC5R, and none at the mMC4R. In fact, only one compound, SKY4-48-8, was able to produce a maximal response (EC_{50} = 7,900 nM) at the mMC4R whereas all of the remaining compounds were unable to produce full activity with respect to the full agonists used in this study, NDP-MSH and SKY4-48-1 (Ac-His-DPhe-Arg-Trp-NH_2), at concentrations up to 100 µM. In contrast, 17 members of this library were found to have antagonist activity with pA_2 values greater than 6.0 (K_i < 1,000 nM) at the mMC4R. A prominent outcome for this library was the presence of an mMC3R agonist/mMC4R antagonist pharmacological profile as illustrated with the most potent mMC3R agonist compound SKY4-48-18 (Figure 4-6a). A total of 9 compounds produced moderate to potent agonist activity (EC_{50} < 1,000 nM) at the mMC3R, in addition to producing antagonist activity at the mMC4R (7.8 < pA_2 < 5.7). This is in contrast to previous reports on melanocortin tetrapeptides in which the SAR tends to favor MC4R potency over the MC3R.[55-59, 62-66, 138-139]

SAR for Agonist Activity

Compounds were most active at the mMC1R, followed by similar activities at the mMC3R and mMC5R, with minimal agonist activity at the mMC4R (Figure 4-6a). Results from substitutions at the first position indicate the mMC1R had a preference for a basic side chain (Arg^1 and His^1), followed by small aromatic sidechains in addition to some intermediate sized aromatics [Phe^1, Tic^1, $DNal(2')^1$], and last, the remaining intermediately sized aromatics and the bulky aromatics [$Nal(2')^1$, Bip^1, $3Bal^1$] were detrimental to the SAR. Activity at the mMC3R and mMC5R were dependent upon having a basic sidechain at the first position to produce a compound with a potency greater than 100 nM. An aromatic sidechain was tolerable with the addition of either a $3Bal^4$ or Tic^4 substitution at the fourth position and resulted in a moderate (>100 nM) to weak micromolar compound. Interestingly, with the $3Bal^4$ or Tic^4 the trends that were observed with the mMC1R at the first position are consistent with the mMC3R and mMC5R, suggesting the amino acid replacements about this scaffold at the first and fourth position may be additive to the overall activity of the peptide since a step-wise increase in activity was observed when a more favorable substitution was incorporated. This would be compared to observing dramatic increases, several orders of magnitude, upon the incorporation of specific pairs of amino acid substitutions.

The amino acid substitutions at the fourth position produced comparable results for agonist activities at the mMC1, mMC3, and mMC5 receptors. The rank order of the amino acid replacements as a function of their resulting potencies were similar for the three receptor subtypes (Tic^4 > $3Bal^4$ > Phe^4 = $Nal(2')^4$ = $DNal(2')^4$ >> Bip^4). The constrained Tic^4 substitution resulted in the most potent analogs at each of the three

receptor subtypes with potencies in the sub- to low-nanomolar ranges (EC_{50} < 10 nM). Compounds containing the sulfur analog of tryptophan, 3Bal[4], tended to mirror the potencies observed for the Tic[4] analogs, albeit none of these analogs reached sub-nanomolar potencies. Fourth position substitutions that resulted in compounds that fell within an intermediate potency range, high nanomolar to micromolar (EC_{50} > 500 nM), were the Phe[4], Nal(2')[4], and DNal(2')[4]. With these particular substitutions, either an Arg[1] or His[1] replacement at the first position was required for the analogs to have activity at the mMC3R and mMC5R. Lastly, compounds containing the bulky Bip[4] amino acid resulted in the weakest activities with most analogs unable to produce any agonist activity at concentrations up to 100 micromolar.

SAR for Antagonist Activity

The double substitution library resulted in wide-ranging antagonist activity at the mMC4R. When the same compound was assayed for antagonist activity at both the central mMC3 and mMC4 receptors, antagonist activity at the mMC4R tended to be on average 8-fold more potent than the observed potency at the mMC3R, a trend observed for other melanocortin antagonists.[52, 67] Similar to the SAR for the agonist activity at the mMC1, mMC3, and mMC5 receptors, the most active compounds contained a Tic[4] substitution, up to pA_2 = 7.8 (K_i = 16 nM) for SKY4-48-18. The 3Bal[4] replacement also decreased antagonist activity with respect to the Tic[4] replacement, similar to the observed trend for agonist activity at the MC1R, MC3R and MC5R. For the Phe[4], Nal(2')[4], and DNal(2')[4] substitutions. Either a basic Arg[1] or His[1] or, interestingly, a DNal(2')[1] replacement was needed to achieve maximal antagonist activity (up to pA_2 = 6.9 or K_i =

126 nM for the DNal(2')^{1}/Phe^{4} analog SKY4-48-33). The Bip^{4} substitution was generally detrimental for mMC4R antagonist activity, with only two of those analogs, SKY4-48-2 and SKY5-146-2, able to produce detectable activity (pA_2 = 5.8 and 6.6, respectively). In addition, SKY4-48-8 was the only compound which resulted in agonist activity at the mMC4R for the whole library and it possessed weak micromolar potency (EC_{50} = 7,900 nM). The most potent mMC4R antagonist, SKY4-48-18, had an Arg^{1}/Tic^{4} substitution which resulted in a pA_2 of 7.8 (K_i = 15 nM); in addition, this compound resulted in nanomolar agonist activity at the mMC3R (EC_{50} = 16 nM). The antagonist activity at the mMC4R was unexpected since studies on the linear tetrapeptide Ac-His-DPhe-Arg-Trp-NH_2 indicate antagonist activity can be conferred through substitutions such as DNal(2') and (pI)DPhe at the second position whereas most substitutions at the first position result in agonist activity.[55, 57] A Tic^{1} replacement at the first position yielded weak antagonists (pA_2 < 6, K_i > 1,000 nM). This is in contrast to the closely related peptide Tic-(pI)DPhe-Arg-Trp-NH_2 which has been reported to strongly bind to both the human MC3R and MC4R (75 and 0.30 nM, respectively), and displays potent antagonist activity at the hMC4R (pA_2 = 9.10, K_i = 0.79 nM, > 35% agonist activation with respect to maximal response).[138] In addition, a Tic substitution on a SHU9119 analog at the same relative position also resulted in potent antagonist activity.[84] All of this suggests the reported TACO scaffold is not only structurally different from compounds based on the endogenous peptides but also elicits different pharmacology when the some of the same residues are replaced.

^{125}I-NDP-MSH Competitive Binding

Reported are the results from the radiolabel competition binding experiments at the mMC3R and mMC4R (Table 4-3). The selection criteria included the nine mMC3R agonists with potencies less than 1,000 nM (SKY6-24-2, SKY4-48-10, SKY4-48-11, SKY4-48-15, SKY4-48-18, SKY4-48-23, SKY6-24-3, SKY4-48-26, and SKY4-48-42). Table 4-3 summarizes the results of two independent experiments each containing two replicates per experiment. The results are tabulated as the mean and standard error of the mean for each compound at the mMC3R and mMC4R. Also included in the table is the calculated fold difference in IC_{50} potency based on the value observed for SKY4-48-1; Ac-His-DPhe-Arg-Trp-NH_2. The IC_{50} value for SKY4-48-1 at the mMC3R was fitted by constraining the top and bottom, complete receptor saturation and complete radiolabel displacement, nonlinear regression parameters to those which were determined for NDP-MSH within the same experiment. This allowed for an estimation of the IC_{50} which was needed in order to numerically compare, in terms of fold difference, the observed changes in IC_{50} potencies within the receptor subtype. The calculated IC_{50} value for SKY4-48-1 is 50 μM at the mMC3R, and this result is in agreement with the previously reported IC_{50} value at the human MC3R (IC_{50} > 10 μM) which has high receptor sequence homology to the mMC3R.[34, 140]

The 9 ligands with EC_{50}s less than 1,000 nM at the mMC3R had binding IC_{50}s less than 5,500 nM. Compared to SKY4-48-1, Ac-His-DPhe-Arg-Trp-NH_2, the fold decrease in IC_{50} ranged from 9-fold for SKY4-48-15 to 120-fold for SKY6-24-3 (IC_{50} = 5,350 and 440 nM, respectively). When compared to the mMC3R agonist function data, the binding data generally complement those observed results. That is to say, compounds

which possessed nanomolar agonist function activity tended to possess similar results for IC_{50} binding values. All of the compounds were greater binders at the mMC4R over the mMC3R. This result is consistent with the other melanocortin ligands, NDP-MSH and Ac-His-DPhe-Arg-Trp-NH_2 (SKY4-48-1) which were included in this study. The binding activity for the selected mMC3R TACOs at the mMC4R tended to be equipotent, IC_{50} < 3-fold difference, compared to SKY4-48-1 (IC_{50} = 121 nM). In addition, relative to the greater than 100-fold increases in binding potencies at the mMC3R, the most potent binder at the mMC4R, SKY4-48-18, possessed just a 9-fold increase (IC_{50} = 13 nM) in binding relative to the tetrapeptide SKY4-48-1. Perhaps the agonist selectivity and nanomolar potencies which were achieved at the mMC3R may be rationalized by the 9- to more than 100-fold increase in binding IC_{50} which was observed relative to the control peptide SKY4-48-1, Ac-His-DPhe-Arg-Trp-NH_2 (Table 4-3, Figure 4-6b).

Is the Ac-Xaa^1-Arg-(pI)DPhe-Xaa-NH_2 Scaffold a chimeric AgRP/MC sequence?

Thus far we have discussed the SAR of the new TACO scaffold, Ac-Xaa^1-Arg-(pI)DPhe-Xaa^4-NH_2, relative to the highly conserved endogenous "His-Phe-Arg-Trp" agonist motif.[35] It appears peptides based on the TACO scaffold share few SAR features with melanocortin compounds which are based on the endogenous agonist peptides, and we contributed some of the observed pharmacology to the unusual reversed Arg-Phe template. However, the possibility cannot be omitted that the reported TACO scaffold is a hybrid combination of the AgRP/AISP signaling sequence "Arg-Phe-Phe" and the core melanocortin signaling sequence "His-Phe-Arg-Trp," and that this could help rationalize additional aspects of the observed SAR. A chimeric NDP-MSH/AGRP peptide, Ac-Ser-

Tyr-Ser-Nle-Glu-His-Arg-Phe-Phe-Gly-Lys-Pro-Val-NH_2, is a more potent stimulator for the mMC3R over the mMC4R (480 nM vs 930 nM).[141] Moreover, a series of disulfide cyclized chimeric α-MSH/ASIP analogs, template Ac-c[Cys-Arg-(X)Phe-Cys]-(X)Trp-NH_2 where X is D or L stereochemistry, are reported to possess hMC3R-selective non-competitive binding.[142] The unusual sequence of the TACO scaffold with respect to the endogenous "His-Phe-Arg-Trp" and "Arg-Phe-Phe" sequences gives additional insights into the requirements for receptor recognition and selectivity for the melanocortin subtypes.

Conclusions

Herein, a double-substitution library of compounds which were pharmacologically characterized at the mouse melanocortin 1, 3, 4, and 5 receptors is reported. The lead compound was identified from a mixture-based positional scan of more than 12.9 million tetrapeptides. Notably, nine compounds demonstrated agonist activity EC_{50} < 1,000 nM at the mMC3R, all of which were observed to be competitive antagonists at the mMC4R. These compounds could be used as molecular probes to explore the mechanism with how the melanocortin-3 and -4 receptors synergistically work together to maintain energy homeostasis. Furthermore, this newly discovered TACO scaffold, Ac-Xaa^1-Arg-(pI)DPhe-Xaa^4-NH_2 is distinct from the classic His-Phe-Arg-Trp melanocortin template sequence. The unique combination of switching residues and sidechain replacements which are required to produce the reported scaffold from the classic signaling sequence illustrate the strength of mixture-based positional scanning to produce new and unbiased ligands.

Experimental Section

Mixture-Based Positional Scan Library

TPI 924 was synthesized by our collaborators at the Torrey Pines Institute for Molecular Studies as previously described[28] using an optimized solid-phase simultaneous multi peptide synthesis approach on p-methylbenzhydrylamine (MBHA) polystyrene resin.[105, 109, 143-144] The library was constructed using 60 different L-, D-, and unnatural amino acids which resulted in 240 acetylated tetrapeptide mixtures, each containing 216,000 acetylated tetrapeptides, with a total diversity of 12,960,000 acetylated tetrapeptides. The 60 different amino acids are Ala, Asp, Glu, Phe, Gly, His, Ile, Lys, Leu, Met, Asn, Pro, Gln, Arg, Ser, Thr, Val, Trp, Tyr, DAla, DAsp, DGlu, DPhe, DHis, DIle, DLys, DLeu, DMet, DAsn, DPro, DGln, DArg, DSer, DThr, DVal, DTrp, DTyr, Nle, DNle, Cha, DCha, PyrAla, DPyrAla, ThiAla, DThiAla, Tic, DTic, (pCl)Phe, (pCl)DPhe, (pI)Phe, (pI)DPhe, (pNO_2)Phe, (pNO_2)DPhe, 2-Nal, 2-DNal, β-Ala, ε-Aminocaproic acid, Met[O_2], dehydPro, and (3I)Tyr.[112, 145]

Single Tetrapeptide Library

The single tetrapeptides described herein were synthesized, by Skye Doering, manually using a combination of microwave-assisted and standard room temperature N-α-Fluorenylmethyloxycarbonyl (Fmoc) solid-phase peptide synthesis on Rink-amide MBHA resin (Peptides International, 0.35 meq/g).[97-98] The peptides were synthesized in parallel in groups of eight compounds. The resin (0.5 mmol scale) was initially swelled in dichloromethane (DCM) for 1 hr. This was followed by resin activation with 15 mL of

20% piperidine in N,N-dimethylformamide (DMF). The reaction was mixed via bubbling the mixture with nitrogen gas for 2 min at room temperature. The reaction vessel was drained, additional 15 mL of 20% piperidine in DMF was added, and the reaction vessel was heated to 75 °C in a microwave (Discover SPS, CEM Corporation) with 30 W power for 4 min. The reaction was allowed to cool and then washed with DMF (3 x 15 mL). Following a positive ninhydrin test,[98] the Fmoc protected amino acid (3.1 eq), N,N,N′,N′-Tetramethyl-O-(1H-benzotriazol-1-yl)uronium hexafluorophosphate (HBTU, Peptides International) (3 eq), and diisopropylethylamine (DIEA, Sigma-Aldrich) (5 eq) were dissolved in DMF and added to the reaction vessel. The vessel was heated to 75 °C in a microwave with 30 W power for 5 min. The amino acid building blocks used in this study were: Fmoc-Arg(Pbf)-OH (Peptides International), Fmoc-3Bal-OH (Bachem), Fmoc-Bip-OH (Synthe Tech), Fmoc-Glu(OtBu)-OH (Peptides International), Fmoc-Gly-OH (Peptides International), Fmoc-His(Trt)-OH (Peptides International), Fmoc-Lys(Boc)-OH (Peptides International), Fmoc-Nle-OH (Peptides International), Fmoc-D-4-I-Phe-OH (AnaSpec), Fmoc-Phe-OH (Peptides International), Fmoc-D-Phe-OH (Peptides International), Fmoc-Pro-OH (Peptides International), Fmoc-Nal(2')-OH (Synthe Tech), Fmoc-D-Nal(2')-OH (Peptides International), Fmoc-Ser(tBu)-OH (Peptides International), Fmoc-Tic-OH (Synthe Tech), Fmoc-Trp(Boc)-OH (Peptides International), Fmoc-Tyr(tBu)-OH (Peptides International), and Fmoc-Val-OH (Peptides International). For coupling Arg the equivalents of the reagents were increased Arg (5 eq), HBTU (5.1 eq), and DIEA (7 eq) as was the microwave coupling time (10 min). For coupling His, the microwave temperature was decreased to 50 °C. After coupling in the microwave, the reaction was allowed to cool and was washed in DMF (3 x 15 mL).

Following a negative ninhydrin test for primary amines, or a chloranil test for secondary amines, the entire deprotection and coupling procedure was repeated for the remaining residues.[98] After coupling the third amino acid residue, the resin was dried and then divided into eight separate reaction wells. With a semi-automatic synthesizer (LabTech 1, Advanced ChemTech), the eight resins were swelled in DCM (10 mL, 1 hr, 350 RPM) and then washed in DMF (3 x 10 mL, 1 min, 350 RPM). The resins were deprotected with 20% piperidine in DMF (10 mL for 2 min, and 10 mL for 18 min). The remaining residue was coupled using the same equivalents as above. The reactions were allowed to couple at RT for 1 hour. Following a negative ninhydrin test for primary amines, or a chloranil test for secondary amines,[98] the resins were deprotected with 20% piperidine in DMF (10 mL 2 min, and 10 mL 18 min at RT), and subsequently acetylated with a 10 mL solution of acetic anhydride and pyridine (3:1) for 30 min at RT. The resin was then washed in DMF (3 x 10 mL) then again in methanol (1 x 10 mL) and dried overnight.

The peptides were cleaved from the resin and globally deprotected in parallel. A 10 mL mixture of trifluoroacetic acid (Sigma-Aldrich), thioanisole (Fluka), triisopropylsilane (Aldrich), and water (91:3:3:3) was added to each well and allowed to stir for 1 hour at RT at 350 RPMs. The mixture was drained and collected into 50 mL Falcon tubes. Upon the addition of cold 0 °C diethyl ether a precipitant was formed. The white precipitant was pelleted using a Sorvall Legend XTR centrifuge with a swinging bucket rotor (4,000 RPM, 4 °C, 4 min). The pellet was washed with additional diethyl ether and pelleted (3 x). The pellet was allowed to dry in a desiccator overnight.

The crude peptides were purified by RP-HPLC with a photodiode array detector (Shimadzu Corp.) on a semi-preparative scale with a flow rate of 5 mL/min on a RP-HPLC C18 bonded column (Vydac 218TP1010, 1 cm x 25 cm) in pairs. Mixtures of crude peptides were combined and purified together in order to decrease instrument time and solvent usage. The collected fractions were concentrated on a rotary evaporator and subsequently lyophilized to a fine white powder. The pure compounds were analytically characterized by RP-HPLC using two different solvent systems. The analytical method was either acetonitrile or methanol in a 10% to 90% gradient in 0.1% TFA in water over 35 minutes at a rate of 1.5 mL/min using an analytical Vydac C18 column (Vydac 218TP104, 4.6 mm x 25 cm) and purity was monitored by integrating the area under the curve at λ=214 nm. The mass was confirmed using a matrix-assisted laser desorption/ionization-time of flight mass spectrometer (MALDI-TOF MS) analysis using an α-cyano-4-hydroxycinnamic acid matrix (AB-Sciex 5800, University of Minnesota Department of Chemistry Mass Spectrometry Laboratory). The control peptides Ac-His-DPhe-Arg-Trp-NH_2 and NDP-MSH were synthesized individually using the microwave method described above. These compounds were also purified individually using the same RP-HLPC instruments.

β-Galactosidase Bioassay

This bioassay was implemented for the primary mixture-based positional scanning library TPI924 by Marvin Dirain. The ligands described in this study were assayed in HEK293 cells stably expressing the mouse melanocortin-1, -3, -4, and -5 receptor subtypes which were cloned into the cells using a $pCDNA_3$ vector which has

been previously described by our laboratory.[67] Stably transfected HEK293 cells were plated with media (Dulbecco's Modified Eagle Medium [DMEM] supplemented with 10% Bovine Serum and 1% Penicillin Streptomycin) into a 10 cm dish such that, 24 hours later the cells reached approximately 40% confluency. Twenty-four hours post plating, the cells were transiently transfected with 4 μg CRE-PBKS per 10 cm plate of cells using the calcium phosphate method.[130] Twenty-four hours post transfection, the cells were plated onto collagen treated Nunclon Delta Surface 96-well plates (Thermo Fischer Scientific) and incubated at 37 °C and 5% CO_2. Forty-eight hours post transfection, the plates were stimulated with the compound mixtures. The compound mixtures were dissolved in water up to a concentration of 1,000 μg/mL and stored at -20 °C until use. The cell media was aspirated and to each well 40 μL of the peptide mixture from TPI 924 (100 μg/mL and 50 μg/mL) in assay media (1.0 mL 1% bovine serum albumin [BSA] in phosphate buffered saline [PBS] and 1.0 mL 100x isobutylmethylxanthine in 98.0 mL DMEM). Controls included NDP-MSH (10^{-6} to 10^{-13} M), forskolin (10 μM), and plain assay media. The plates were incubated at 37 °C and 5% CO_2 for six hours. Post stimulation, the media was aspirated and 50 μL of lysis buffer (250 mM Tris-HCl pH=8.0, Triton X-100 in water) was added. The plates were stored at -80 °C for up to two weeks.

The plates were thawed, assessed for protein content, and substrate was added to develop the plates. Protein content was assessed by adding, 10 μL of cell lysate was added to 200 μL of BioRad dye solution (1:4 dilution with water) in another 96 well plate, and the absorbance was read using a 96 well plate reader (Molecular Devices) at λ = 595 nm. To the remaining 40 μL of cell lysate, 40 μL of, 37 °C, 0.5% BSA in PBS was

added in addition to 150 μL of the β-galactosidase substrate (60 mM Na_2HPO_4, 1 mM $MgCl_2$, 10 mM KCl, 50 mM 2-mercaptoethanol, and 660 μM 2-nitrophenyl β-D-galactopyranoside). The plates were incubated at 37 °C and periodically read on the 96 well plate reader until the absorbance at λ = 405 nm reached approximately 1.0 relative absorbance units for the positive controls. The β-galactosidase activity was normalized to both protein content and maximal response of the positive controls.

AlphaScreen Bioassay

This bioassay was used to produce the dose-response curves and subsequent EC_{50} determination for the reported TACO library. The ligands described in this study were assayed by Katie Freeman and Sathya Schnell in HEK293 cells stably expressing the mouse melanocortin-1, -3, -4, and -5 receptor subtypes which were cloned into the cells using a $pCDNA_3$ vector which has been previously described by our laboratory.[28] The cAMP signaling was directly measured using the AlphaScreen (Perkin-Elmer, Cat#6760635M) assay protocol as described by manufacturer as previously reported.[68, 97, 136] Cells were grown in an incubator at 37 °C with 5% CO_2 in cell media [Dulbecco's modified Eagle's medium (DMEM) containing 10% newborn calf serum (NCS) and 1% penicillin/streptomycin] in 10 cm plates to 70-95% confluency the day of the assay.

Cells were disassociated with 1 mL 37 °C Versene solution (Gibco), re-suspended in 5 mL 37 °C cell media, and pelleted by centrifugation at 800 RPM for 5 min at room temperature (Sorvall Legend XTR centrifuge, swinging bucket rotor). The supernatant was subsequently aspirated and the cell pellet was re-suspended in 37 °C Dulbecco's phosphate buffered saline solution (DPBS 1X without $CaCl_2$ or $MgCl_2$, Gibco). The cells

were manually counted using a hemocytometer (10 µL cell mixture added to 10 µL of Trypan blue BioRad dye). The cells were again centrifuged (800 RPM, 5 min, RT) and the supernatant was aspirated. The cell pellet was then re-suspended in a solution of freshly made stimulation buffer [Hank's Balanced Salt Solution (HBSS 10 X without $NaHCO_3$ or phenol red, Gibco), 0.5 mM isobutylmethylxanthine (IBMX), 5 mM HEPES buffer solution (1 M, Gibco), 0.1% bovine serum albumin (BSA) in Milli-Q water, pH=7.4] to a final concentration of 10,000 cells/µL.

A solution of cells and anti-cAMP acceptor beads in stimulation buffer was then prepared (1,000 cells/µL and 0.5 µg/µL AlphaScreen anti-cAMP acceptor beads in stimulation buffer). The 10 µL of the cell/acceptor bead solution was then added each well in a 384-well microplate (OptiPlate-384, Perkin-Elmer). To each well an additional 5 µL of ligand was added and the concentration of the ligand was adjusted such that the final concentration in the well reflected the desired concentration. The plate was then sealed and incubated at room temperature in the dark for two hours. Compounds included on each plate were NDP-MSH (10^{-6} to 10^{-12} M), forskolin (10^{-4} M), and stimulation buffer alone (blank control). The compounds described in this study were initially assayed from 10^{-4} to 10^{-10} M and the range was adjusted accordingly in later experiments.

The light sensitive biotinylated cAMP/streptavidin coated donor bead mixture in lysis buffer was prepared, 30 min prior to the end of the initial two hour plate incubation, under green light (0.5 µg/µL AlphaScreen donor beads and 0.62 µM AlphaScreen cAMP biotinylated tracer in a solution of 10% Tween-20, 5 mM HEPES, and 0.1% BSA in Milli-Q water, pH=7.4). Post the initial plate incubation, 10 µL of the biotinylated cAMP/streptavidin donor bead lysis buffer was added to each well under green light. The

plate was resealed, covered with aluminum foil, and incubated for a second two hour incubation in the dark. After incubation, the plate was read via an EnSpire Alpha Plate Reader (Perkin-Elmer) using a protocol preset by the manufacturer. The data were fitted with dose-response curves and EC_{50} values were calculated by a nonlinear regression using GraphPad Prism (v4.0) software.

^{125}I-NDP-MSH Preparation and Purification

NDP-MSH was monoradioiodinated for the use in competition binding assays by Robert Speth. The peptide was radioiodinated with $Na^{125}I$ using the previously described chloramine T procedure.[146] The monoradioiodinated peptide was resolved from the uniodinated and diradioiodinated peptide via RP-HPLC using a C18 reverse phase column eluted isocratically with an acetonitrile:trimethylamine phosphate (pH 3.0) mobile phase. The column eluate containing the monoradioiodinated peptide was diluted in a solvent mixture (2 parts 24% acetonitrile: 76% triethylamine phosphate, pH 3.0: 1 part milliQ water) containing a 2 mg/mL bovine albumin stabilizer. The resulting yield (lot number: 150326A) was 1.9 mL contining 1126 μCi of monoiodinated NDP-MSH with a theoretical specific activity of 2175 Ci/mmol. The radioligand was stored at -80°C in a lead pig until use.

^{125}I-NDP-MSH Competitive Binding Assay

This bioassay was used to produce the dose-response curves and subsequent IC_{50} determination for selected compounds from the reported TACO library (the 10 most potent EC_{50} values at the mMC3R) at the mMC3R and mMC4R. Using the HEK293 cells stably transfected with the selected mouse melanocortin receptors, as described above,

were used in this assay. Cells were plated into 12-well treated polystyrene plates (Corning Life Sciences, Cat. # 353043) 48-hours prior to the binding experiment such that each well reached greater than 90% confluency the day of the assay. On the day of the assay, media was aspirated and a 500 μL solution of 0.1% BSA in DMEM containing the experimental compound (10^{-4} to 10^{-10} M) and a constant 100,000 cpm/well ^{125}I NDP-MSH were added each well. The plates were incubated at 37°C with 5% CO_2 for 1 hour. Post incubation, the media was aspirated, each well was washed with 500 μL assay media, and cells were lysed with 500 μL of 0.1 M NaOH and 500 μL of 1% Triton x-100.

Following a 10-15 minute room temperature incubation, the cell lysate mixture was transferred to 12x75 mm polystyrene tubes and the radioactivity was quantified using a WIZARD^2 Automatic Gamma Counter (Perkin-Elmer). The specific binding for each well was determined by subtracting the counts obtained from the cell lysate which was incubated with the non-radioactive 10^{-6} M NDP-MSH. Each experiment included the experimental determination of the specific binding for NDP-MSH as a positive control. The specific binding for each compound was normalized to 100% relative to the specific binding determined for non-radiolabeled NDP-MSH. The data were analyzed using GraphPad Prism (v4.0; GraphPad, Inc), and dose-response curves in addition to the corresponding IC_{50} values were calculated by a non-linear regression method. Each reported value represents the mean and standard error of the mean (SEM) of, at least, two independent experiments each containing two experimental replicates.

Chapter 4 Tables and Figures:

Table 4-1: Summary of agonist and antagonist data collected at the mMC3R and mMC4R

		mMC3R		mMC4R	
ID	**Sequence**	**Agonist EC_{50} ± SEM (nM)**	**Antagonist pA_2 ± SEM**	**Agonist EC_{50} ± SEM (nM)**	**Antagonist pA_2 ± SEM**
NDP-MSH	Ac-Ser-Tyr-Ser-Nle-Glu-His-DPhe-Arg-Trp-Gly-Lys-Pro-Val-NH_2	0.09 ± 0.01	Full Agonist	0.8 ± 0.1	Full Agonist
SKY4-48-1	Ac-His-DPhe-Arg-Trp-NH_2	73 ± 10	Full Agonist	16 ± 3	Full Agonist
SKY6-24-2	Ac-His-Arg-(pI)DPhe-Tic-NH_2	40 ± 7	Full Agonist	> 100,000	7.0 ± 0.2
SKY4-48-2	Ac-Arg-Arg-(pI)DPhe-Bip-NH_2	45% @ 100 µM	5.3 ± 0.1	32% @ 100 µM	5.8 ± 0.1
SKY4-48-3	Ac-His-Arg-(pI)DPhe-Bip-NH_2	53% @ 100 µM	No Activity	43% @ 100 µM	No Activity
SKY4-48-4	Ac-Bip-Arg-(pI)DPhe-Bip-NH_2	> 100,000	No Activity	24% @ 100 µM	No Activity
SKY4-48-5	Ac-3Bal-Arg-(pI)DPhe-Bip-NH_2	51% @ 100 µM	No Activity	35% @ 100 µM	No Activity
SKY5-146-1	Ac-Tic-Arg-(pI)DPhe-Bip-NH_2	100,000	No Activity	> 100,000	No Activity
SKY4-48-7	Ac-Phe-Arg-(pI)DPhe-Bip-NH_2	30% @ 100 µM	No Activity	> 100,000	No Activity
SKY4-48-8	Ac-Nal(2')-Arg-(pI)DPhe-Bip-NH_2	14,000 ± 1,100	Full Agonist	7,900 ± 1,300	Full Agonist
SKY5-146-2	Ac-DNal(2')-Arg-(pI)DPhe-Bip-NH_2	30% @ 100 µM	5.6 ± 0.2	42% @ 100 µM	6.6 ± 0.1
SKY4-48-10	Ac-Arg-Arg-(pI)DPhe-3Bal-NH_2	160 ± 40	Full Agonist	24% @ 100 µM	6.6 ± 0.1
SKY4-48-11	Ac-His-Arg-(pI)DPhe-3Bal-NH_2	460 ± 50	Full Agonist	47% @ 100 µM	6.4 ± 0.1

SKY4-48-12	Ac-Bip-Arg-(pI)DPhe-3Bal-NH_2	2,300 ± 920	Full Agonist	> 100,000	No Activity
SKY4-48-13	Ac-3Bal-Arg-(pI)DPhe-3Bal-NH_2	2,500 ± 770	Full Agonist	> 100,000	5.7 ± 0.3
SKY4-48-14	Ac-Tic-Arg-(pI)DPhe-3Bal-NH_2	8,900 ± 2,400	Full Agonist	> 100,000	5.2 ± 0.1
SKY4-48-15	Ac-Phe-Arg-(pI)DPhe-3Bal-NH_2	930 ± 520	Full Agonist	> 100,000	5.7 ± 0.1
SKY4-48-16	Ac-Nal(2')-Arg-(pI)DPhe-3Bal-NH_2	1,500 ± 530	Full Agonist	> 100,000	6.0 ± 0.7
SKY4-48-17	Ac-DNal(2')-Arg-(pI)DPhe-3Bal-NH_2	4,000 ± 1,300	Full Agonist	45% @ 100 µM	6.6 ± 0.1
SKY4-48-18	Ac-Arg-Arg-(pI)DPhe-Tic-NH_2	16 ± 3	Full Agonist	> 100,000	7.8 ± 0.3
SKY4-48-20	Ac-Bip-Arg-(pI)DPhe-Tic-NH_2	13,000 ± 3,300	Full Agonist	> 100,000	5.7 ± 0.1
SKY4-48-21	Ac-3Bal-Arg-(pI)DPhe-Tic-NH_2	2,500 ± 190	Full Agonist	37% @ 100 µM	6.2 ± 0.1
SKY6-24-1	Ac-Tic-Arg-(pI)DPhe-Tic-NH_2	3,900 ± 940	Full Agonist	36% @ 100 µM	6.0 ± 0.2
SKY4-48-23	Ac-Phe-Arg-(pI)DPhe-Tic-NH_2	610 ± 200	Full Agonist	> 100,000	6.3 ± 0.1
SKY4-48-24	Ac-Nal(2')-Arg-(pI)DPhe-Tic-NH_2	3,000 ± 940	Full Agonist	33% @ 100 µM	6.4 ± 0.1
SKY6-24-3	Ac-DNal(2')-Arg-(pI)DPhe-Tic-NH_2	600 ± 210	Full Agonist	32% @ 100 µM	6.4 ± 0.1
SKY4-48-26	Ac-Arg-Arg-(pI)DPhe-Phe-NH_2	540 ± 190	Full Agonist	> 100,000	5.7 ± 0.1
SKY5-146-3	Ac-His-Arg-(pI)DPhe-Phe-NH_2	1,100 ± 240	Full Agonist	> 100,000	5.6 ± 0.1
SKY4-48-28	Ac-Bip-Arg-(pI)DPhe-Phe-NH_2	77% @ 100 µM	No Activity	> 100,000	5.6 ± 0.1
SKY5-146-4	Ac-3Bal-Arg-(pI)DPhe-Phe-NH_2	37% @ 100 µM	No Activity	> 100,000	No Activity

SKY4-48-30	Ac-Tic-Arg-(pI)DPhe-Phe-NH_2	> 100,000	No Activity	> 100,000	No Activity
SKY4-48-31	Ac-Phe-Arg-(pI)DPhe-Phe-NH_2	50% @ 100 μM	No Activity	> 100,000	No Activity
SKY4-48-32	Ac-Nal(2') -Arg-(pI)DPhe-Phe-NH_2	42% @ 100 μM	No Activity	> 100,000	No Activity
SKY4-48-33	Ac-DNal(2') -Arg-(pI)DPhe-Phe-NH_2	> 100,000	5.7 ± 0.1	> 100,000	6.9 ± 0.1
SKY4-48-34	Ac-Arg-Arg-(pI)DPhe-Nal(2')-NH_2	51% @ 100 μM	5.8 ± 0.1	> 100,000	6.1 ± 0.1
SKY4-48-35	Ac-His-Arg-(pI)DPhe-Nal(2')-NH_2	57% @ 100 μM	5.6 ± 0.1	35% @ 100 μM	6.1 ± 0.2
SKY4-48-36	Ac-Bip-Arg-(pI)DPhe-Nal(2')-NH_2	> 100,000	No Activity	> 100,000	No Activity
SKY4-48-37	Ac-3Bal-Arg-(pI)DPhe-Nal(2')-NH_2	> 100,000	No Activity	> 100,000	No Activity
SKY4-48-38	Ac-Tic-Arg-(pI)DPhe-Nal(2')-NH_2	> 100,000	No Activity	> 100,000	5.9 ± 0.1
SKY4-48-39	Ac-Phe-Arg-(pI)DPhe-Nal(2')-NH_2	44% @ 100 μM	No Activity	> 100,000	5.9 ± 0.1
SKY4-48-40	Ac-Nal(2')-Arg-(pI)DPhe-Nal(2')-NH_2	39% @ 100 μM	No Activity	> 100,000	No Activity
SKY5-146-5	Ac-DNal(2')-Arg-(pI)DPhe-Nal(2')-NH_2	43% @ 100 μM	5.4 ± 0.1	39% @ 100 μM	6.7 ± 0.1
SKY4-48-42	Ac-Arg-Arg-(pI)DPhe-DNal(2')-NH_2	57 ± 15	Full Agonist	> 100,000	6.4 ± 0.1
SKY4-48-43	Ac-His-Arg-(pI)DPhe-DNal(2')-NH_2	5,000 ± 2,100	Full Agonist	50% @ 100 μM	5.5 ± 0.1
SKY4-48-44	Ac-Bip-Arg-(pI)DPhe-DNal(2')-NH_2	32% @ 100 μM	No Activity	> 100,000	No Activity
SKY4-48-45	Ac-3Bal-Arg-(pI)DPhe-DNal(2')-NH_2	34% @ 100 μM	No Activity	38% @ 100 μM	No Activity
SKY4-48-46	Ac-Tic-Arg-(pI)DPhe-DNal(2')-NH_2	42% @ 100 μM	No Activity	33% @ 100 μM	No Activity

SKY4-48-47	Ac-Phe-Arg-(pI)DPhe-DNal(2')-NH_2	22% @ 100 μM	No Activity	> 100,000	6.1 ± 0.4
SKY4-48-48	Ac-Nal(2')-Arg-(pI)DPhe-DNal(2')-NH_2	31% @ 100 μM	No Activity	> 100,000	No Activity
SKY4-48-49	Ac-DNal(2')-Arg-(pI)DPhe-DNal(2')-NH_2	40% @ 100 μM	5.6 ± 0.1	37% @ 100 μM	5.9 ± 0.1

Summary of all the function data at the selected mMC3R and mMC4R using the AlphaScreen. All of the compounds were assessed for agonist activity up to a concentration of 100 μM and values are represented as EC_{50} in nM. Compounds which did not produce a full dose-response curve were tabulated as a percent of the NDP-MSH maximal positive control, and compounds with < 20% activity were denoted as EC_{50} > 100,000. These experiments were performed with duplicate replicates in three independent experiments. Compounds were assessed for antagonist activity if they did not produce a full dose-response. Antagonist activity was assessed by co-administering NDP-MSH and the compound at concentrations of 10,000 nM, 5,000 nM, 1,000 nM, and 500 nM and measuring the resulting shift in EC_{50} and calculating a subsequent pA_2 value [-Log(K_i)] via a Schild analysis.[51] The antagonist experiment was performed in triplicate unless there was no shift in EC_{50} activity was observed in which case it was tabulated as "no activity."

Table 4-2: Summary of Agonist Data Collected at the mMC1R and mMC5R

ID	Sequence	mMC1R EC_{50} ± SEM (nM)	mMC5R EC_{50} ± SEM (nM)
NDP-MSH	Ac-Ser-Tyr-Ser-Nle-Glu-His-DPhe-Arg-Trp-Gly-Lys-Pro-Val-NH_2	0.02 ± 0.001	0.18 ± 0.02
SKY4-48-1	Ac-His-DPhe-Arg-Trp-NH_2	20 ± 1	3.0 ± 0.5
SKY6-24-2	Ac-His-Arg-(pI)DPhe-Tic-NH_2	0.71 ± 0.04	17 ± 3
SKY4-48-2	Ac-Arg-Arg-(pI)DPhe-Bip-NH_2	44% @ 100 µM	5,000 ± 1,600
SKY4-48-3	Ac-His-Arg-(pI)DPhe-Bip-NH_2	> 100,000	69,000 ± 31,000
SKY4-48-4	Ac-Bip-Arg-(pI)DPhe-Bip-NH_2	> 100,000	> 100,000
SKY4-48-5	Ac-3Bal-Arg-(pI)DPhe-Bip-NH_2	> 100,000	72,000 ± 28,000
SKY5-146-1	Ac-Tic-Arg-(pI)DPhe-Bip-NH_2	39% @ 100 µM	71,000 ± 29,000
SKY4-48-7	Ac-Phe-Arg-(pI)DPhe-Bip-NH_2	67% @ 100 µM	68,000 ± 32,000
SKY4-48-8	Ac-Nal(2')-Arg-(pI)DPhe-Bip-NH_2	7,600 ± 1,200	8,300 ± 1,600
SKY5-146-2	Ac-DNal(2')-Arg-(pI)DPhe-Bip-NH_2	> 100,000	67,000 ± 33,000
SKY4-48-10	Ac-Arg-Arg-(pI)DPhe-3Bal-NH_2	56 ± 20	210 ± 52
SKY4-48-11	Ac-His-Arg-(pI)DPhe-3Bal-NH_2	70 ± 7	270 ± 67
SKY4-48-12	Ac-Bip-Arg-(pI)DPhe-3Bal-NH_2	3,100 ± 490	5,500 ± 2,900
SKY4-48-13	Ac-3Bal-Arg-(pI)DPhe-3Bal-NH_2	1,800 ± 590	18,000 ± 7,800
SKY4-48-14	Ac-Tic-Arg-(pI)DPhe-3Bal-NH_2	38% @ 100 µM	26,000 ± 7,200
SKY4-48-15	Ac-Phe-Arg-(pI)DPhe-3Bal-NH_2	330 ± 180	1,300 ± 480
SKY4-48-16	Ac-Nal(2')-Arg-(pI)DPhe-3Bal-NH_2	460 ± 210	5,400 ± 2,900
SKY4-48-17	Ac-DNal(2')-Arg-(pI)DPhe-3Bal-NH_2	210 ± 50	> 100,000
SKY4-48-18	Ac-Arg-Arg-(pI)DPhe-Tic-NH_2	0.51 ± 0.08	8.8 ± 0.7
SKY4-48-20	Ac-Bip-Arg-(pI)DPhe-Tic-NH_2	440 ± 70	16,000 ± 8,000
SKY4-48-21	Ac-3Bal-Arg-(pI)DPhe-Tic-NH_2	72 ± 26	4,100 ± 1,300
SKY6-24-1	Ac-Tic-Arg-(pI)DPhe-Tic-NH_2	93 ± 26	570 ± 110
SKY4-48-23	Ac-Phe-Arg-(pI)DPhe-Tic-NH_2	8 ± 3	200 ± 70
SKY4-48-24	Ac-Nal(2')-Arg-(pI)DPhe-Tic-NH_2	54 ± 18	4,400 ± 2,700
SKY6-24-3	Ac-DNal(2')-Arg-(pI)DPhe-Tic-NH_2	7 ± 2	250 ± 70
SKY4-48-26	Ac-Arg-Arg-(pI)DPhe-Phe-NH_2	55 ± 9	340 ± 90
SKY5-146-3	Ac-His-Arg-(pI)DPhe-Phe-NH_2	92 ± 19	680 ± 140
SKY4-48-28	Ac-Bip-Arg-(pI)DPhe-Phe-NH_2	2,600 ± 1,600	69% @ 100 µM
SKY5-146-4	Ac-3Bal-Arg-(pI)DPhe-Phe-NH_2	1,200 ± 450	35% @ 100 µM
SKY4-48-30	Ac-Tic-Arg-(pI)DPhe-Phe-NH_2	3,500 ± 1,200	21% @ 100 µM
SKY4-48-31	Ac-Phe-Arg-(pI)DPhe-Phe-NH_2	600 ± 110	52% @ 100 µM
SKY4-48-32	Ac-Nal(2') -Arg-(pI)DPhe-Phe-NH_2	760 ± 600	49% @ 100 µM
SKY4-48-33	Ac-DNal(2') -Arg-(pI)DPhe-Phe-NH_2	540 ± 210	> 100,000
SKY4-48-34	Ac-Arg-Arg-(pI)DPhe-Nal(2')-NH_2	210 ± 100	1,000 ± 350
SKY4-48-35	Ac-His-Arg-(pI)DPhe-Nal(2')-NH_2	350 ± 90	2,900 ± 1,100
SKY4-48-36	Ac-Bip-Arg-(pI)DPhe-Nal(2')-NH_2	23% @ 100 µM	21% @ 100 µM

SKY4-48-37	Ac-3Bal-Arg-(pI)DPhe-Nal(2')-NH_2	12,000 ± 4,000	50% @ 100 μM
SKY4-48-38	Ac-Tic-Arg-(pI)DPhe-Nal(2')-NH_2	66% @ 100 μM	48% @ 100 μM
SKY4-48-39	Ac-Phe-Arg-(pI)DPhe-Nal(2')-NH_2	1,000 ± 750	61% @ 100 μM
SKY4-48-40	Ac-Nal(2')-Arg-(pI)DPhe-Nal(2')-NH_2	3,800 ± 2,200	45% @ 100 μM
SKY5-146-5	Ac-DNal(2')-Arg-(pI)DPhe-Nal(2')-NH_2	1,200 ± 390	40% @ 100 μM
SKY4-48-42	Ac-Arg-Arg-(pI)DPhe-DNal(2')-NH_2	280 ± 140	500 ± 100
SKY4-48-43	Ac-His-Arg-(pI)DPhe-DNal(2')-NH_2	3,700 ± 2,400	47% @ 100 μM
SKY4-48-44	Ac-Bip-Arg-(pI)DPhe-DNal(2')-NH_2	5,300 ± 1,100	55% @ 100 μM
SKY4-48-45	Ac-3Bal-Arg-(pI)DPhe-DNal(2')-NH_2	36% @ 100 μM	41% @ 100 μM
SKY4-48-46	Ac-Tic-Arg-(pI)DPhe-DNal(2')-NH_2	770 ± 90	74% @ 100 μM
SKY4-48-47	Ac-Phe-Arg-(pI)DPhe-DNal(2')-NH_2	3,800 ± 1,500	39% @ 100 μM
SKY4-48-48	Ac-Nal(2')-Arg-(pI)DPhe-DNal(2')-NH_2	53% @ 100 μM	40% @ 100 μM
SKY4-48-49	Ac-DNal(2')-Arg-(pI)DPhe-DNal(2')-NH_2	4,000 ± 850	43% @ 100 μM

Summary of all the function data at the selected mouse melanocortin receptors using the ALPHA screen. NDP-MSH and assay media served as both positive and negative controls, respectively. Forskolin served as an additional positive control due to the fact it independently activates adenylate cyclase. All of the compounds were assessed for agonist activity up to a concentration of 100 μM and values are represented as EC_{50} in nM. Compounds which did not produce a full dose-response curve were tabulated as a percent of the NDP-MSH maximal positive control, and compounds with < 20% activity were denoted as EC_{50} > 100,000. These experiments were performed in triplicate.

Table 4-3: Summary of ^{125}I-NDP-MSH Binding Displacement of Selected TACOs at the mMC3R and mMC4R

		mMC3R (IC_{50})		mMC4R (IC_{50})	
Compound	**Sequence**	**Mean ± SEM (nM)**	**Fold Diff.**	**Mean ± SEM (nM)**	**Fold Diff.**
NDP-MSH	Ac-Ser-Tyr-Ser-Nle-Glu-His-DPhe-Arg-Trp-Gly-Lys-Pro-Val-NH_2	5.3 ± 0.7		2.0 ± 0.2	
SKY4-48-1	Ac-His-DPhe-Arg-Trp-NH_2	50500 ± 500	1.0	121 ± 39	1.0
SKY6-24-2	Ac-His-Arg-(pI)DPhe-Tic-NH_2	975 ± 225	52	83 ± 13	1
SKY4-48-10	Ac-Arg-Arg-(pI)DPhe-3Bal-NH_2	965 ± 135	52	93 ± 6	1
SKY4-48-11	Ac-His-Arg-(pI)DPhe-3Bal-NH_2	3400 ± 300	15	275 ± 35	-2
SKY4-48-15	Ac-Phe-Arg-(pI)DPhe-3Bal-NH_2	5350 ± 250	9	850 ± 40	-7
SKY4-48-18	Ac-Arg-Arg-(pI)DPhe-Tic-NH_2	550 ± 120	92	13 ± 3	9
SKY4-48-23	Ac-Phe-Arg-(pI)DPhe-Tic-NH_2	2500 ± 600	20	135 ± 15	1
SKY6-24-3	Ac-DNal(2')-Arg-(pI)DPhe-Tic-NH_2	420 ± 50	120	43 ± 7	3
SKY4-48-26	Ac-Arg-Arg-(pI)DPhe-Phe-NH_2	6500 ± 600	8	455 ± 85	-4
SKY4-48-42	Ac-Arg-Arg-(pI)DPhe-DNal(2')-NH_2	440 ± 70	115	220 ± 10	-2

The 10 most potent TACOs at the mMC3R were selected for ^{125}I NDP-MSH radiolabel competition binding experiments. The compounds were assayed at both the mMC3R and mMC4R, and the reported values are the mean and standard error of the mean of two independent experiments each consisting of duplicate replicates. In addition, NDP-MSH and SKY4-48-1, Ac-His-DPhe-Arg-Trp-NH_2, are included for assay control and reference purposes. The fold difference (Fold Diff.) is in reference to SKY4-48-1.

Table 4-4: Summary of the analytical information for the single tetrapeptides synthesized and characterized in this study. Purity for these compounds is >95%

ID	k' Solvent 1 (Acetonitrile)	k' Solvent 2 (Methanol)	Purity (%)	Observed Mass [M+1]	Calculated Exact Mass
NDP-MSH	4.2	7.8	98.6	*824.0 [M+2]	1645.84
SKY4-48-1	4.4	6.6	> 99	686.3	685.34
SKY6-24-2	6.0	10.7	> 99	785.3	784.23
SKY4-48-2	8.3	12.7	99.1	868.3	867.30
SKY4-48-3	8.3	12.8	> 99	849.3	848.26
SKY4-48-4	11.4	16.0	> 99	935.3	934.30
SKY4-48-5	10.6	15.4	97.1	915.3	914.24
SKY5-146-1	9.8	15.3	99.8	871.3	870.27
SKY4-48-7	9.9	14.8	95.2	859.3	858.27
SKY4-48-8	10.8	15.6	97.5	909.3	908.28
SKY5-146-2	10.2	15.5	99.9	909.3	908.28
SKY4-48-10	7.5	11.8	97.3	846.3	847.24
SKY4-48-11	7.5	12.0	> 99	829.3	828.20
SKY4-48-12	10.9	15.6	> 99	915.2	914.24
SKY4-48-13	12.5	15.0	> 99	895.2	894.18
SKY4-48-14	14.7	14.1	98.4	851.3	850.21
SKY4-48-15	9.7	14.3	> 99	839.2	838.21
SKY4-48-16	10.7	15.1	97.8	889.2	888.22
SKY4-48-17	10.1	14.6	> 99	889.3	888.22
SKY4-48-18	7.0	10.7	> 99	804.2	803.27
SKY4-48-20	10.6	15.0	> 99	871.3	870.27
SKY4-48-21	9.7	14.2	99.3	851.2	850.21
SKY6-24-1	7.9	13.0	95.2	807.3	806.24
SKY4-48-23	9.0	13.0	> 99	795.3	794.24
SKY4-48-24	9.7	14.3	> 99	845.2	844.25
SKY6-24-3	8.7	13.5	> 99	845.3	844.25
SKY4-48-26	6.5	10.7	> 99	792.3	791.27
SKY5-146-3	6.2	10.8	> 99	773.2	772.23
SKY4-48-28	10.1	15.0	96.8	859.3	858.27
SKY5-146-4	9.0	14.6	> 99	839.2	838.21
SKY4-48-30	8.6	13.2	96.0	795.2	794.24
SKY4-48-31	8.8	13.1	> 99	783.2	782.24

SKY4-48-32	6.1	14.3	98.6	833.1	832.25
SKY4-48-33	9.1	13.6	> 99	833.3	832.25
SKY4-48-34	7.6	11.8	> 99	842.4	841.28
SKY4-48-35	9.5	12.0	> 99	823.1	822.24
SKY4-48-36	11.0	15.6	> 99	909.2	908.28
SKY4-48-37	10.0	14.9	97.2	889.2	888.22
SKY4-48-38	9.4	14.2	96.8	845.3	844.25
SKY4-48-39	9.3	14.2	96.3	833.3	832.25
SKY4-48-40	10.2	15.0	> 99	883.3	882.26
SKY5-146-5	9.7	15.0	> 99	883.3	882.26
SKY4-48-42	7.3	11.6	> 99	842.3	841.28
SKY4-48-43	7.3	11.5	97.4	823.2	822.24
SKY4-48-44	9.8	15.2	> 99	909.1	908.28
SKY4-48-45	10.0	14.5	>99	889.2	888.22
SKY4-48-46	9.1	13.5	> 99	845.3	844.25
SKY4-48-47	9.0	13.6	98.0	833.2	832.25
SKY4-48-48	10.0	14.6	> 99	883.3	882.26
SKY4-48-49	10.0	14.4	> 99	883.3	882.26

The k’ is defined as [(Retention Time – Solvent Time)/Retention Time]. The compounds were assessed for purity using two different HPLC solvent systems. Solvent system 1 was a 10% to 90% acetonitrile gradient in 0.1% TFA in water over 35 minutes at a rate of 1.5 mL/min using an analytical Vydac C18 column (Vydac 218TP104). Solvent system 2 was a 10% to 90% methanol gradient in 0.1% TFA in water over 35 minutes using the same flow rate and column as solvent system 1. The purity was assessed by integrating the area under the curve at λ=214 nm. The mass was confirmed using a matrix-assisted laser desorption/ionization-time of flight mass spectrometer (MALDI-TOF MS) using a cyano-4-hydroxycinnamic acid matrix (AB-Sciex 5800, University of Minnesota Department of Chemistry Mass Spectrometry Laboratory). *Note, the mass of NDP-MSH was confirmed using electrospray ionization-time of flight (ESI-TOF) spectrometer

(Bruker BioTOF II, University of Minnesota Department of Chemistry Mass Spectrometry Laboratory).

Figure 4-1: Amino acid building blocks for the reported library

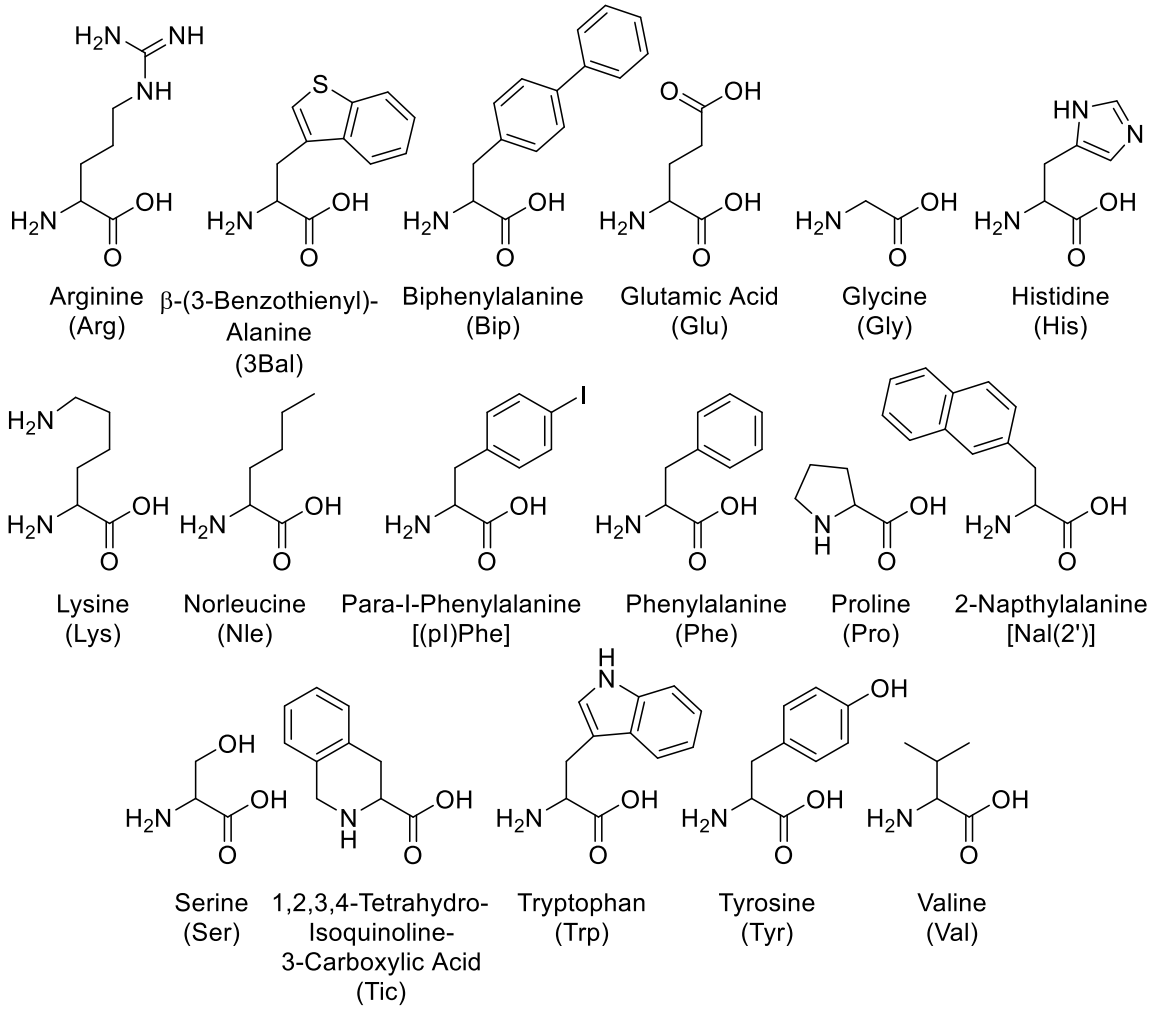

Illustration of the building blocks used within this study. The stereochemistry is not included, however, it is included in the compound sequences.

Figure 4-2: Parallel Purification Method Used in this Study

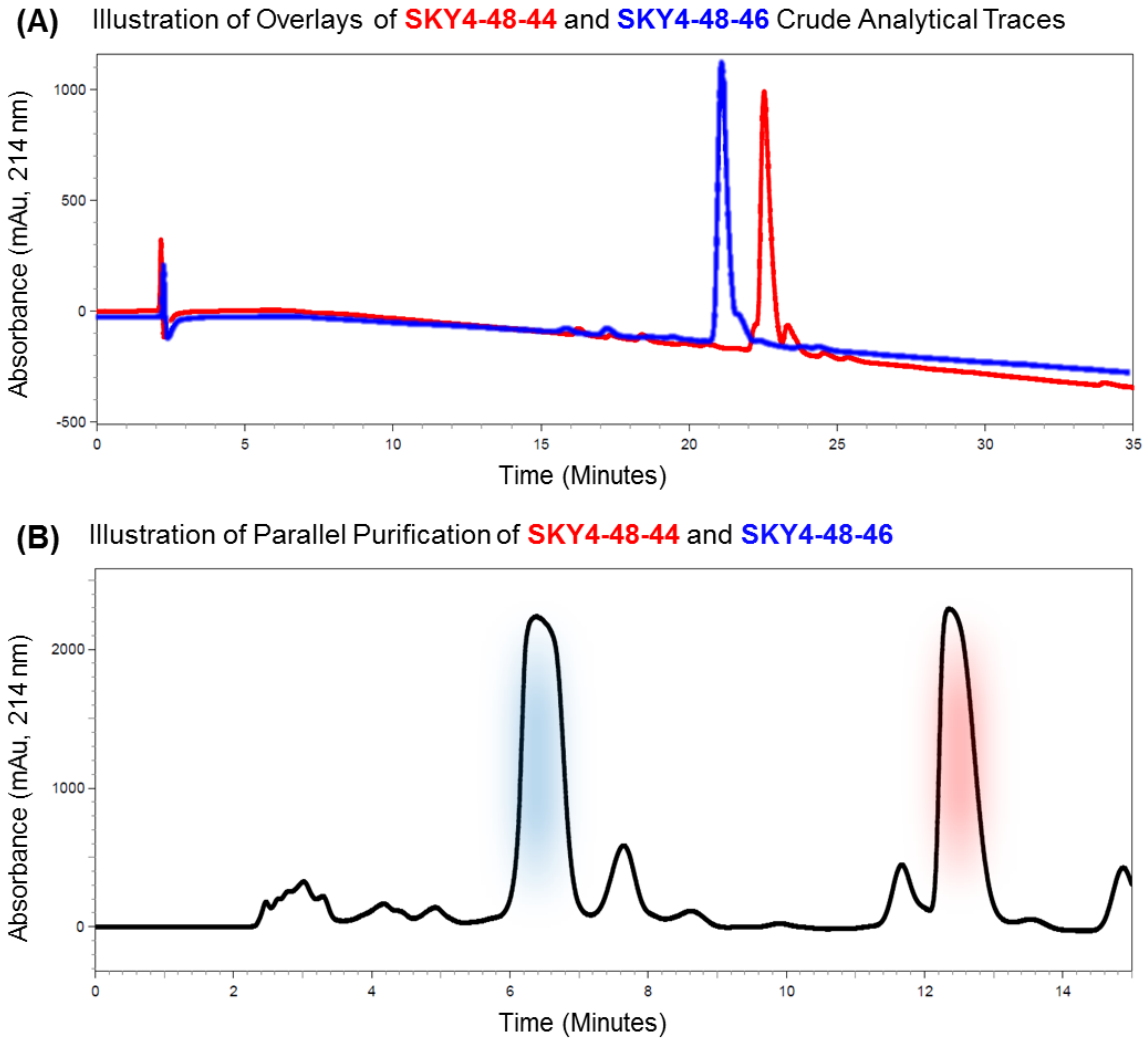

Illustration of the RP-HPLC traces observed while implementing the parallel purification method used in this study. Crude peptides were selected for parallel purification when (A) overlays of the crude analytical traces (10% to 90% acetonitrile gradient in 0.1% trifluoroacetic acid in water over 35 minutes at 1.5 mL/min using an analytical 10 micron C18, 4.6 x 250 mm, Vydac Cat#218TP104) had the desired peptides within 5 minutes of

each other and did not introduce impurities into the other peptide. The semipreparative parallel purification (B) could be achieved with a 15 minute separation method (typically 40% to 50% acetonitrile gradient in 0.1% trifluoroacetic acid in water over 15 minutes at 5 mL/min using a semipreparative 10 micron C18, 10 x 250 mm, Vydac Cat#218TP1010).

Figure 4-3: Summary of agonist activity, -Log(EC50), as a function of the first and fourth sidechain substitutions at the mouse melanocortin-1 and -5 receptors for the scaffold Ac-Xaa^{1}-(pI)DPhe-Arg-Xaa^{4}-NH$_2$

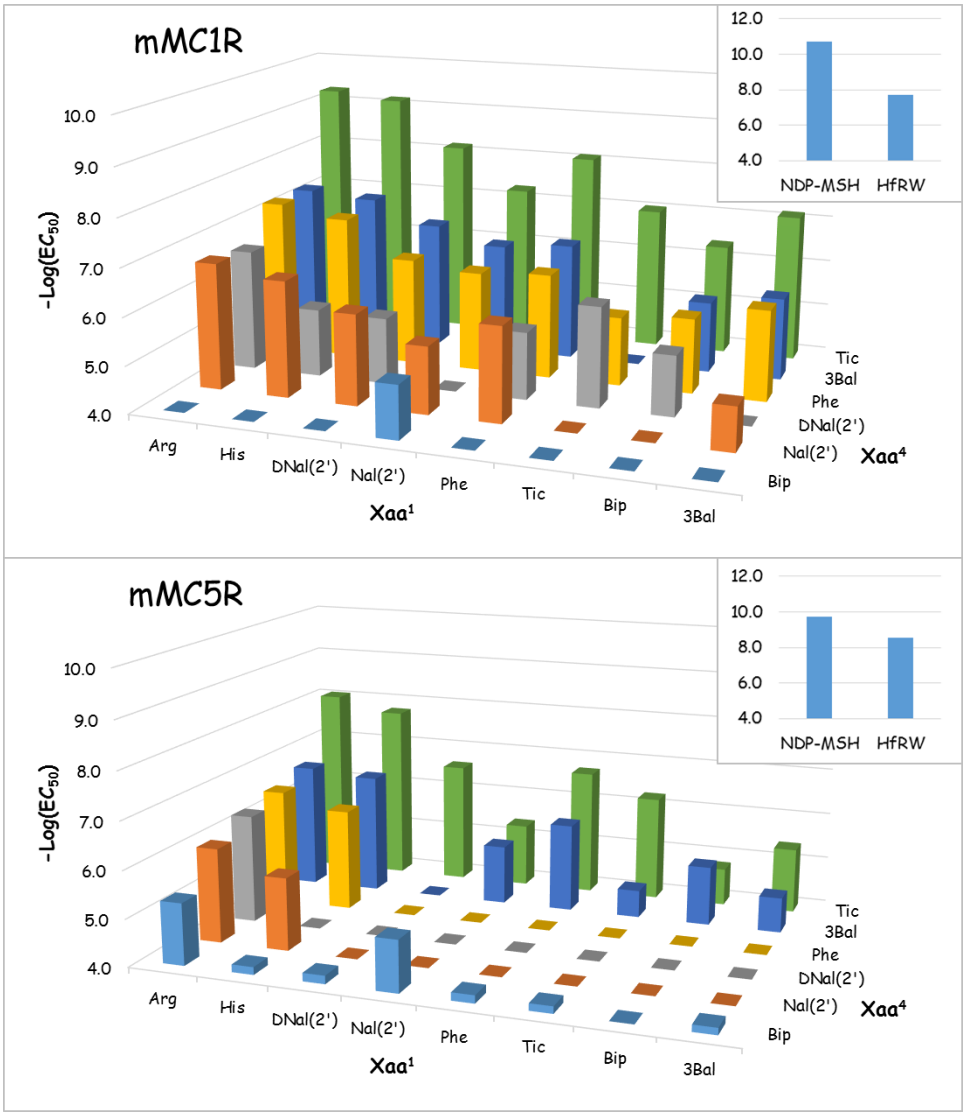

The positive controls include the peptide NDP-MSH and the CHL peptide with the sequence, Ac-His-DPhe-Arg-Trp-NH$_2$, indicated as "HfRW."

Figure 4-4: Summary of agonist activity, -Log(EC_{50}), as a function of the first and fourth sidechain substitutions at the mouse melanocortin-3 and -4 receptors for the scaffold Ac-Xaa^1-(pI)DPhe-Arg-Xaa^4-NH_2

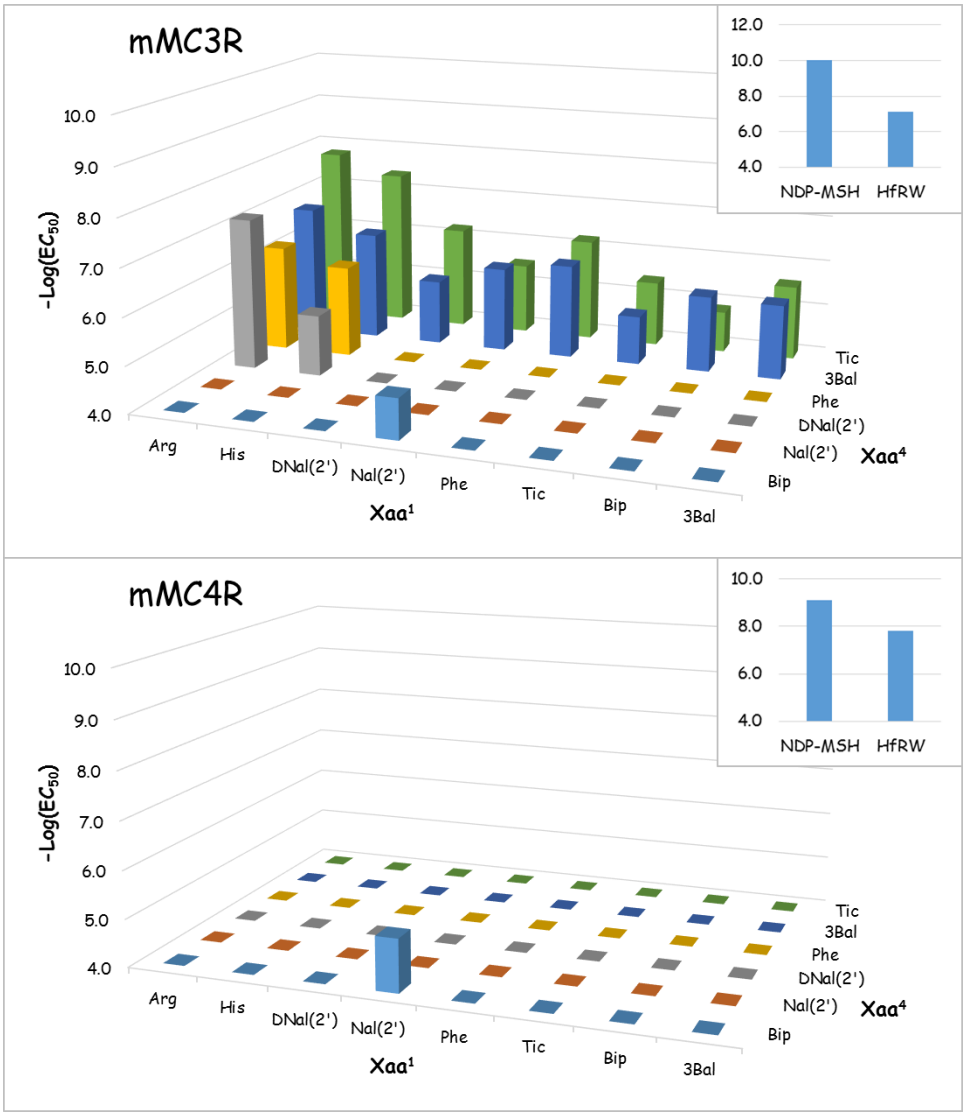

The positive controls include the peptide NDP-MSH and the CHL peptide with the sequence, Ac-His-DPhe-Arg-Trp-NH_2, indicated as "HfRW."

Figure 4-5: Summary of antagonist activity, pA_2, as a function of the first and fourth sidechain substitutions at the mouse melanocortin-3 and -4 receptors for the scaffold Ac-Xaa^1-(pI)DPhe-Arg-Xaa^4-NH_2

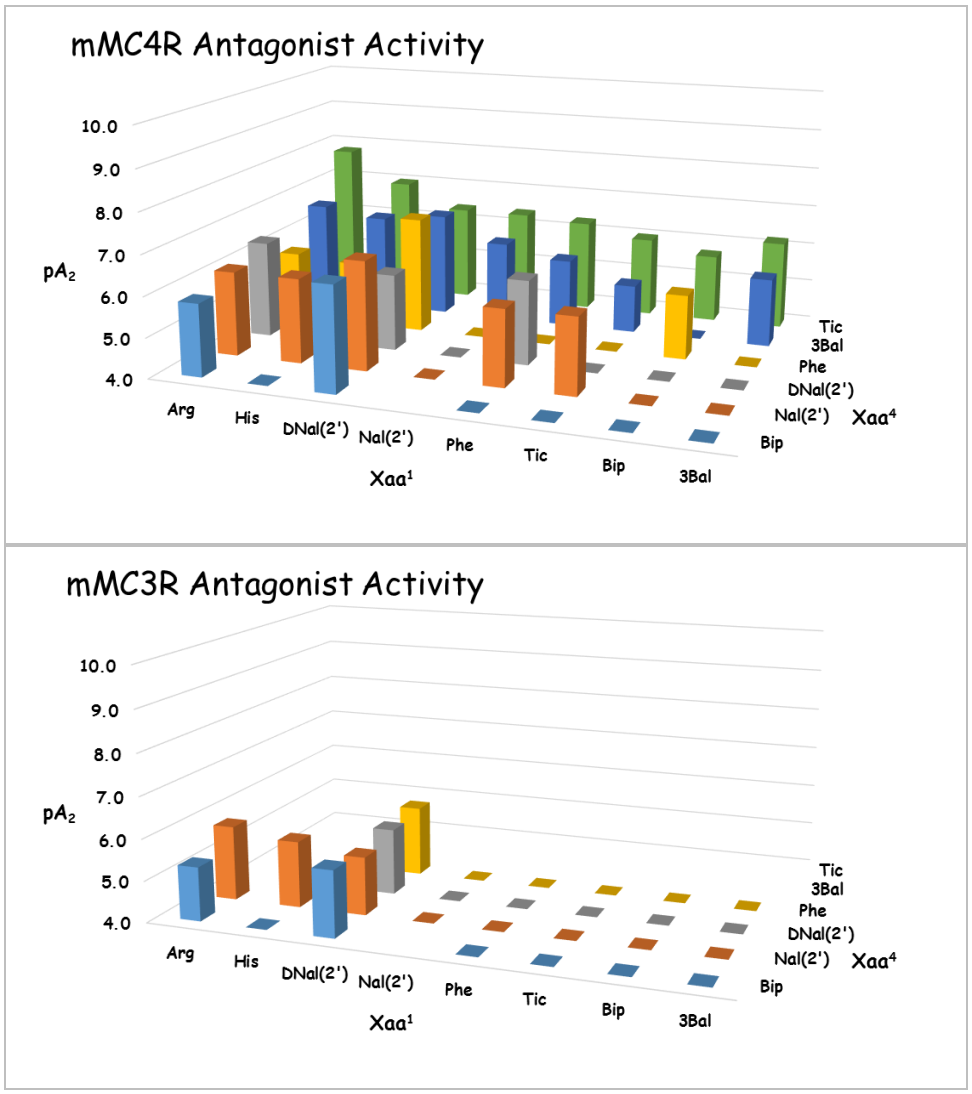

Figure 4-6: Illustration of the pharmacological profile observed for SKY4-48-18 at the selected mouse melanocortin receptors

(A) Comparing Function Dose-Response Curves for SKY4-48-18 [Ac-Arg-Arg-(pI)DPhe-Tic-NH_2] at the Selected MCRs

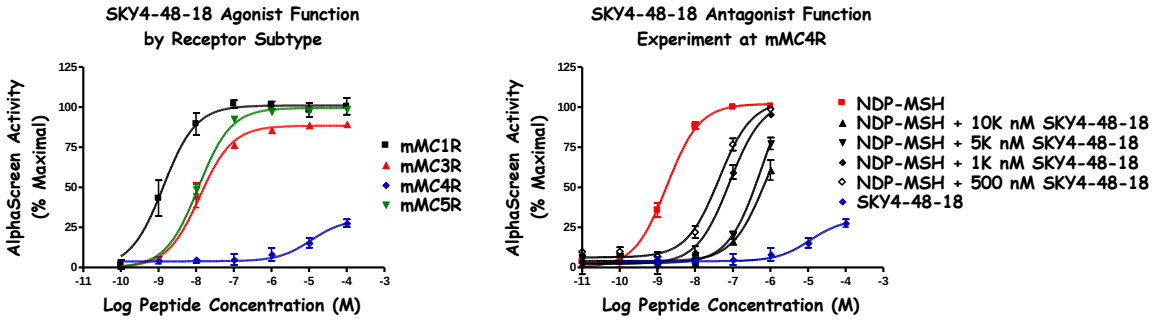

(B) Comparison of Binding and Function for SKY4-48-1 (Ac-His-DPhe-Arg-Trp-NH_2) and SKY6-24-2 [Ac-His-Arg-(pI)DPhe-Tic-NH_2] at the mMC3R and mMC4R

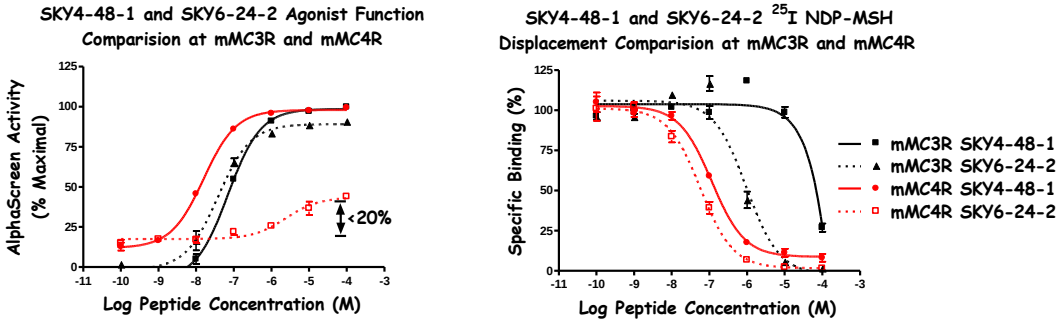

Compound SKY4-48-18 had a unique pharmacological profile. The compound displayed potent nanomolar agonist activity at the mouse melanocortin-1, -3, and -5 receptor subtypes (EC_{50} < 20 nM) and strong antagonist activity at the mouse melanocortin-4 receptor subtype (pA_2 = 7.8). This compound was the most potent activity out of all of the compounds produced within this study. A total of nine compounds produced moderate to potent agonist activity (EC_{50} < 1,000 nM) at the mMC3R in addition to producing antagonist activity at the mMC4R (7.8 < pA_2 < 5.7).

Figure 4-7: Tetrapeptide Agonist Compound (TACO) Symbol

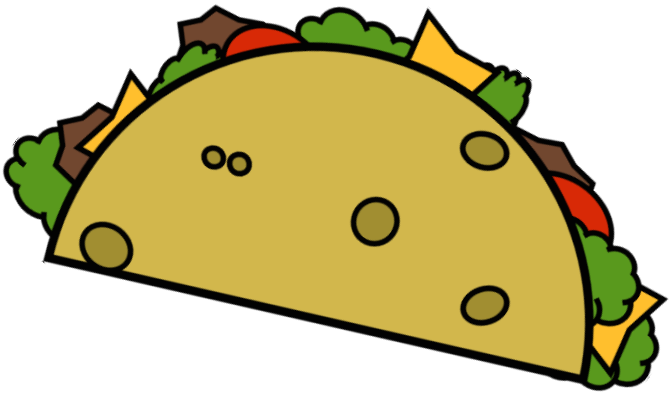

Chapter 5

Retro-Inversion of a Potent Melanocortin Tetrapeptide Agonist Compound (TACO) Produces a Selective (Greater Than 100-Fold) Melanocortin-3 Receptor Antagonist

All peptides were synthesized, purified, and characterized by Skye Doering under the supervision of Carrie Haskell-Luevano, with the exception of Ac-His-(pI)DPhe-Arg-Trp-NH_2, CJL1-20, which was synthesized first by Cody Lensing and then purchased from Peptides International. Function and binding assays were designed and performed by Katie Freeman, Sathya Schnell, and Skye Doering. The data were analyzed by Skye Doering and Carrie Haskell-Luevano. The ^{125}I-NDP-MSH radiolabel was radioiodinated by Robert Speth. This work is currently in preparation for dissemination.

Introduction:

As discussed in Chapter 1, there is an unmet need in the field to identify more drug-like melanocortin ligands that are selective for the MC3R over the MC4R. Concisely, the rationale for this is to develop compounds that could fully elucidate the function of the MC3R in an *in vivo* system were everything is present. These compounds could potentially be utilized as therapeutics addressing weight management and overall energy homeostasis and which are devoid of the side effects, such as hypertension, that are observed with the administration of MC4R selective compounds.[75]

Chapter 4 discussed the identification of a first-in-class melanocortin tetrapeptide ligand via mixture-based positional scanning wherein the results from an *in vitro* whole

cell intracellular cAMP accumulation assay indicated the tetrapeptide SKY6-24-2, Ac-His-Arg-(pI)DPhe-Tic-NH_2, was an agonist at the mMC3R and an antagonist at the mMC4R (EC_{50} = 40 nM and pA_2 = 7.0, respectively). With the TACO template, Ac-Xaa^1-Arg-(pI)DPhe-Xaa^4-NH_2, I constructed double substitution library. Eight amino acid substitutions at the first position and six amino acid substitutions at the fourth position resulted in 48 (8x6) individual compounds. The general result observed from the intracellular cAMP accumulation and the ^{125}I-NDP-MSH radiolabel binding assays indicated the potency at both the mMC3R and the mMC4R could be tuned; however, attempts to achieve selectivity for either the mMC3R or the mMC4R proved futile. Even so, nanomolar activity at both receptor subtypes was observed. Since the desired potency had been achieved, albeit without receptor subtype selectivity, we decided to perform a chemotopographical study on the TACO scaffold to better understand the requirements for each of the receptor subtypes with the hope we could then develop selectivity at each of the receptors.

The TACO scaffold contained a key structural difference from the conserved melanocortin signaling sequence His-Phe-Arg-Trp wherein the Phe and Arg residues were in a reversed order. We postulated by studying the Arg-Phe structural motif, both the sequence order and chemical topology of the sidechains, we could identify ligands specifically targeting the mMC3R and diminish activity at the mMC4R. Reported in this chapter is the identification of a selective MC3R antagonist with no detectable agonist/antagonist activity at the MC4R.

Library Design

Based upon the observed SAR profile for the TACO scaffold and the lead tetrapeptide SKY6-24-2, Ac-His-Arg-(pI)DPhe-Tic-NH_2, it was hypothesized that the resultant activity may be due to the amino acid positions which were held constant among all members of the compound library. These were the Arg^2 and $(pI)DPhe^3$ substitutions along the tetrapeptide sequence. Relative to the endogenous melanocortin signaling sequence "His-Phe-Arg-Trp," the arginine and substituted phenylalanine residues were in the reversed order. We speculated the Arg-(pI)DPhe dipeptide sequence was a new melanocortin pharmacophore.

It was at this juncture we designed two separate but related compound libraries to probe the importance of the side chain positions (sequence) in addition to the relative orientation (D vs. L) of the side chains. It was postulated these chemotopographical studies would produce different molecular requirements for each of the receptor subtypes, and ultimately, the desired selectivity could be achieved without sacrificing ligand potency.

The first library consisted of α-MSH and NDP-MSH analogs in addition to two melanocortin tetrapeptide ligands, sequence Ac-His-(X)DPhe-Arg-Trp-NH_2 where X is an hydrogen or iodine replacement. The analogs reversed the sequence of the (D or L)Phe^7 and Arg^8 (using α-MSH numbering) residues. This made for a total of eight compounds. We hypothesized that a loss of activity would indicate the TACO scaffold is a unique pharmacophore, different from the core melanocortin signaling motif and could be exploited in the generation of receptor selective ligands.

The second library consisted of retro-inverso analogs of the lead TACO peptide SKY6-24-2. With this library the relative three dimensional orientation of the Arg and Phe sidechains would be conserved. However, the amide backbone would be presented in the reversed orientation (Figure 5-1). By definition, a retro-inverso isomer is a peptide where the direction of the sequence is reversed and the chirality of each of the sidechain stereocenters are switched.[147] Relative to the parent peptide, a retro-inverso isomer has a similar three dimensional orientation of the sidechains, with exception of the end groups, and the amide backbone is reversed (Figure 5-2). It has been postulated this type of peptide modification increases enzymatic stability and therefore prolongs the action of a peptide with minimal disturbance to the orientation of the sidechain functionalities, however, a word of caution, in practice this type of modification often results in peptides which are enzymatically stable but ligand potency is catastrophically sacrificed.[147-149] Yet, we were cautiously optimistic in this since there was some literature precedence for similar modifications with melanocortin ligands, in addition, the retro-inversion of the TACO scaffold would resemble, in sequence, the endogenous melanocortin signaling motif (Figure 5-3).

Studies on the melanocortin ligands indicate the receptors are able to accommodate retro-inverso isomers in addition to other closely related isomers including the all D-pentapeptide of α-MSH(5-9) and the complete retro-inverso analog of α-MSH.[150-151] However, additional reports indicate some melanocortin scaffolds are sensitive to backbone modification. A series of naphthalene and indole containing peptides with reduced amide backbone was reported to possess modest micromolar binding affinities.[152] In addition, our laboratory previously reported on a polyamine, fully

reduced, melanocortin peptide with the sequence Phe-DPhe-Arg-Trp-NH_2 which was a weak antagonist at both the mMC3R and mMC4R.[62] Furthermore, we are currently conducting a study on a library of fully reduced peptides with sequences derived from a mixture-based positional scan deconvolution and preliminary results indicate micromolar intracellular cAMP accumulation at the mMC3R and mMC4R (Chapter 6). Taking all of these results together we envisioned the retro-inverso isomer of the tetrapeptide Ac-His-Arg-(pI)DPhe-Tic-NH_2 would retain activity since it would contain a Phe and Arg sequence similar to the core melanocortin signaling motif, "His-Phe-Arg-Trp" (Figure 5-1). In addition, if the Phe and Arg dipeptide sequence presented itself similar to the melanocortin peptides which contain the core signaling motif, then the amide bond backbone would have the same orientation as those active ligands (Figure 5-3).

Relative to the parent compound, Ac-His-Arg-(pI)DPhe-Tic-NH_2, the retro-inverso isomer, Ac-DTic-(pI)LPhe-DArg-DHis-NH_2, contains several spatial imperfections that do not allow for the isomers to perfectly superimpose over each other, and some of these potential issues were addressed in the library design (Figure 5-1). The first design consideration in the library is the end group problem wherein the N terminal acetyl group and the C terminal amide are not palindromic with respect to each other. To produce a mimetic for the C terminal amide, the N terminal of the retro-inverso compounds were synthesized to contain either an N terminal acetyl or less bulky formyl groups (Figure 5-1). The second design consideration addressed in the construction of the retro-inverso library was the spatial imperfection introduced by the backbone constrained Tic side chain. Since the nitrogen atom within the 1,2,3,4-tetrahydroisoquinoline heterocycle is part of the peptide backbone, the Tic residue on the retro-inverso isomer

has moved by one bond relative to the parent isomer (Figure 5-1). This issue was addressed by synthesizing the retro-isomer containing the correct DTic[1] substitution, in addition to an analog containing a DTic[1] to DPhe[1] replacement which could allow for the aromatic functionality of the DPhe residue to adopt a confirmation mimicking the orientation of the Tic[4] residue on the parent compound Ac-His-Arg-(pI)DPhe-Tic-NH_2.

Results and Discussion:

Library Synthesis

All compounds were synthesized by microwave assisted standard Nα-fluorenylmethyloxycarbonyl (Fmoc) solid phase peptide synthesis (SPPS) on Rink amide MBHA resin using N,N,N′,N′-tetramethyl-O-(1H-benzotriazol-1-yl)uronium hexafluorophosphate (HBTU) and diisopropylethylamine (DIEA) coupling conditions.[98, 153] Resin (0.1 mmol scale) was swelled in dichloromethane (DCM) and activated in a 20% solution of piperidine in N,N-dimethylformamide (DMF). An Nα-Fmoc amino acid possessing a trifluoroacetic acid labile sidechain (3.1 eq), HBTU (3 eq), and DIEA (5 eq) dissolved in DMF were added to the activated resin and coupled with microwave assistance (75°C, 30W, 5 min). Completion of the reaction was qualitatively monitored by a Kaiser test for the presence of a primary amine, and the chloranil test was utilized for the presence of a secondary amine.[98] After reaction completion, the Nα-Fmoc was removed with 20% solution of piperidine in DMF. The reaction was stirred with nitrogen bubbles for 2 min at room temperature and drained. Additional Fmoc deprotection solution was added to the reaction vessel and was reacted using microwave assistance (75 °C, 30W, 4 min). The coupling and deprotection cycles were repeated in an iterative

manner until the peptide was completed. The peptide was either acetylated by a 1:3 mixture of pyridine and acetic anhydride or formylated by a 1:1 mixture of formic acid and acetic anhydride which *in situ* formed the mixed anhydride and then preferentially formylated the free amine (30 min, room temperature). Note, the addition of formic acid to acetic anhydride is exceedingly exothermic and the formation of the mixed anhydride should be performed at 0°C. Following the final capping, either formylation or acetylation, the resin was washed in DMF, DCM, and MeOH. The final wash in MeOH shrinks the resin and produces a less clumpy resin after drying.

The completed peptides were globally deprotected and cleaved from the resin using a cleavage solution of TFA:thioanisole:water:triisopropylsilane (91:3:3:3) stirred, via nitrogen bubbles, for two hours at room temperature. The peptide/cleavage mixture was collected and precipitated upon the addition of 0°C diethyl ether. The precipitant was pelleted and supernatant was discarded (Sorvall, swinging bucket rotor, 4°C, 4K RPM, 4 min). The pellet was washed in additional ether and pelleted three times, and the pellet was dried overnight under a vacuum in a desiccator.

The compounds were purified by reverse phase high pressure liquid chromatography (RP-HPLC) on a semi-preparative scale (Vydac 218TP1010, 1 cm x 25 cm) to a purity greater than 95% (absorbance at λ = 214 nm). The purified compounds were lyophilized to a fine white powder and analytically characterized. They were assessed for purity by analytical (10 micron, 4.6 x 250 mm, Vydac) RP-HPLC using two solvent systems. Additionally, the mass of the compounds were confirmed by matrix-assisted laser desorption/ionization-time of flight (MALDI-TOF) mass spectrometry

(University of Minnesota Spectrometry Laboratory). A summary of the collected analytical data is available in Table 5-3.

AlphaScreen Assay

All of the analogs were assessed for agonist activity through direct measurement of cAMP intracellular accumulation via the AlphaScreen cAMP assay (Perkin-Elmer) at concentrations up to 100 μM in HEK293 cells stably expressing the mouse MC1, 3, 4, and 5 cloned receptors. Briefly, the cells were stably transfected with a plasmid containing the clone receptor, a $pcDNA_3$ vector, and G418 selection. In a 384-well format, cells, AlphaScreen acceptor beads with anti-cAMP antibodies, and compound were mixed and incubated. Post incubation, light sensitive AlphaScreen cAMP coated donor beads and lysis buffer solution was added to each well and incubated. The response was read using an Enspire (Perkin-Elmer) plate reader using the manufactures' preset protocol. The presence of intracellular cAMP caused a dissociation of the acceptor/donor bead complex, loss of energy transfer via a high energy singlet oxygen species, and the subsequent loss of signal was observed. Each plate contained NDP-MSH, forskolin, and basal controls. The complete experimental details are described below (experimental section). If compounds failed to achieve a full dose-response at the mMC3R or mMC4R, they were assessed for antagonist activity where compounds were co-dosed with the potent melanocortin analog NDP-MSH, and any apparent shifts in EC_{50} for NDP-MSH were recorded and a Schild analysis was performed to produce a pA_2 value [$pA_2 = -Log(K_i)$].[51] The results from this study are tabulated in Table 5-1; in addition, the amino

acid building blocks used in this study are illustrated in Figure 5-4. The complete experimental protocol is available in Chapter 4.

^{125}I-NDP-MSH Radiolabel Binding Assay

The retro-inverso compounds SKY5-122-1 and SKY5-122-2 were selected for radiolabel binding experiments at the mMC3R and mMC4R. In addition, NDP-MSH and SKY4-48-1, Ac-His-DPhe-Arg-Trp-NH_2, were included for assay controls and reference purposes. The compounds were assessed for their ability to competitively displace radiolabeled ^{125}I-NDP-MSH. Briefly, cells stably expressing the cloned receptor subtypes were plated in a 12-well format, and the experimental compounds were assayed from 10^{-4} to 10^{-10} M in the presence of a constant 100,000 cpm/well ^{125}I-NDP-MSH. Upon washing and cell lysis, the radioactivity for each well was determined using a WIZARD2 Automatic Gamma Counter (Perkin-Elmer). From these data, the specific binding was experimentally determined and a corresponding IC_{50} value was calculated. Note each reported value represents the mean and standard error of the mean (SEM) of at least two independent experiments containing two experimental replicates. The complete experimental details for this assay are in Chapter 4. The results from the experiments are tabulated in Table 5-2 and illustrations of the specific binding curves are in Figure 5-5.

Reversing the Phe-Arg Pharmacophore (Scaffold 1)

At the mMC3R, α-MSH had an EC_{50} value of 0.13 nM while the corresponding (Arg^7, Phe^8) α-MSH reverse analog yielded 45,000-fold decreased potency (5,800 nM). A similar decrease in potency was observed for NDP-MSH and the corresponding (Arg^7, $DPhe^8$) NDP-MSH reverse analog (0.05 nM and 1,800 nM, respectively). There were

similar results, ranging from 21,000- to 45,000-fold decreased potency, observed for α-MSH, NDP-MSH, and their Arg-Phe reversed analogs at the mMC1, mMC4, and mMC5 receptors; however, switching the DPhe-Arg residues in the tetrapeptide Ac-His-DPhe-Arg-Trp-NH_2 to Ac-His-Arg-DPhe-Trp-NH_2 was not as detrimental to the potency at some of the receptors.

The well-studied CHL-tetrapeptide Ac-His-DPhe-Arg-Trp-NH_2 is a potent agonist at all four of the selected melanocortin receptor subtypes (20, 73, 16, and 3.0 nM, for the mMC1, 3, 4, and 5 receptors, respectively) and the corresponding reverse analog SKY5-146-6, Ac-His-Arg-DPhe-Trp-NH_2, yielded micromolar agonists at the mMC1, mMC3, and mMC5 receptors and no agonist activity up to concentrations of 100 μM at the mMC4R. The closely related halogenated tetrapeptide Ac-His-(pI)DPhe-Arg-Trp-NH_2, CJL-1-20, and the reverse analog SKY5-146-7 yielded a similar pharmacological pattern.

The reverse analog of Ac-His-(pI)DPhe-Arg-Trp-NH_2, SKY5-146-7, and the lead compound SKY6-24-2 differ by a Trp^4 to Tic^4 substitution, and this Trp^4 to Tic^4 replacement resulted in a 380-fold increase in potency at the mMC1R, a 12-fold increase in potency at the mMC3R, a complete elimination of agonist potency at the mMC4R, and a 40-fold increase in potency at the mMC5R. This suggests for tetrapeptides the reverse in the Phe and Arg may be detrimental to activity, yet agonist activity at the mMC1, 3, and 5 receptors can be rescued with an amino acid replacement at the fourth position. In addition, the lack of activity observed at the MC4R results in a centrally selective MC3R agonists. It can be envisioned the double substitution library reported above is simply a combination phenylalanine/arginine reversal and fourth position replacement of the

previously reported melanocortin ligands. This modification could be used to produce additional MC3R agonists from previously reported melanocortin tetrapeptides and pentapeptides.

Retro-Inversion of TACO Tetrapeptides (Scaffold 2)

The four retro-inverso analogs (SKY5-122-1, SKY5-122-2, SKY5-142-A, and SKY5-148) of Ac-His-DPhe-Arg-Trp-NH_2 (SKY4-48-1), with sidechains arranged in a similar chemical topology to the parent compound but with reversed amide bond backbone, produced little to no measureable agonist activity up to concentrations of 100 µM at all four of the selected receptor subtypes (Table 5-1). These results are consistent with a previous report.[150] The small library of retro-inverso compounds of the lead peptide SKY6-24-2, Ac-His-Arg-(pI)DPhe-Tic-NH_2, which investigated different terminal modifications and backbone constrained amino acids and their effects on retro-inverso analogs, produced little to no agonist activity at the mMC3, mMC4, and mMC5 receptors yet were relatively potent inverse agonists at the mMC1R, although, additional experiments would be required at the mMC1R to confirm the observed activity (Table 5-1). Subsequent antagonist analysis for the compounds at the mMC3R/mMC4R subtypes, in addition to, the specific binding determination for two of the retro-inverso compounds, SKY5-122-1 and SKY5-122-2, yielded exciting results.

The retro-inversion of the TACO scaffold yielded a series of potent antagonists that were selective for the mMC3R over the mMC4R. The potencies for the four retro-inverso compounds ranged from a pA_2 of 7.2 to 6.4 (K_i = 63 and 398 nM, respectively) at the mMC3R, and the antagonist activity observed at the mMC4R was at or below the

limit of quantitation for the assay ($pA_2 < 5.5$ or $K_I > 3{,}100$ nM). Figure 5-6 illustrates the antagonist pharmacology for SKY5-122-1, the most potent mMC3R antagonist, at both the mMC3R and mMC4R. At the mMC3R, log shifts in potency can be observed for NDP-MSH with increasing concentrations of SKY5-122-1, whereas no shifts were observed at the mMC4R. Figure 5-6 also illustrates the pharmacology for the peptide when it is assayed alone and the limited agonist activity at concentrations up to 100 μM for both receptor subtypes. Similar but less potent results were observed for SKY5-122-2, which had the $DPhe^1$ substitution in addition to the corresponding formylated N terminal analogs SKY5-142-A and SKY5-148. In addition to the antagonist activity at the mMC3R and no activity at the mMC4R, there was no activity observed at the mMC5R ($EC_{50} > 100$ μM) and some inverse activity at the mMC1R. Further experiments would be required to fully characterize the observed inverse agonism at the mMC1R and to assess if the observed result has any relevance *in vivo*.

The specific binding for SKY5-122-1 and SKY5-122-2 reflected a similar selectivity trend for the mMC3R over the mMC4R (Table 5-2 and Figure 5-5). Both compounds were approximately 10-fold more potent at the mMC3R over the mMC4R (800 and 3,500 nM vs 6,700 and 39,500 nM, respectively). Compared to SKY4-48-1, Ac-His-DPhe-Arg-Trp-NH_2, SKY5-122-1 and SKY5-122-2 were more potent binders at the mMC3R (14- to 64-fold decrease in IC_{50}) and possessed decreased binding affinity at the mMC4R (55- to 326-fold increase in IC_{50}). Most, if not all, reports on MC3R selective compounds have been primarily limited to analogs of α-MSH and γ-MSH.[80-85] However, there is one common feature at the sixth position, using α-MSH numbering, between the tetrapeptides reported herein and the longer analogs.

The replacement of the sixth position on α-MSH analogs with bulky yet sterically constrained substitutions yields ligands that are selective MC3R antagonists.[85] Figure 5-7 aligns the sequences of two reported compounds that possessed antagonist selective activity for the MC3R over the MC4R, in addition to the most potent selective MC3R antagonist reported herein, SKY5-122-1; all of these compounds are aligned relative to the endogenous melanocortin ligand α-MSH. Consistent to the previous report, the substitution of a sterically constrained aromatic residue at the sixth position (using α-MSH numbering) appears to achieve selective antagonist activity at the MC3R over the MC4R.[85] Herein is, to the best of our knowledge, the first report of a selective MC3R antagonist consisting of a tetrapeptide sequence.

Conclusions:

All of these results, when taken together, suggest the reversal of the Arg and Phe residues did not result in the observed increase in selectivity of the previously reported TACO scaffold for the MC3R over the MC4R. Reversing the sequence in known melanocortin ligands was disastrous for activity at all of the tested receptor subtypes, indicating the "reversed" Arg-Phe di-peptide sequence was not a general strategy for increasing mMC3R selectivity over all melanocortin ligand scaffold systems. The retro-inverso TACO peptides resulted in selective antagonist activity at the mMC3R over the mMC4R. The sequence of these peptides was similar to the endogenous melanocortin signaling sequence, when the sequences were aligned from their N to C termini yet most of the chiral centers were scrambled. The retro-inverso TACO peptide stereocenters were D-L-D-D whereas the stereocenters for the core signaling motif in α-MSH were L-L-L-L

and L-D-L-L for NDP-MSH. Taking these two aspects of the TACO motif together, it may be concluded that the "reversed" TACO scaffold is indeed a novel pharmacophore distinctly different from the endogenous "His-Phe-Arg-Trp" motif.

In summary, we explored the importance of the backbone direction and chemical topology of the previously reported TACO scaffold (Chapter 4) which was an agonist at the MC3R and an antagonist at the MC4R. We postulated the reversed "Arg-Phe" sequence, relative to the conserved "His-Phe-Arg-Trp" motif, was a new melanocortin pharmacophore and by studying the requirements for each receptor subtype we could achieve selectivity for one of the receptor subtypes while maintaining potency. We constructed a series of MSH analogs studying the importance of side chain position in addition to a series of retro-inverso tetrapepetide analogs. We discovered the mMC3 and mMC4 receptor subtypes have different molecular requirements which allowed for us to serendipitously identify a selective mMC3R antagonist compound.

Experimental Section:

The peptide library described above was synthesized and purified using identical chemistry and reagents as reported in Chapter 4 and described in Chapter 2. The solid phase synthesis method was modified while synthesizing the "reversed" MSH analogs. The common C terminal fragments for α-MSH and NDP-MSH, in addition to their corresponding "reversed" analogs, were synthesized together. Upon coupling the Trp^9 residue, the resin was then split into four equal aliquots and then the remaining residues for each of the analogs were coupled. After completing the synthesis of the four peptides, they were cleaved and purified in parallel as previously described. The AlphaScreen

cAMP bioassay, ^{125}I-NDP-MSH preparation and purification, and ^{125}I-NDP-MSH competitive binding assay all used identical protocols described in Chapter 4.

Chapter 5 Tables and Figures:

Table 5-1: Selected melanocortin ligands and their "reverse analogs"

			mMC1R	mMC3R	mMC4R	mMC5R
Cpmd ID	Type	Sequence	EC_{50} ± SEM	EC_{50} ± SEM	EC_{50} ± SEM	EC_{50} ± SEM
SKY2-125-4	α-MSH	Ac-Ser-Tyr-Ser-Met-Glu-His-Phe-Arg-Trp-Gly-Lys-Pro-Val-NH_2	0.14 ± 0.03	0.13 ± 0.07	1.9 ± 0.6	0.07 ± 0.03
SKY2-125-5	(Arg^7, Phe^8) α-MSH	Ac-Ser-Tyr-Ser-Met-Glu-His-Arg-Phe-Trp-Gly-Lys-Pro-Val-NH_2	3,000 ± 900	5,800 ± 1,200	44,000 ± 30,000	2,600 ± 930
NDP-MSH	NDP-MSH	Ac-Ser-Tyr-Ser-Nle-Glu-His-DPhe-Arg-Trp-Gly-Lys-Pro-Val-NH_2	0.02 ± 0.01	0.05 ± 0.01	0.3 ± 0.1	0.05 ± 0.01
SKY2-125-3	(Arg^7, Phe^8) NDP-MSH	Ac-Ser-Tyr-Ser-Nle-Glu-His-Arg-DPhe-Trp-Gly-Lys-Pro-Val-NH_2	380 ± 70	1,800 ± 200	9,500 ± 3,000	1,600 ± 230
SKY4-48-1	Reference	Ac-His-DPhe-Arg-Trp-NH_2	20 ± 1	73 ± 10	16 ± 3	3.0 ± 0.5
SKY5-146-6	Rev. Tetra.	Ac-His-Arg-DPhe-Trp-NH_2	1,300 ± 500	21,000 ± 7,000 Full Agonist	> 100,000 pA_2 = No Activity	21,000 ± 5,000
SKY5-121	Retro. Tetra.	Ac-DTrp-DArg-Phe-DHis-NH_2	> 100,000	> 100,000 pA_2 = No Activity	> 100,000 pA_2 = No Activity	29% @ 100 µM
CJL-1-20	CJL Data	Ac-His-(pI)DPhe-Arg-Trp-NH_2	12 ± 2	56% @ 100 µM pA_2 = 6.8 ± 0.1	44% @ 100 µM pA_2 = 8.6 ± 0.1	2.7 ± 1.1
SKY5-146-7	Rev. Tetra.	Ac-His-Arg-(pI)DPhe-Trp-NH_2	270 ± 130	500 ± 170 Full Agonist	29% @ 100 µM pA_2 = 6.0 ± 0.1	690 ± 120
SKY6-24-2	Reference	Ac-His-Arg-(pI)DPhe-Tic-NH_2	0.71 ± 0.05	40 ± 7 Full Agonist	> 100,000 pA_2 = 7.0 ± 0.2	17 ± 3
SKY5-122-2	Retro. Tetra.	Ac-DPhe-(pI)Phe-DArg-DHis-NH_2	*720 ± 130	> 100,000 pA_2 = 6.4 ± 0.1	16% @ 100 µM pA_2 = No Activity	> 100,000
SKY5-142-A	Retro. Tetra.	For-DPhe-(pI)Phe-DArg-DHis-NH_2	*420 ± 99	> 100,000 pA_2 = 6.7 ± 0.1	47% @ 100 µM pA_2 = No Activity	> 100,000
SKY5-122-1	Retro. Tetra.	Ac-DTic-(pI)Phe-DArg-DHis-NH_2	*22 ± 9	> 100,000 pA_2 = 7.2 ± 0.1	42% @ 100 µM pA_2 = 5.5 ± 0.1	> 100,000
SKY5-148	Retro. Tetra.	For-DTic-(pI)Phe-DArg-DHis-NH_2	*40 ± 7	> 100,000 pA_2 = 6.8 ± 0.1	71% @ 100 µM pA_2 = 5.4 ± 0.1	> 100,000
*Inverse agonist activity observed						

Summary of all the function data at the selected mouse melanocortin receptors using the AlphaScreen. NDP-MSH and assay media served as both positive and negative controls, respectively. Forskolin served as an additional positive control due to the fact it independently activates adenylate cyclase from the melanocortin receptors. All of the compounds were assessed for agonist activity up to a concentration of 100 μM and values are represented as EC_{50} in nM. Compounds which did not produce a full dose-response curve were tabulated as a percent of the NDP-MSH maximal positive control, and compounds with < 20% activity were denoted as EC_{50} > 100,000 nM. These experiments were performed in triplicate. Compounds were assessed for antagonist activity at the mMC3R and mMC4R if they did not produce a full dose-response. Antagonist activity was assessed by co-administering NDP-MSH and the compound at concentrations of 10,000, 5,000, 1,000, and 500 nM and measuring the resulting shift in EC_{50} and calculating a subsequent pA_2 value [-Log(K_i)] via a Schild analysis.[51] The antagonist experiment was performed in triplicate unless there was no shift in EC_{50} activity was observed in which case it was tabulated as "no activity."

Table 5-2: Summary of the Binding Data for NDP-MSH, SKY4-48-1, SKY5-122-1, and SKY5-122-2

Compound	Sequence	mMC3R Mean ± SEM (nM)	Fold Diff.	mMC4R Mean ± SEM (nM)	Fold Diff.
NDP-MSH	Ac-Ser-Tyr-Ser-Nle-Glu-His-DPhe-Arg-Trp-Gly-Lys-Pro-Val-NH_2	5.3 ± 0.7		2.0 ± 0.2	
SKY4-48-1	Ac-His-DPhe-Arg-Trp-NH_2	50,500 ± 500	1.0	121 ± 39	1.0
SKY5-122-1	Ac-DTic-(pI)LPhe-DArg-DHis-NH_2	800 ± 170	-64	6,700 ± 400	55
SKY5-122-2	Ac-DPhe-(pI)LPhe-DArg-DHis-NH_2	3,500 ± 1,300	-14	39,500 ± 10,500	326

Summary of the specific binding data for two of the retro-invsero TACO analogues (SKY5-122-1 and SKY5-122-2). The peptides SKY4-48-1 in addition to NSP-MSH were used as control compounds. The numbers reported are the mean and corresponding standard error of the mean for, at least, two independent experiments each containing duplicate replicates for each concentration tested.

Table 5-3: Summary of Analytical Data for Retro-TACO and "Reversed" Melanocortin Analogs

Cpmd ID	Type	Sequence	k' System 1 Acetonitrile	k' System 2 Methanol	Calculated Exact Mass	Observed MALDI-MS [M+1]
SKY2-125-4	α-MSH	Ac-Ser-Tyr-Ser-Met-Glu-His-Phe-Arg-Trp-Gly-Lys-Pro-Val-NH_2	4.9	8.9	1664.9	833.3 (2+)
SKY2-125-5	(Arg^7, Phe^8) α-MSH	Ac-Ser-Tyr-Ser-Met-Glu-His-Arg-Phe-Trp-Gly-Lys-Pro-Val-NH_2	4.7	8.6	1664.9	833.3 (2+)
SKY2-125-2	NDP-MSH	Ac-Ser-Tyr-Ser-Nle-Glu-His-DPhe-Arg-Trp-Gly-Lys-Pro-Val-NH_2	5.0	9.3	1646.9	824.3 (2+)
SKY2-125-3	(Arg^7, Phe^8) NDP-MSH	Ac-Ser-Tyr-Ser-Nle-Glu-His-Arg-DPhe-Trp-Gly-Lys-Pro-Val-NH_2	5.1	9.3	1646.9	824.8 (2+)
SKY5-146-6	Rev. Tetra.	Ac-His-Arg-DPhe-Trp-NH_2	6.3	9.4	685.3	686.3
SKY5-121	Retro. Tetra.	Ac-DTrp-DArg-Phe-DHis-NH_2	5.3	8.2	685.3	686.2
CJL-1-20	CJL Data	Ac-His-(pI)DPhe-Arg-Trp-NH_2	3.4	6.1	811.7	812.4*
SKY5-146-7	Rev. Tetra.	Ac-His-Arg-(pI)DPhe-Trp-NH_2	7.4	11.2	811.2	812.2
SKY5-122-2	Retro. Tetra.	Ac-DPhe-(pI)Phe-DArg-DHis-NH_2	7.3	11.7	772.2	773.0
SKY5-142-A	Retro. Tetra.	For-DPhe-(pI)Phe-DArg-DHis-NH_2	7.2	11.7	758.2	759.1
SKY5-122-1	Retro. Tetra.	Ac-DTic-(pI)Phe-DArg-DHis-NH_2	7.5	11.9	784.23	784.7
SKY5-148	Retro. Tetra.	For-DTic-(pI)Phe-DArg-DHis-NH_2	7.4	11.7	770.2	771.0

The k' is defined as [(Retention Time – Solvent Time)/Retention Time]. The compounds were assessed for purity using two different HPLC solvent systems. Solvent system 1 was a 10% to 90% acetonitrile gradient in 0.1% TFA in water over 35 minutes at a rate of 1.5 mL/min using an analytical Vydac C18 column (Vydac 218TP104). Solvent system 2 was a 10% to 90% methanol gradient in 0.1% TFA in water over 35 minutes using the same flow rate and column as solvent system 1. The purity was assessed by integrating the area under the curve at λ=214 nm and is greater than 95%. The mass was confirmed using a matrix-assisted laser desorption/ionization-time of flight mass spectrometer (MALDI-TOF MS) using a cyano-4-hydroxycinnamic acid matrix (AB-Sciex 5800, University of Minnesota Department of Chemistry Mass Spectrometry Laboratory). *Note, the mass of CJL-1-20 was confirmed using electrospray ionization-time of flight (ESI-TOF) spectrometer (Bruker BioTOF II, University of Minnesota Department of Chemistry Mass Spectrometry Laboratory).

Figure 5-1: SKY6-24-2 and the Retro-Inverso Isomers

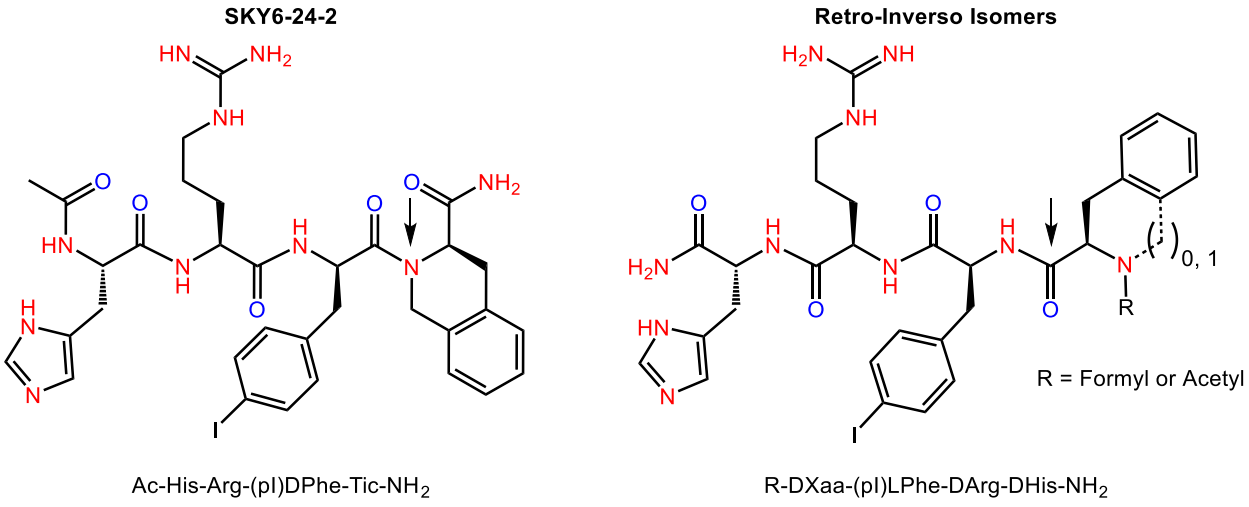

Above illustrates how SKY6-24-2 and the corresponding retro-inverso isomers possess similar spatial orientation of the residue sidechains when SKY6-24-2 is drawn with the backbone going from the N termini to C termini and the retro-inverso isomer analogs are drawn with their backbone in the opposite C termini to N termini orientation.

Figure 5-2: Relationship Between an all-L-Peptide and the Retro-Inverso Isomer

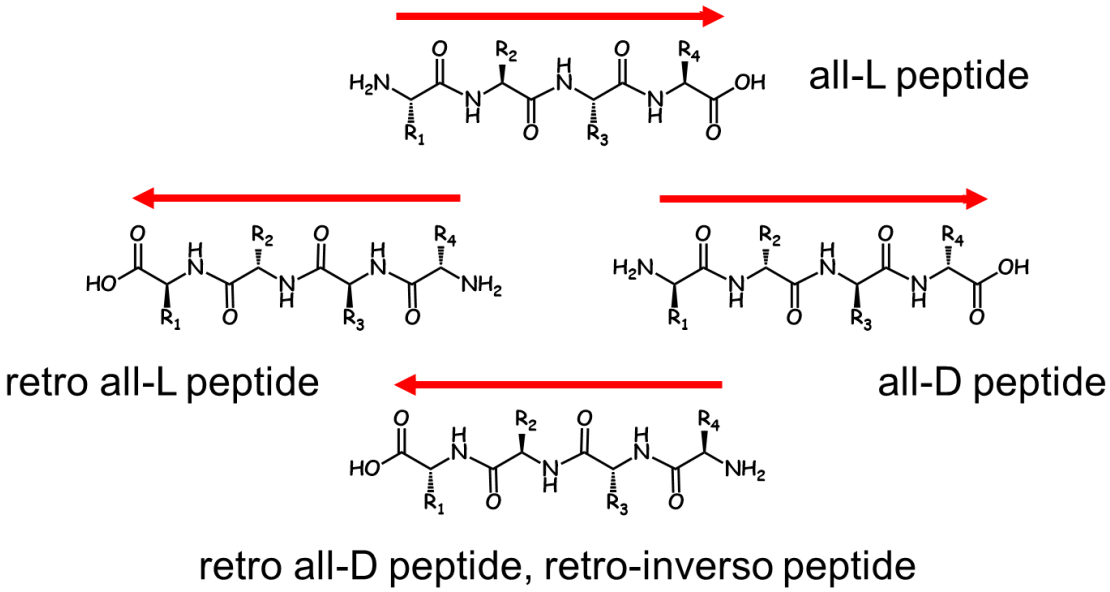

Figure 5-3: Illustration Comparing the Sequence Alignment of α-MSH to the Retro-Inverso TACO Isomer

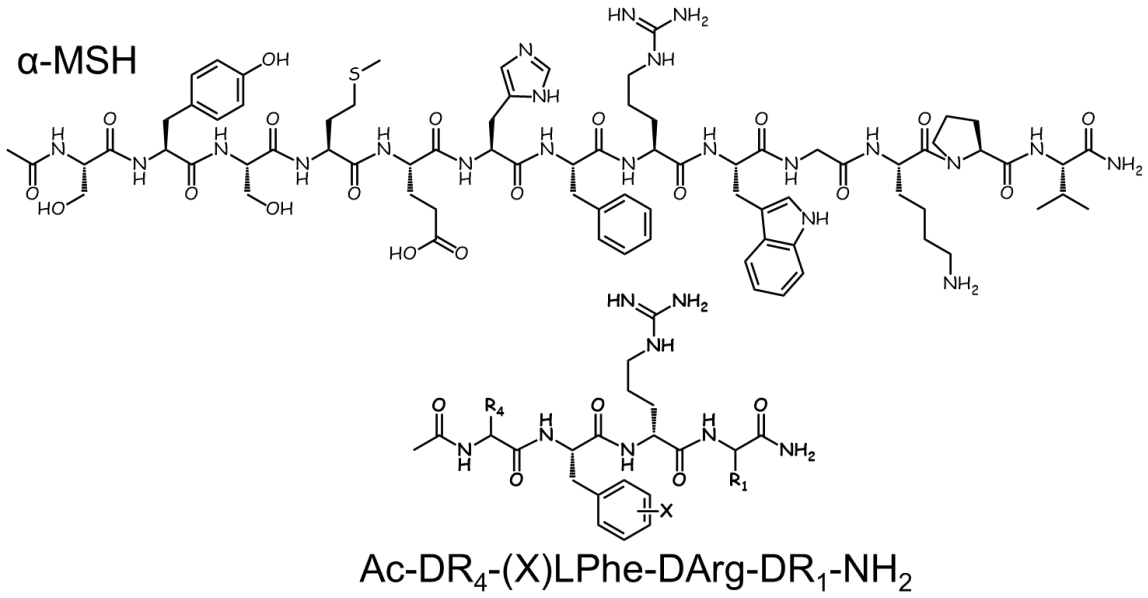

Relative to α-MSH, the retro-inverso TACO scaffold contains the Phe[2] and D-Arg[3] residues in the same sequence as what is found in the core "His-Phe-Arg-Trp" melanocortin motif, and the stereochemistry of the D-Arg[3] residue is opposite from the natural L configuration of the Arg[8] in α-MSH.

Figure 5-4: Amino Acid Building blocks

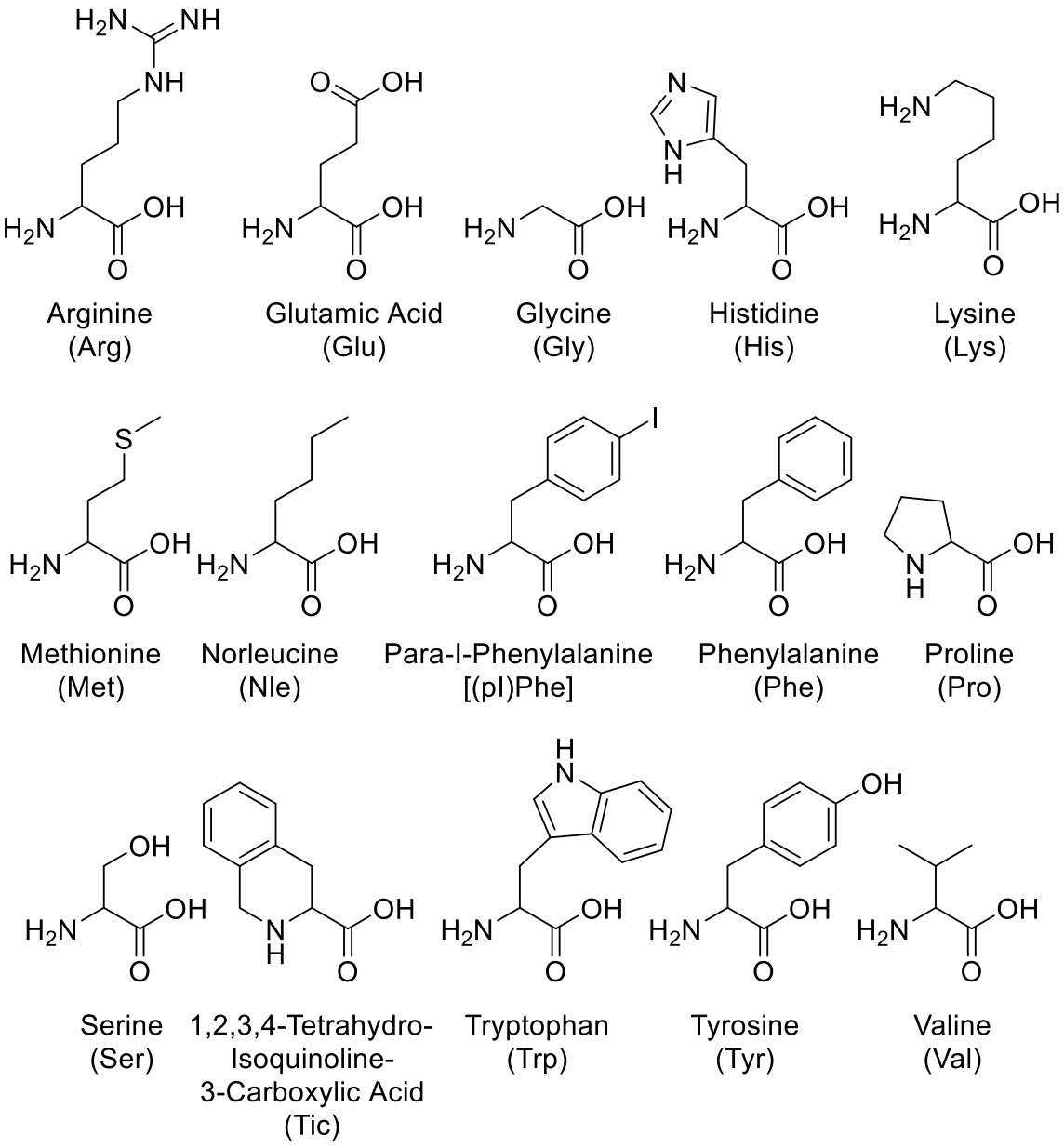

Figure 5-5: Observed Dose-Response Curves for the Competitive Displacement of ^{125}I-NDP-MSH for the Reported Retro-Inverso Compounds

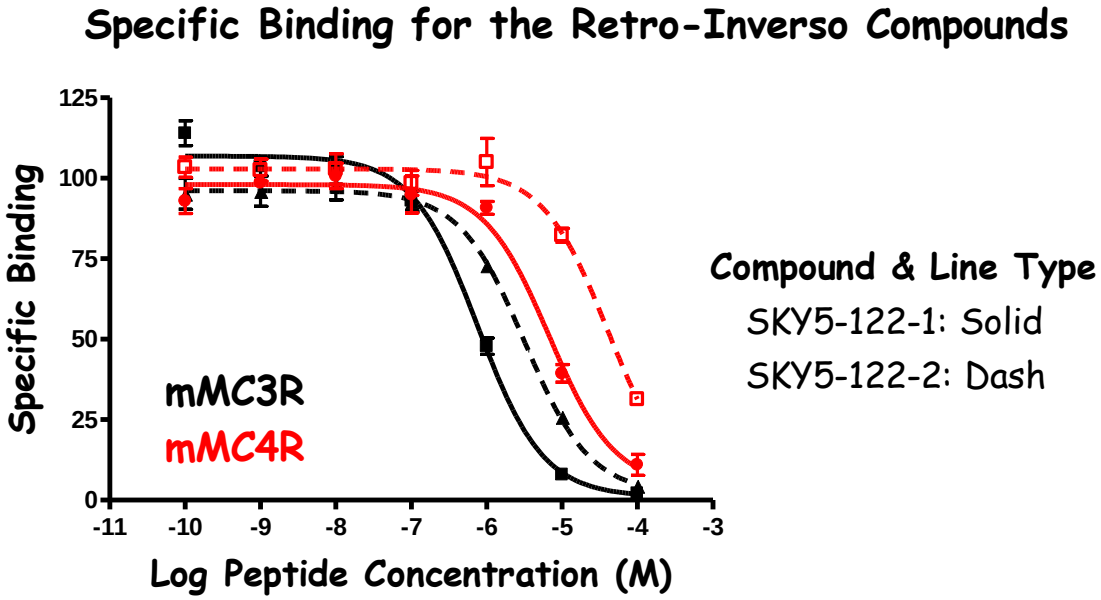

Figure 5-6: Illustration of Antagonist Plots for the Most Potent Retro-Inverso Compound SKY5-122-1

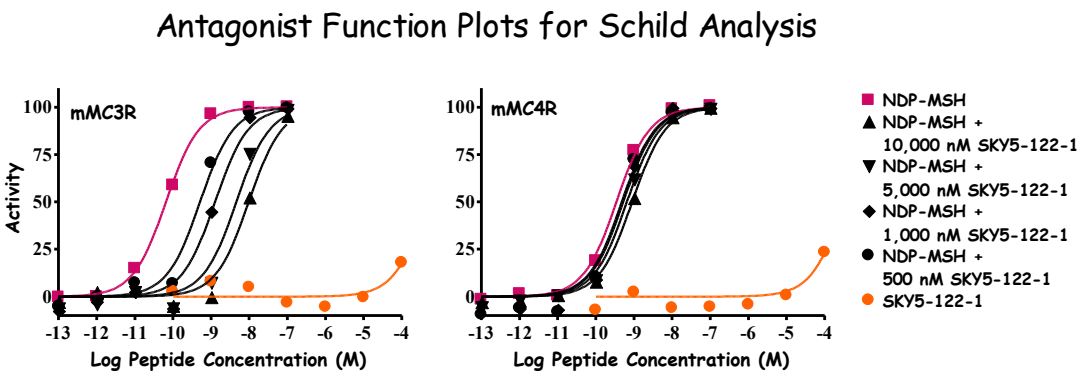

The most potent retro-inverso compound was SKY5-122-1. The compound was assayed for agonist activity from 10^{-10} to 10^{-4} M, and all of the data is included in the plot above. However, the activity observed at 10^{-4} M is likely an artifact of the assay since the cells appear stressed at that concentration.

Figure 5-7: Comparing SKY5-122-1 to α-MSH and a selective MC3R antagonist

α-MSH: Ac-S-Y-S-Met-Glu-His-Phe-Arg-Trp-Gly-Lys-P-V-NH_2

Aba-2: Ac-Nle-c[Asp-Aba-DPhe-Arg-Trp-Lys]-NH_2

Aba-4: Ac-Nle-c[Asp-Aba-DNal-Arg-Trp-Lys]-NH_2

SKY5-122-1: Ac-DTic-(pI)Phe-DArg-DHis-NH_2

*Note: Aba = 4-amino-1,2,4,5-tetrahydro-2-benzazepin-3-one

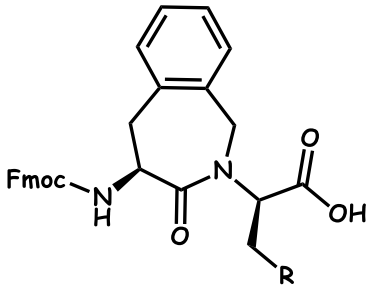

Bibliography

1. Mendis, S.; Chestnov, O.; World Health, O., *Global status report on noncommunicable diseases 2014*. World Health Organization: Geneva, 2014.
2. Ogden, C. L.; Carroll, M. D.; Kit, B. K.; Flegal, K. M., Prevalence of childhood and adult obesity in the united states, 2011-2012. *JAMA* **2014,** *311* (8), 806-814.
3. Finkelstein, E. A.; Trogdon, J. G.; Cohen, J. W.; Dietz, W., Annual Medical Spending Attributable To Obesity: Payer-And Service-Specific Estimates. *Health Aff.* **2009,** *28* (5), w822-w831.
4. Farooqi, I. S.; Keogh, J. M.; Yeo, G. S.; Lank, E. J.; Cheetham, T.; O'Rahilly, S., Clinical spectrum of obesity and mutations in the melanocortin 4 receptor gene. *N. Engl. J. Med.* **2003,** *348* (12), 1085-95.
5. Chen, K. Y.; Muniyappa, R.; Abel, B. S.; Mullins, K. P.; Staker, P.; Brychta, R. J.; Zhao, X. C.; Ring, M.; Psota, T. L.; Cone, R. D.; Panaro, B. L.; Gottesdiener, K. M.; Van der Ploeg, L. H. T.; Reitman, M. L.; Skarulis, M. C., RM-493, a Melanocortin-4 Receptor (MC4R) Agonist, Increases Resting Energy Expenditure in Obese Individuals. *J Clin Endocr Metab* **2015,** *100* (4), 1639-1645.
6. Kievit, P.; Halem, H.; Marks, D. L.; Dong, J. Z.; Glavas, M. M.; Sinnayah, P.; Pranger, L.; Cowley, M. A.; Grove, K. L.; Culler, M. D., Chronic Treatment With a Melanocortin-4 Receptor Agonist Causes Weight Loss, Reduces Insulin Resistance, and Improves Cardiovascular Function in Diet-Induced Obese Rhesus Macaques. *Diabetes* **2013,** *62* (2), 490-497.
7. Kumar, K. G.; Sutton, G. M.; Dong, J. Z.; Roubert, P.; Plas, P.; Halem, H. A.; Culler, M. D.; Yang, H.; Dixit, V. D.; Butler, A. A., Analysis of the therapeutic functions of novel melanocortin receptor agonists in MC3R-and MC4R-deficient C57BL/6J mice. *Peptides* **2009,** *30* (10), 1892-1900.
8. Chhajlani, V.; Wikberg, J. E., Molecular cloning and expression of the human melanocyte stimulating hormone receptor cDNA. *FEBS Lett.* **1992,** *309* (3), 417-20.
9. Mountjoy, K. G.; Robbins, L. S.; Mortrud, M. T.; Cone, R. D., The cloning of a family of genes that encode the melanocortin receptors. *Science* **1992,** *257* (5074), 1248-1251.
10. Roselli-Rehfuss, L.; Mountjoy, K. G.; Robbins, L. S.; Mortrud, M. T.; Low, M. J.; Tatro, J. B.; Entwistle, M. L.; Simerly, R. B.; Cone, R. D., Identification of a receptor for gamma melanotropin and other proopiomelanocortin peptides in the hypothalamus and limbic system. *Proc. Natl. Acad. Sci. U.S.A.* **1993,** *90* (19), 8856-60.
11. Mountjoy, K. G.; Mortrud, M. T.; Low, M. J.; Simerly, R. B.; Cone, R. D., Localization of the melanocortin-4 receptor (MC4-R) in neuroendocrine and autonomic control circuits in the brain. *Mol. Endocrinol.* **1994,** *8* (10), 1298-308.

12. Gantz, I.; Konda, Y.; Tashiro, T.; Shimoto, Y.; Miwa, H.; Munzert, G.; Watson, S. J.; DelValle, J.; Yamada, T., Molecular cloning of a novel melanocortin receptor. *J. Biol. Chem.* **1993,** *268* (11), 8246-50.
13. Gantz, I.; Miwa, H.; Konda, Y.; Shimoto, Y.; Tashiro, T.; Watson, S. J.; Delvalle, J.; Yamada, T., Molecular-cloning, expression, and gene localization of a 4th melanocortin receptor. *J. Biol. Chem.* **1993,** *268* (20), 15174-15179.
14. Gantz, I.; Shimoto, Y.; Konda, Y.; Miwa, H.; Dickinson, C. J.; Yamada, T., Molecular cloning, expression, and characterization of a fifth melanocortin receptor. *Biochem. Biophys. Res. Commun.* **1994,** *200* (3), 1214-20.
15. Haynes, R. C., Jr., The activation of adrenal phosphorylase by the adrenocorticotropic hormone. *J. Biol. Chem.* **1958,** *233* (5), 1220-2.
16. Joppa, M. A.; Gogas, K. R.; Foster, A. C.; Markison, S., Central infusion of the melanocortin receptor antagonist agouti-related peptide (AgRP(83-132)) prevents cachexia-related symptoms induced by radiation and colon-26 tumors in mice. *Peptides* **2007,** *28* (3), 636-642.
17. Barrett, C. E.; Modi, M. E.; Zhang, B. C.; Walum, H.; Inoue, K.; Young, L. J., Neonatal melanocortin receptor agonist treatment reduces play fighting and promotes adult attachment in prairie voles in a sex-dependent manner. *Neuropharmacology* **2014,** *85*, 357-366.
18. Van der Ploeg, L. H.; Martin, W. J.; Howard, A. D.; Nargund, R. P.; Austin, C. P.; Guan, X.; Drisko, J.; Cashen, D.; Sebhat, I.; Patchett, A. A.; Figueroa, D. J.; DiLella, A. G.; Connolly, B. M.; Weinberg, D. H.; Tan, C. P.; Palyha, O. C.; Pong, S. S.; MacNeil, T.; Rosenblum, C.; Vongs, A.; Tang, R.; Yu, H.; Sailer, A. W.; Fong, T. M.; Huang, C.; Tota, M. R.; Chang, R. S.; Stearns, R.; Tamvakopoulos, C.; Christ, G.; Drazen, D. L.; Spar, B. D.; Nelson, R. J.; MacIntyre, D. E., A role for the melanocortin 4 receptor in sexual function. *Proc. Natl. Acad. Sci. U.S.A.* **2002,** *99* (17), 11381-6.
19. Giuliani, D.; Neri, L.; Canalini, F.; Calevro, A.; Ottani, A.; Vandini, E.; Sena, P.; Zaffe, D.; Guarini, S., NDP-α-MSH induces intense neurogenesis and cognitive recovery in Alzheimer transgenic mice through activation of melanocortin MC4 receptors. *Mol. Cell. Neurosci.* **2015,** *67*, 13-21.
20. Suzuki, I.; Cone, R. D.; Im, S.; Nordlund, J.; Abdel-Malek, Z. A., Binding of melanotropic hormones to the melanocortin receptor MC1R on human melanocytes stimulates proliferation and melanogenesis. *Endocrinology* **1996,** *137* (5), 1627-1633.
21. Sawyer, T. K.; Sanfilippo, P. J.; Hruby, V. J.; Engel, M. H.; Heward, C. B.; Burnett, J. B.; Hadley, M. E., 4-Norleucine, 7-D-phenylalanine-alpha-melanocyte-stimulating hormone: a highly potent alpha-melanotropin with ultralong biological activity. *Proc. Natl. Acad. Sci. U.S.A.* **1980,** *77* (10), 5754-8.
22. Schiöth, H. B.; Chhajlani, V.; Muceniece, R.; Klusa, V.; Wikberg, J. E. S., Major pharmacological distinction of the ACTH receptor from other melanocortin receptors. *Life Sci.* **1996,** *59* (10), 797-801.

23. Chen, W. B.; Kelly, M. A.; OpitzAraya, X.; Thomas, R. E.; Low, M. J.; Cone, R. D., Exocrine gland dysfunction in MC5-R-deficient mice: Evidence for coordinated regulation of exocrine gland function by melanocortin peptides. *Cell* **1997,** *91* (6), 789-798.
24. Xiang, Z.; Proneth, B.; Dirain, M. L.; Litherland, S. A.; Haskell-Luevano, C., Pharmacological Characterization of 30 Human Melanocortin-4 Receptor Polymorphisms with the Endogenous Proopiomelanocortin-Derived Agonists, Synthetic Agonists, and the Endogenous Agouti-Related Protein Antagonist. *Biochemistry* **2010,** *49* (22), 4583-4600.
25. Xiang, Z. M.; Litherland, S. A.; Sorensen, N. B.; Proneth, B.; Wood, M. S.; Shaw, A. M.; Millard, W. J.; Haskell-Luevano, C., Pharmacological characterization of 40 human melanocortin-4 receptor polymorphisms with the endogenous proopiomelanocortin-derived agonists and the Agouti-related protein (AGRP) antagonist. *Biochemistry* **2006,** *45* (23), 7277-7288.
26. Proneth, B.; Xiang, Z. M.; Pogozheva, I. D.; Litherland, S. A.; Gorbatyuk, O. S.; Shaw, A. M.; Millard, W. J.; Mosberg, H. I.; Haskell-Luevano, C., Molecular mechanism of the constitutive activation of the L250Q human melanocortin-4 receptor polymorphism. *Chemical Biology & Drug Design* **2006,** *67* (3), 215-229.
27. Xiang, Z. M.; Pogozheva, I. D.; Sorenson, N. B.; Wilczynski, A. M.; Holder, J. R.; Litherland, S. A.; Millard, W. J.; Mosberg, H. I.; Haskell-Luevano, C., Peptide and small molecules rescue the functional activity and agonist potency of dysfunctional human melanocortin-4 receptor polymorphisms. *Biochemistry* **2007,** *46* (28), 8273-8287.
28. Haslach, E. M.; Huang, H.; Dirain, M.; Debevec, G.; Geer, P.; Santos, R. G.; Giulianotti, M. A.; Pinilla, C.; Appel, J. R.; Doering, S. R.; Walters, M. A.; Houghten, R. A.; Haskell-Luevano, C., Identification of tetrapeptides from a mixture based positional scanning library that can restore nM full agonist function of the L106P, I69T, I102S, A219V, C271Y, and C271R human melanocortin-4 polymorphic receptors (hMC4Rs). *J. Med. Chem.* **2014,** *57* (11), 4615-28.
29. Nakanishi, S.; Inoue, A.; Kita, T.; Inoue, A.; Nakamura, M.; Chang, A. C. Y.; Cohen, S. N.; Numa, S., Nucleotide sequence of cloned cDNA for bovine corticotropin-[beta]-lipotropin precursor. *Nature* **1979,** *278* (5703), 423-427.
30. Büch, T. R. H.; Heling, D.; Damm, E.; Gudermann, T.; Breit, A., Pertussis Toxin-sensitive Signaling of Melanocortin-4 Receptors in Hypothalamic GT1-7 Cells Defines Agouti-related Protein as a Biased Agonist. *J. Biol. Chem.* **2009,** *284* (39), 26411-26420.
31. Mo, X. L.; Tao, Y. X., Activation of MAPK by inverse agonists in six naturally occurring constitutively active mutant human melanocortin-4 receptors. *Biochim. Biophys. Acta.* **2013,** *1832* (12), 1939-48.
32. Ghamari-Langroudi, M.; Digby, G. J.; Sebag, J. A.; Millhauser, G. L.; Palomino, R.; Matthews, R.; Gillyard, T.; Panaro, B. L.; Tough, I. R.; Cox, H. M.; Denton, J. S.; Cone, R. D., G-protein-independent coupling of MC4R to Kir7.1 in hypothalamic neurons. *Nature* **2015,** *520* (7545), 94-98.

33. Cone, R. D., *The melanocortin receptors*. Humana Press: Totowa, N.J., 2000; p x, 551 p.
34. Irani, B. G.; Holder, J. R.; Todorovic, A.; Wilczynski, A. M.; Joseph, C. G.; Wilson, K. R.; Haskell-Luevano, C., Progress in the development of melanocortin receptor selective ligands. *Current Pharmaceutical Design* **2004,** *10* (28), 3443-3479.
35. Hruby, V. J.; Wilkes, B. C.; Hadley, M. E.; Al-Obeidi, F.; Sawyer, T. K.; Staples, D. J.; de Vaux, A. E.; Dym, O.; Castrucci, A. M.; Hintz, M. F.; et al., Alpha-Melanotropin: the minimal active sequence in the frog skin bioassay. *J. Med. Chem.* **1987,** *30* (11), 2126-30.
36. Otsuka, H.; Inouye, K., Syntheses of peptides related to the N-terminal structure of corticotropin. III. The synthesis of L-histidyl-L-phenylalanyl-L-arginyl-L-tryptophan, the smallest peptide exhibiting the melanocyte-stimulating and the lipolytic activities. *Bull. Chem. Soc. Jpn.* **1964,** *37* (10), 1465-1471.
37. Bultman, S. J.; Michaud, E. J.; Woychik, R. P., Molecular characterization of the mouse agouti locus. *Cell* **1992,** *71* (7), 1195-1204.
38. Miller, M. W.; Duhl, D. M.; Vrieling, H.; Cordes, S. P.; Ollmann, M. M.; Winkes, B. M.; Barsh, G. S., Cloning of the mouse agouti gene predicts a secreted protein ubiquitously expressed in mice carrying the lethal yellow mutation. *Genes. Dev.* **1993,** *7* (3), 454-67.
39. Ollmann, M. M.; Wilson, B. D.; Yang, Y. K.; Kerns, J. A.; Chen, Y. R.; Gantz, I.; Barsh, G. S., Antagonism of central melanocortin receptors in vitro and in vivo by Agouti-related protein. *Science* **1997,** *278* (5335), 135-138.
40. Tota, M. R.; Smith, T. S.; Mao, C.; MacNeil, T.; Mosley, R. T.; Van der Ploeg, L. H. T.; Fong, T. M., Molecular Interaction of Agouti Protein and Agouti-Related Protein with Human Melanocortin Receptors. *Biochemistry* **1999,** *38* (3), 897-904.
41. Wilczynski, A.; Wang, X. S.; Joseph, C. G.; Xiang, Z.; Bauzo, R. M.; Scott, J. W.; Sorensen, N. B.; Shaw, A. M.; Millard, W. J.; Richards, N. G.; Haskell-Luevano, C., Identification of Putative Agouti-Related Protein(87−132)-Melanocortin-4 Receptor Interactions by Homology Molecular Modeling and Validation Using Chimeric Peptide Ligands. *J. Med. Chem.* **2004,** *47* (9), 2194-2207.
42. Joseph, C. G.; Wang, X. S.; Scott, J. W.; Bauzo, R. M.; Xiang, Z.; Richards, N. G.; Haskell-Luevano, C., Stereochemical Studies of the Monocyclic Agouti-Related Protein (103−122) Arg-Phe-Phe Residues: Conversion of a Melanocortin-4 Receptor Antagonist into an Agonist and Results in the Discovery of a Potent and Selective Melanocortin-1 Agonist. *J. Med. Chem.* **2004,** *47* (27), 6702-6710.
43. Fan, W.; Boston, B. A.; Kesterson, R. A.; Hruby, V. J.; Cone, R. D., Role of melanocortinergic neurons in feeding and the agouti obesity syndrome. *Nature* **1997,** *385* (6612), 165-168.
44. Irani, B. G.; Xiang, Z. M.; Yarandi, H. N.; Holder, J. R.; Moore, M. C.; Bauzo, R. M.; Proneth, B.; Shaw, A. M.; Millard, W. J.; Chambers, J. B.; Benoit, S. C.; Clegg, D.

J.; Haskell-Luevano, C., Implication of the melanocortin-3 receptor in the regulation of food intake. *Eur. J. Pharmacol.* **2011,** *660* (1), 80-87.
45. Holder, J. R.; Haskell-Luevano, C., Melanocortin ligands: 30 years of structure-activity relationship (SAR) studies. *Medicinal Research Reviews* **2004,** *24* (3), 325-356.
46. Hruby, V. J.; Cai, M. Y., Design of Peptide and Peptidomimetic Ligands with Novel Pharmacological Activity Profiles. *Annu Rev Pharmacol* **2013,** *53*, 557-+.
47. Hruby, V. J.; Cai, M. Y.; Cain, J.; Nyberg, J.; Trivedi, D., Design of novel melanocortin receptor ligands: Multiple receptors, complex pharmacology, the challenge. *Eur. J. Pharmacol.* **2011,** *660* (1), 88-93.
48. Alobeidi, F.; Hadley, M. E.; Pettitt, B. M.; Hruby, V. J., Design of a New Class of Superpotent Cyclic Alpha-Melanotropins Based on Quenched Dynamic Simulations. *J. Am. Chem. Soc.* **1989,** *111* (9), 3413-3416.
49. Alobeidi, F.; Castrucci, A. M. D.; Hadley, M. E.; Hruby, V. J., Potent and Prolonged Acting Cyclic Lactam Analogs of Alpha-Melanotropin - Design Based on Molecular-Dynamics. *J. Med. Chem.* **1989,** *32* (12), 2555-2561.
50. Hadley, M. E., Discovery that a melanocortin regulates sexual functions in male and female humans. *Peptides* **2005,** *26* (10), 1687-1689.
51. Schild, H. O., pA, a new scale for the measurement of drug antagonism. *Br. J. Pharmacol.* **1947,** *2* (3), 189-206.
52. Hruby, V. J.; Lu, D. S.; Sharma, S. D.; Castrucci, A. D.; Kesterson, R. A.; Alobeidi, F. A.; Hadley, M. E.; Cone, R. D., Cyclic lactam alpha-melanotropin analogs of Ac-Nle(4)-Cyclo[Asp(5),D-Phe(7),Lys(10)] alpha-melanocyte-stimulating hormone-(4-10)-NH2 with bulky aromatic-amino-acids at position-7 show high antagonist potency and selectivity at specific melanocortin receptors. *J. Med. Chem.* **1995,** *38* (18), 3454-3461.
53. Haskell-Luevano, C.; Holder, J. R.; Monck, E. K.; Bauzo, R. M., Characterization of melanocortin NDP-MSH agonist peptide fragments at the mouse central and peripheral melanocortin receptors. *J. Med. Chem.* **2001,** *44* (13), 2247-2252.
54. Yang, Y.; Fong, T. M.; Dickinson, C. J.; Mao, C.; Li, J. Y.; Tota, M. R.; Mosley, R.; Van der Ploeg, L. H. T.; Gantz, I., Molecular determinants of ligand binding to the human melanocortin-4 receptor. *Biochemistry* **2000,** *39* (48), 14900-14911.
55. Holder, J. R.; Bauzo, R. M.; Xiang, Z. M.; Haskell-Luevano, C., Structure-activity relationships of the melanocortin tetrapeptide Ac-His-DPhe-Arg-Trp-NH2 at the mouse melanocortin receptors. 1. Modifications at the His position. *J. Med. Chem.* **2002,** *45* (13), 2801-2810.
56. Holder, J. R.; Xiang, Z. M.; Bauzo, R. M.; Haskell-Leuvano, C., Structure-activity relationships of the melanocortin tetrapeptide Ac-His-D-Phe-Arg-Trp-NH2 at the mouse melanocortin receptors. 4. Modifications at the Trp position. *J. Med. Chem.* **2002,** *45* (26), 5736-5744.

57. Holder, J. R.; Bauzo, R. M.; Xiang, Z. M.; Haskell-Luevano, C., Structure-activity relationships of the melanocortin tetrapeptide Ac-His-DPhe-Arg-Trp-NH2 at the mouse melanocortin receptors: Part 2 modifications at the Phe position. *J. Med. Chem.* **2002,** *45* (14), 3073-3081.
58. Holder, J. R.; Xiang, Z. M.; Bauzo, R. M.; Haskell-Luevano, C., Structure-activity relationships of the melanocortin tetrapeptide Ac-His-DPhe-Arg-Trp-NH2 at the mouse melanocortin receptors - Part 3: modifications at the Arg position. *Peptides* **2003,** *24* (1), 73-82.
59. Holder, J. R.; Bauzo, R. M.; Xiang, Z. M.; Scott, J.; Haskell-Luevano, C., Design and pharmacology of peptoids and peptide-peptoid hybrids based on the melanocortin agonists core tetrapeptide sequence. *Bioorg. Med. Chem. Lett.* **2003,** *13* (24), 4505-4509.
60. Holder, J. R.; Haskell-Luevano, C., Melanocortin tetrapeptides modified at the N-terminus, His, Phe, Arg, and Trp positions. In *Melanocortin System*, Cone, R. D., Ed. 2003; Vol. 994, pp 36-48.
61. Holder, J. R.; Marques, F. F.; Xiang, Z. M.; Bauzo, R. M.; Haskell-Luevano, C., Characterization of aliphatic, cyclic, and aromatic N-terminally "capped" His-D-Phe-Arg-Trp-NH2 tetrapeptides at the melanocortin receptors. *Eur. J. Pharmacol.* **2003,** *462* (1-3), 41-52.
62. Todorovic, A.; Holder, J. R.; Scott, J. W.; Haskell-Luevano, C., Synthesis and activity of the melanocortin Xaa-d-Phe-Arg-Trp-NH tetrapeptides with amide bond modifications. *The journal of peptide research : official journal of the American Peptide Society* **2004,** *63* (3), 270-8.
63. Joseph, C. G.; Sorensen, N. B.; Wood, M. S.; Xiang, Z.; Moore, M. C.; Haskell-Luevano, C., Modified melanocortin tetrapeptide Ac-His-dPhe-Arg-Trp-NH at the arginine side chain with ureas and thioureas. *The journal of peptide research : official journal of the American Peptide Society* **2005,** *66* (5), 297-307.
64. Todorovic, A.; Holder, J. R.; Bauzo, R. M.; Scott, J. W.; Kavanagh, R.; Abdel-Malek, Z.; Haskell-Luevano, C., N-terminal fatty acylated HiS-DPhe-Arg-Trp-NH2 tetrapeptides: Influence of fatty acid chain length on potency and selectivity at the mouse melanocortin receptors and human melanocytes. *J. Med. Chem.* **2005,** *48* (9), 3328-3336.
65. Boeglin, D.; Xiang, Z.; Sorenson, N. B.; Wood, M. S.; Haskell-Luevano, C.; Lubell, W. D., Aza-scanning of the potent melanocortin receptor agonist Ac-His-D-Phe-Arg-Trp-NH. *Chem. Biol. Drug Des.* **2006,** *67* (4), 275-83.
66. Proneth, B.; Pogozheva, I. D.; Portillo, F. P.; Mosberg, H. I.; Haskell-Luevano, C., Melanocortin tetrapeptide Ac-His-DPhe-Arg-Trp-NH(2) modified at the para position of the benzyl side chain (DPhe): Importance for mouse melanocortin-3 receptor agonist versus antagonist activity. *J. Med. Chem.* **2008,** *51* (18), 5585-5593.
67. Doering, S. R.; Todorovic, A.; Haskell-Luevano, C., Melanocortin antagonist tetrapeptides with minimal agonist activity at the mouse melanocortin-3 receptor. *A.C.S. Med. Chem. Lett.* **2015,** *6* (2), 123-7.

68. Singh, A.; Tala, S. R.; Flores, V.; Freeman, K.; Haskell-Luevano, C., Synthesis and Pharmacology of alpha/beta(3)-Peptides Based on the Melanocortin Agonist Ac-His-dPhe-Arg-Trp-NH2 Sequence. *A.C.S. Med. Chem. Lett.* **2015,** *6* (5), 568-72.
69. Kopanchuk, S.; Veiksina, S.; Mutulis, F.; Mutule, I.; Yahorava, S.; Mandrika, I.; Petrovska, R.; Rinken, A.; Wikberg, J. E. S., Kinetic evidence for tandemly arranged ligand binding sites in melanocortin 4 receptor complexes. *Neurochem. Int.* **2006,** *49* (5), 533-542.
70. Smith, P. E., Experimental Ablation of the Hypophysis in the Frog Embryo. *Science* **1916,** *44* (1130), 280-282.
71. Allen, B. M., Effects of the Extirpation of the Anterior Lobe of the Hypophysis of Rana Pipiens. *Biological Bulletin* **1917,** *32* (3), 117-130.
72. Poggioli, R.; Vergoni, A. V.; Bertolini, A., ACTH-(1–24) and α-MSH antagonize feeding behavior stimulated by kappa opiate agonists. *Peptides* **1986,** *7* (5), 843-848.
73. Good, D. J., Obese Mouse Models. In *Sourcebook of Models for Biomedical Research*, Conn, P. M., Ed. Humana Press: Totowa, NJ, 2008; pp 683-702.
74. Michaud, E. J.; Bultman, S. J.; Klebig, M. L.; van Vugt, M. J.; Stubbs, L. J.; Russell, L. B.; Woychik, R. P., A molecular model for the genetic and phenotypic characteristics of the mouse lethal yellow (Ay) mutation. *Proceedings of the National Academy of Sciences* **1994,** *91* (7), 2562-2566.
75. Greenfield, J. R.; Miller, J. W.; Keogh, J. M.; Henning, E.; Satterwhite, J. H.; Cameron, G. S.; Astruc, B.; Mayer, J. P.; Brage, S.; See, T. C.; Lomas, D. J.; O'Rahilly, S.; Farooqi, I. S., Modulation of Blood Pressure by Central Melanocortinergic Pathways. *New Engl J Med* **2009,** *360* (1), 44-52.
76. Atalayer, D.; Robertson, K. L.; Haskell-Luevano, C.; Andreasen, A.; Rowland, N. E., Food demand and meal size in mice with single or combined disruption of melanocortin type 3 and 4 receptors. *Am. J. Physiol. Regul. Integr. Comp. Physiol.* **2010,** *298* (6), R1667-74.
77. Ni, X. P.; Butler, A. A.; Cone, R. D.; Humphreys, M. H., Central receptors mediating the cardiovascular actions of melanocyte stimulating hormones. *J. Hypertens.* **2006,** *24* (11), 2239-2246.
78. Wessells, H.; Fuciarelli, K.; Hansen, J.; Hadley, M. E.; Hruby, V. J.; Dorr, R.; Levine, N., Synthetic melanotropic peptide initiates erections in men with psychogenic erectile dysfunction: double-blind, placebo controlled crossover study. *J. Urol.* **1998,** *160* (2), 389-93.
79. Joseph, C. G.; Yao, H.; Scott, J. W.; Sorensen, N. B.; Marnane, R. N.; Mountjoy, K. G.; Haskell-Luevano, C., gamma(2)-Melanocyte stimulation hormone (gamma(2)-MSH) truncation studies results in the cautionary note that gamma(2)-MSH is not selective for the mouse MC3R over the mouse MC5R. *Peptides* **2010,** *31* (12), 2304-2313.

80. Carotenuto, A.; Merlino, F.; Cai, M.; Brancaccio, D.; Yousif, A. M.; Novellino, E.; Hruby, V. J.; Grieco, P., Discovery of novel potent and selective agonists at the melanocortin-3 receptor. *J. Med. Chem.* **2015,** *58* (24), 9773-9778.
81. Grieco, P.; Balse, P. M.; Weinberg, D.; MacNeil, T.; Hruby, V. J., D-amino acid scan of gamma-melanocyte-stimulating hormone: Importance of Trp(8) on human MC3 receptor selectivity. *J. Med. Chem.* **2000,** *43* (26), 4998-5002.
82. Kavarana, M. J.; Trivedi, D.; Cai, M. Y.; Ying, J. F.; Hammer, M.; Cabello, C.; Grieco, P.; Han, G. X.; Hruby, V. J., Novel cyclic templates of alpha-MSH give highly selective and potent antagonists/agonists for human melanocortin-3/4 receptors. *J. Med. Chem.* **2002,** *45* (12), 2644-2650.
83. Grieco, P.; Cai, M.; Han, G.; Trivedi, D.; Campiglia, P.; Novellino, E.; Hruby, V. J., Further structure-activity studies of lactam derivatives of MT-II and SHU-9119: Their activity and selectivity at human melanocortin receptors 3, 4, and 5. *Peptides* **2007,** *28* (6), 1191-1196.
84. Grieco, P.; Lavecchia, A.; Cai, M. Y.; Trivedi, D.; Weinberg, D.; MacNeil, T.; Van der Ploeg, L. H. T.; Hruby, V. J., Structure-activity studies of the melanocortin peptides: Discovery of potent and selective affinity antagonists for the hMC3 and hMC4 receptors. *J. Med. Chem.* **2002,** *45* (24), 5287-5294.
85. Ballet, S.; Mayorov, A. V.; Cai, M. Y.; Tymecka, D.; Chandler, K. B.; Palmer, E. S.; Van Rompaey, K.; Misicka, A.; Tourwe, D.; Hruby, V. J., Novel selective human melanocortin-3 receptor ligands: Use of the 4-amino-1,2,4,5-tetrahydro-2-benzazepin-3-one (Aba) scaffold. *Bioorg. Med. Chem. Lett.* **2007,** *17* (9), 2492-2498.
86. Prevention, C. f. D. C. a., Prevalence of Self-Reported Obesity Among U.S. Adults by State and Territory, BRFSS, 2014. **2014**.
87. Merrifield, R. B., Solid Phase Peptide Synthesis. I. The Synthesis of a Tetrapeptide. *J. Am. Chem. Soc.* **1963,** *85* (14), 2149-2154.
88. Kempe, M.; Barany, G., CLEAR: A Novel Family of Highly Cross-Linked Polymeric Supports for Solid-Phase Peptide Synthesis1,2. *J. Am. Chem. Soc.* **1996,** *118* (30), 7083-7093.
89. Sarin, V. K.; Kent, S. B. H.; Merrifield, R. B., Properties of swollen polymer networks. Solvation and swelling of peptide-containing resins in solid-phase peptide synthesis. *J. Am. Chem. Soc.* **1980,** *102* (17), 5463-5470.
90. Matsueda, G. R.; Stewart, J. M., A p-methylbenzhydrylamine resin for improved solid-phase synthesis of peptide amides. *Peptides* **1981,** *2* (1), 45-50.
91. Chang, C.-D.; Meienhofer, J., Solid-Phase Peptide Synthesis Using Mild Base Cleavage of NαFluorenylmethyloxycarbonylamino acids, Exemplified by a Synthesis of Dihydrosomatostatin. *Int. J. Pept. Protein Res.* **1978,** *11* (3), 246-249.
92. Carpino, L. A.; Han, G. Y., 9-Fluorenylmethoxycarbonyl function, a new base-sensitive amino-protecting group. *J. Am. Chem. Soc.* **1970,** *92* (19), 5748-5749.

93. Carpino, L. A.; Han, G. Y., 9-Fluorenylmethoxycarbonyl amino-protecting group. *The Journal of Organic Chemistry* **1972,** *37* (22), 3404-3409.
94. Murray, J. K.; Aral, J.; Miranda, L. P., Solid-Phase Peptide Synthesis Using Microwave Irradiation. *Methods Mol Biol* **2011,** *716*, 73-88.
95. Michels, T.; Dolling, R.; Haberkorn, U.; Mier, W., Acid-mediated prevention of aspartimide formation in solid phase peptide synthesis. *Org. Lett.* **2012,** *14* (20), 5218-21.
96. Isidro-Llobet, A.; Alvarez, M.; Albericio, F., Amino Acid-Protecting Groups. *Chem. Rev.* **2009,** *109* (6), 2455-2504.
97. Tala, S. R.; Schnell, S. M.; Haskell-Luevano, C., Microwave-assisted solid-phase synthesis of side-chain to side-chain lactam-bridge cyclic peptides. *Bioorg. Med. Chem. Lett.* **2015,** *25* (24), 5708-5711.
98. Stewart, J. M.; Young, J. D., *Solid phase peptide synthesis*. 2nd ed.; Pierce Chemical Co.: Rockford, Ill., 1984; p xvi, 176 p.
99. Kaiser, E.; Colescott, R. L.; Bossinger, C. D.; Cook, P. I., Color test for detection of free terminal amino groups in the solid-phase synthesis of peptides. *Anal. Biochem.* **1970,** *34* (2), 595-598.
100. Judkowski, V.; Pinilla, C.; Schroder, K.; Tucker, L.; Sarvetnick, N.; Wilson, D. B., Identification of MHC Class II-Restricted Peptide Ligands, Including a Glutamic Acid Decarboxylase 65 Sequence, that Stimulate Diabetogenic T Cells from Transgenic BDC2.5 Nonobese Diabetic Mice. *The Journal of Immunology* **2001,** *166* (2), 908-917.
101. Appel, J. R.; Campbell, G. D.; Buencamino, J.; Houghten, R. A.; Pinilla, C., Characterization of antigen-antibody interactions using single substitution analogs and mixture-based synthetic combinatorial libraries. *Journal of Peptide Research* **1998,** *52* (5), 346-355.
102. Appel, J. R.; Johnson, J.; Narayanan, V. L.; Houghten, R. A., Identification of novel antitumor agents from mixture-based synthetic combinatorial libraries using cell-based assays. *Mol. Divers.* **1998,** *4* (2), 91-102.
103. Vanderah, T. W.; Largent-Milnes, T.; Lai, J.; Porreca, F.; Houghten, R. A.; Menzaghi, F.; Wisniewski, K.; Stalewski, J.; Sueiras-Diaz, J.; Galyean, R.; Schteingart, C.; Junien, J.-L.; Trojnar, J.; Rivière, P. J. M., Novel d-amino acid tetrapeptides produce potent antinociception by selectively acting at peripheral κ-opioid receptors. *Eur. J. Pharmacol.* **2008,** *583* (1), 62-72.
104. Lebl, M., Parallel Personal Comments on "Classical" Papers in Combinatorial Chemistry. *J. Comb. Chem.* **1999,** *1* (1), 3-24.
105. Houghten, R. A., General method for the rapid solid-phase synthesis of large numbers of peptides: specificity of antigen-antibody interaction at the level of individual amino acids. *Proc. Natl. Acad. Sci. U.S.A.* **1985,** *82* (15), 5131-5.
106. Houghten, R. A., Means for sequential solid phase organic synthesis and methods using the same. Google Patents: 1986.

107. Santos, R. G.; Giulianotti, M. A.; Dooley, C. T.; Pinilla, C.; Appel, J. R.; Houghten, R. A., Use and Implications of the Harmonic Mean Model on Mixtures for Basic Research and Drug Discovery. *Acs Comb Sci* **2011,** *13* (3), 337-344.
108. Houghten, R. A.; Wilson, D. B.; Pinilla, C., Drug discovery and vaccine development using mixture-based synthetic combinatorial libraries. *Drug Discovery Today* **2000,** *5* (7), 276-285.
109. Ostresh, J. M.; Winkle, J. H.; Hamashin, V. T.; Houghten, R. A., Peptide libraries: Determination of relative reaction rates of protected amino acids in competitive couplings. *Biopolymers* **1994,** *34* (12), 1681-1689.
110. Burgess, K.; Liaw, A. I.; Wang, N., Combinatorial Technologies Involving Reiterative Division/Coupling/Recombination: Statistical Considerations. *J. Med. Chem.* **1994,** *37* (19), 2985-2987.
111. Geysen, H. M.; Rodda, S. J.; Mason, T. J., A priori delineation of a peptide which mimics a discontinuous antigenic determinant. *Mol. Immunol.* **1986,** *23* (7), 709-715.
112. Pinilla, C.; Appel, J. R.; Blanc, P.; Houghten, R. A., Rapid identification of high affinity peptide ligands using positional scanning synthetic peptide combinatorial libraries. *BioTechniques* **1992,** *13* (6), 901-905.
113. Maria Waldhoer; Selena E. Bartlett, a.; Whistler, J. L., Opioid Receptors. *Annu. Rev. Biochem* **2004,** *73* (1), 953-990.
114. *The opiate receptors*. 2nd ed.. ed.; New York : Springer Science+Business Media, LLC: New York, 2011.
115. Aldrich, J. V.; McLaughlin, J. P., Peptide Kappa Opioid Receptor Ligands: Potential for Drug Development. *The AAPS Journal* **2009,** *11* (2), 312-322.
116. Dooley, C. T.; Ny, P.; Bidlack, J. M.; Houghten, R. A., Selective Ligands for the μ, δ, and κ Opioid Receptors Identified from a Single Mixture Based Tetrapeptide Positional Scanning Combinatorial Library. *J. Biol. Chem.* **1998,** *273* (30), 18848-18856.
117. Vanderah, T. W.; Lai, J.; Schteingart, C. D.; Trojnar, J.; Riviere, P. J. M.; Junien, J.-L., FE200041 (D-Phe-D-Phe-D-Nle-D-Arg-NH 2): A peripheral efficacious κ opioid agonist with unprecedented selectivity. *J. Pharmacol. Exp. Ther.* **2004,** *310* (1), 326-333.
118. Chalmers, D. T.; Jones, J. B.; Spencer, R. H., Peripheral kappa receptor agonists for reducing pain and inflammation. Google Patents: 2015.
119. Hensler, M. E.; Bernstein, G.; Nizet, V.; Nefzi, A., Pyrrolidine bis-cyclic guanidines with antimicrobial activity against drug-resistant Gram-positive pathogens identified from a mixture-based combinatorial library. *Bioorg. Med. Chem. Lett.* **2006,** *16* (19), 5073-5079.
120. Chang, Y. P.; Banerjee, J.; Dowell, C.; Wu, J. H.; Gyanda, R.; Houghten, R. A.; Toll, L.; McIntosh, J. M.; Armishaw, C. J., Discovery of a Potent and Selective alpha 3 beta 4 Nicotinic Acetylcholine Receptor Antagonist from an alpha-Conotoxin Synthetic Combinatorial Library. *J. Med. Chem.* **2014,** *57* (8), 3511-3521.

121. Yongye, A. B.; Appel, J. R.; Giulianotti, M. A.; Dooley, C. T.; Medina-Franco, J. L.; Nefzi, A.; Houghten, R. A.; Martinez-Mayorga, K., Identification, structure-activity relationships and molecular modeling of potent triamine and piperazine opioid ligands. *Biorg. Med. Chem.* **2009,** *17* (15), 5583-5597.
122. Pinilla, C.; Appel, J. R.; Borras, E.; Houghten, R. A., Advances in the use of synthetic combinatorial chemistry: Mixture-based libraries. *Nat. Med.* **2003,** *9* (1), 118-122.
123. Chen, W. B.; Shields, T. S.; Stork, P. J. S.; Cone, R. D., A colorimetric assay for measuring activation of G(S)-coupled and G(Q)-coupled signaling pathways. *Anal. Biochem.* **1995,** *226* (2), 349-354.
124. Gantz, I.; Tashiro, T.; Barcroft, C.; Konda, Y.; Shimoto, Y.; Miwa, H.; Glover, T.; Munzert, G.; Yamada, T., Localization of the Genes Encoding the Melanocortin-2 (Adrenocorticotropic Hormone) and Melanocortin-3 Receptors to Chromosomes 18p11.2 and 20q13.2-Q13.3 by Fluorescence in-Situ Hybridization. *Genomics* **1993,** *18* (1), 166-167.
125. Eipper, B. A.; Mains, R. E., Structure and Biosynthesis of Pro-Adrenocorticotropin/Endorphin and Related Peptides. *Endocr Rev* **1980,** *1* (1), 1-27.
126. Cheung, A. W. H.; Danho, W.; Swistok, J.; Qi, L.; Kurylko, G.; Franco, L.; Yagaloff, K.; Chen, L., Structure-activity relationship of linear peptide Bu-His-DPhe-Arg-Trp-Gly-NH2 at the human melanocortin-1 and-4 receptors: Arginine substitution. *Bioorg. Med. Chem. Lett.* **2002,** *12* (17), 2407-2410.
127. Cheung, A. W. H.; Danho, W.; Swistok, J.; Qi, L. D.; Kurylko, G.; Rowan, K.; Yeon, M.; Franco, L.; Chu, X. J.; Chen, L.; Yagaloff, K., Structure-activity relationship of linear peptide Bu-His-DPhe-Arg-Trp-Gly-NH2 at the human melanocortin-1 and-4 receptors: Histidine substitution. *Bioorg. Med. Chem. Lett.* **2003,** *13* (1), 133-137.
128. Todorovic, A. Peptide, Peptidomimetic and Small Molecule Based Ligands Targeting Melanocortin Receptor System. University of Florida, 2006.
129. Ellacott, K. L.; Morton, G. J.; Woods, S. C.; Tso, P.; Schwartz, M. W., Assessment of feeding behavior in laboratory mice. *Cell Metab.* **2010,** *12* (1), 10-7.
130. Chen, C. A.; Okayama, H., Calcium phosphate-mediated gene transfer: a highly efficient transfection system for stably transforming cells with plasmid DNA. *BioTechniques* **1988,** *6* (7), 632-638.
131. Day, J. W.; Ottaway, N.; Patterson, J. T.; Gelfanov, V.; Smiley, D.; Gidda, J.; Findeisen, H.; Bruemmer, D.; Drucker, D. J.; Chaudhary, N.; Holland, J.; Hembree, J.; Abplanalp, W.; Grant, E.; Ruehl, J.; Wilson, H.; Kirchner, H.; Lockie, S. H.; Hofmann, S.; Woods, S. C.; Nogueiras, R.; Pfluger, P. T.; Perez-Tilve, D.; DiMarchi, R.; Tschop, M. H., A new glucagon and GLP-1 co-agonist eliminates obesity in rodents. *Nat Chem Biol* **2009,** *5* (10), 749-757.
132. Finan, B.; Ma, T.; Ottaway, N.; Müller, T. D.; Habegger, K. M.; Heppner, K. M.; Kirchner, H.; Holland, J.; Hembree, J.; Raver, C.; Lockie, S. H.; Smiley, D. L.; Gelfanov,

V.; Yang, B.; Hofmann, S.; Bruemmer, D.; Drucker, D. J.; Pfluger, P. T.; Perez-Tilve, D.; Gidda, J.; Vignati, L.; Zhang, L.; Hauptman, J. B.; Lau, M.; Brecheisen, M.; Uhles, S.; Riboulet, W.; Hainaut, E.; Sebokova, E.; Conde-Knape, K.; Konkar, A.; DiMarchi, R. D.; Tschöp, M. H., Unimolecular Dual Incretins Maximize Metabolic Benefits in Rodents, Monkeys, and Humans. *Science Translational Medicine* **2013,** *5* (209), 209ra151-209ra151.
133. Finan, B.; Yang, B.; Ottaway, N.; Smiley, D. L.; Ma, T.; Clemmensen, C.; Chabenne, J.; Zhang, L.; Habegger, K. M.; Fischer, K.; Campbell, J. E.; Sandoval, D.; Seeley, R. J.; Bleicher, K.; Uhles, S.; Riboulet, W.; Funk, J.; Hertel, C.; Belli, S.; Sebokova, E.; Conde-Knape, K.; Konkar, A.; Drucker, D. J.; Gelfanov, V.; Pfluger, P. T.; Muller, T. D.; Perez-Tilve, D.; DiMarchi, R. D.; Tschop, M. H., A rationally designed monomeric peptide triagonist corrects obesity and diabetes in rodents. *Nat. Med.* **2015,** *21* (1), 27-36.
134. Haskell-Luevano, C.; Sawyer, T. K.; Hendrata, S.; North, C.; Panahinia, L.; Stum, M.; Staples, D. J.; Castrucci, A. M. D.; Hadley, M. E.; Hruby, V. J., Truncation studies of alpha-melanotropin peptides identify tripeptide analogues exhibiting prolonged agonist bioactivity. *Peptides* **1996,** *17* (6), 995-1002.
135. Houghten, R. A.; Pinilla, C.; Appel, J. R.; Blondelle, S. E.; Dooley, C. T.; Eichler, J.; Nefzi, A.; Ostresh, J. M., Mixture-based synthetic combinatorial libraries. *J. Med. Chem.* **1999,** *42* (19), 3743-3778.
136. Ericson, M. D.; Schnell, S. M.; Freeman, K. T.; Haskell-Luevano, C., A fragment of the Escherichia coli ClpB heat-shock protein is a micromolar melanocortin 1 receptor agonist. *Bioorg. Med. Chem. Lett.* **2015,** *25* (22), 5306-5308.
137. Danho, W.; Swistok, J.; Cheung, A. W. H.; Kurylko, G.; Franco, L.; Chu, X. J.; Chen, L.; Yagaloff, K., Structure-activity relationship of linear peptide Bu-His(6)-DPhe(7)-Arg(8)-Trp(9)-Gly(10)-NH2 at the human melanocortin-1 and-4 receptors: DPhe(7) and Trp(9) substitution. *Bioorg. Med. Chem. Lett.* **2003,** *13* (4), 649-652.
138. Ye, Z. X.; MacNeil, T.; Weinberg, D. H.; Kalyani, R. N.; Tang, R.; Strack, A. M.; Murphy, B. A.; Mosley, R. T.; MacIntyre, D. E.; Van der Ploeg, L. H. T.; Patchett, A. A.; Wyvratt, M. J.; Nargund, R. R., Structure-activity relationship of linear tetrapeptides Tic-DPhe-Arg-Trp-NH2 at the human melanocortin-4 receptor and effects on feeding behaviors in rat. *Peptides* **2005,** *26* (10), 2017-2025.
139. Koikov, L. N.; Ebetino, F. H.; Solinsky, M. G.; Cross-Doersen, D.; Knittel, J. J., Sub-nanomolar hMC1R agonists by end-capping of the melanocortin tetrapeptide His-D-Phe-Arg-Trp-NH(2). *Bioorg. Med. Chem. Lett.* **2003,** *13* (16), 2647-50.
140. Haskell-Luevano, C.; Hendrata, S.; North, C.; Sawyer, T. K.; Hadley, M. E.; Hruby, V. J.; Dickinson, C.; Gantz, I., Discovery of prototype peptidomimetic agonists at the human melanocortin receptors MC1R and MC4R. *J. Med. Chem.* **1997,** *40* (14), 2133-9.

141. Joseph, C. G.; Wilczynski, A.; Holder, J. R.; Xiang, Z. M.; Bauzo, R. M.; Scott, J. W.; Haskell-Luevano, C., Chimeric NDP-MSH and MTII melanocortin peptides with agouti-related protein (AGRP) Arg-Phe-Phe amino acids possess agonist melanocortin receptor activity. *Peptides* **2003,** *24* (12), 1899-1908.
142. Mayorov, A. V.; Cai, M. Y.; Palmer, E. S.; Liu, Z. H.; Cain, J. P.; Vagner, J.; Trivedi, D.; Hruby, V. J., Solid-phase peptide head-to-side chain cyclodimerization: Discovery of C-2-symmetric cyclic lactam hybrid alpha-melanocyte-stimulating hormone (MSH)/agouti-signaling protein (ASIP) analogues with potent activities at the human melanocortin receptors. *Peptides* **2010,** *31* (10), 1894-1905.
143. Tam, J. P.; Heath, W. F.; Merrifield, R. B., An SN2 deprotection of synthetic peptides with a low concentration of hydrofluoric acid in dimethyl sulfide: evidence and application in peptide synthesis. *J.A.C.S.* **1983,** *105* (21), 6442-6455.
144. Houghten, R. A.; Bray, M. K.; Degraw, S. T.; Kirby, C. J., Simplified procedure for carrying out simultaneous multiple hydrogen fluoride cleavages of protected peptide resins. *Int. J. Pept. Protein Res.* **1986,** *27* (6), 673-8.
145. Dooley, C. T.; Houghten, R. A., The use of positional scanning synthetic peptide combinatorial libraries for the rapid determination of opioid receptor ligands. *Life Sci.* **1993,** *52* (18), 1509-1517.
146. Hunter, W. M.; Greenwood, F. C., Preparation of Iodine-131 Labelled Human Growth Hormone of High Specific Activity. *Nature* **1962,** *194* (4827), 495-496.
147. Goodman, M.; Chorev, M., On the concept of linear modified retro-peptide structures. *Acc. Chem. Res.* **1979,** *12* (1), 1-7.
148. Chorev, M.; Goodman, M., A dozen years of retro-inverso peptidomimetics. *Acc. Chem. Res.* **1993,** *26* (5), 266-273.
149. Chorev, M.; Shavitz, R.; Goodman, M.; Minick, S.; Guillemin, R., Partially Modified Retro-Inverso-Enkephalinamides - Topochemical Long-Acting Analogs Invitro and Invivo. *Science* **1979,** *204* (4398), 1210-1212.
150. Weeden, T.; Stefano, J.; Duan, S.; Edling, A.; Hou, L.; Chuang, W.-L.; Perricone, M. A.; Pan, C.; Dzuris, J. L., A retro-inverso α-melanocyte stimulating hormone analog with MC1R-binding selectivity. *J. Pept. Sci.* **2011,** *17* (1), 47-55.
151. Hano, K.; Koida, M.; Kubo, K.; Yajima, H., Evaluation of the physiological properties of d-histidyl-d-phenylalanyl-d-arginyl-d-tryptophyl-glycine in frog melanocyte. *Biochimica et Biophysica Acta (BBA) - General Subjects* **1964,** *90* (1), 201-204.
152. Mutulis, F.; Mutule, I.; Lapins, M.; Wikberg, J. E. S., Reductive amination products containing naphthalene and indole moieties bind to melanocortin receptors. *Bioorg. Med. Chem. Lett.* **2002,** *12* (7), 1035-1038.
153. Fields, G. B.; Noble, R. L., Solid phase peptide synthesis utilizing 9-fluorenylmethoxycarbonyl amino acids. *Int. J. Pept. Protein Res.* **1990,** *35* (3), 161-214.